Development of Automatic Vehicle Pedals Lock System with GPS and GSM Tracking for Controlling Drunk Driving

Sewagegn Zewudie Tegegne

Office of Graduate Studies

Adama Science and Technology University

February, 2022

Adama, Ethiopia

Development of Automatic Vehicle Pedals Lock System with GPS and GSM Tracking for Controlling Drunk Driving

Sewagegn Zewudie Tegegne

A Thesis Submitted to
The Department of Mechanical Engineering
School of Mechanical, Chemical and Materials Engineering

Presented in Partial Fulfilment of the Requirement for Master of Science in Automotive Engineering

Office of Graduate Studies
Adama Science and Technology University

February, 2022
Adama, Ethiopia

Development of Automatic Vehicle Pedals Lock System with GPS and GSM Tracking for Controlling Drunk Driving

Sewagegn Zewudie Tegegne

Advisor: Dr. Ramesh Babu Nallamothu

Co-Advisor: Dr. Harish Kalla

A Thesis Submitted to

The Department of Mechanical Engineering

School of Mechanical, Chemical and Materials Engineering

Presented in Partial Fulfilment of the Requirement for Master of Science in Automotive Engineering

Office of Graduate Studies

Adama Science and Technology University

February, 2022

Adama, Ethiopia

DECLARATION

I hereby declare that this master's thesis entitled "Development of Automatic Vehicle Pedals Lock System with GPS and GSM Tracking for Controlling Drunk Driving" partially fulfills the requirements for the award of the Master of Science degree in Automotive Engineering. It is an authentic record of my original work. That is, it has not been submitted to any other university for a degree, diploma, or diploma award. All sources of material used in this thesis have been acknowledged by citation.

Sewagegn Zewudie Tegegne	________________	________________
Name of student	Signature	Date

RECOMMENDATION

We, the advisors of this thesis, hereby certify that we have read the revised version of the thesis entitled "Development of Automatic Vehicle Pedals Lock System with GPS and GSM Tracking for Controlling Drunk Driving" prepared under our guidance by Sewagegn Zewudie submitted in partial fulfilment of the requirements for Master of Science in automotive engineering. Therefore, we recommend the submission of the revised version of the thesis to the department following the applicable procedures.

Dr. Ramesh Babu Nallamothu	________________	________________
Advisor	Signature	Date
Dr. Harish Kalla	________________	________________
Co-Advisor	Signature	Date

APPROVAL PAGE

We, the advisors of the thesis entitled "Development of Automatic Vehicle Pedals Lock System with GPS and GSM Tracking for Controlling Drunk Driving" and developed by Sewagegn Zewudie, hereby certify that the recommendation and suggestions made by the board of examiners are appropriately incorporated into the final version of the thesis.

____________________	________________	________________
Advisor	Signature	Date
____________________	________________	________________
Co-Advisor	Signature	Date

We, the undersigned, members of the Board of Examiners of the thesis by Sewagegn Zewudie have read and evaluated the thesis entitled "Development of Automatic Vehicle Pedals Lock System with GPS and GSM Tracking for Controlling Drunk Driving" and examined the candidate during the open defence. This is, therefore, to certify that the thesis is accepted for partial fulfilment of the requirement of Master of Science in Automotive Engineering.

____________________	________________	________________
Chairperson	Signature	Date
____________________	________________	________________
Internal Examiner	Signature	Date
____________________	________________	________________
External Examiner	Signature	Date

Finally, approval and acceptance of the thesis is contingent upon submission of its final copy to the Office of Postgraduate Studies (OPGS) through the Department Graduate Council (DGC) and School Graduate Committee (SGC).

____________________	________________	________________
Department Head	Signature	Date
____________________	________________	________________
School Dean	Signature	Date
____________________	________________	________________
Office of Postgraduate Studies, Dean	Signature	Date

ACKNOWLEDGEMENT

First of all, I would like to thank almighty God for giving me everything. Next, I would like to express my sincere gratitude to my teacher and advisor Dr. Ramesh Babu Nallamothu for his guidance and advice to complete this thesis. I would like to thank my co-advisor Dr. Harish Kalla for his great advice and help in designing the prototype, helping me write a program for the hardware prototype and Proteus simulation. Finally, I would like to thank my teachers, friends, and families for their significant contribution, help, support, and advice.

TABLE OF CONTENTS

LIST OF FIGURES

LIST OF TABLES

ACRONYMS

ABS	Antilock brake system
BAC	Blood alcohol concentration
BrAC	Breath alcohol content
BBR	Blood to breath ratio
CSi	Chest severity index
CG	Centre of gravity
DC	Direct current
GPS	Global position system
FMVSS	Federal motor vehicle safety standard
FHWA	Federal Highway Administration
GSM	Global System for Mobile Communication
LCD	Liquid crystal display
LSTC	Livermore Software Technology
HIC	Head injury criterion
MCECS	Microprocessor-based car engine-control system
NCAC	National Crash Analysis Centre
NHTSA	National Highway Traffic Safety Administration
RTI	Road traffic injury
SAE	Society of automotive engineering
SMS	Short Message Service
NEMA	National Electrical Manufacturers Association

NOMENCLATURE

A	Area(m^2)
a	Acceleration of the vehicle (m/s^2)
c	Position of mass centre
d	Pitch diameter (mm)
d_c	Minor diameter (mm)
g	Acceleration Due to Gravity (m/s^2)
h	Thread depth (mm)
H	Height of the C.G. of the vehicle above the road surface (m)
l	Wheel base(m)
m	Mass of the vehicle in (kg)
n	Number of engaged threads
p	Pitch (mm)
R	Normal reaction force between the ground and the wheels (N)
s	Distance (m)
t	time (s)
T	Torque required for rotate the screw (N. m)
v	Speed (m/s)
W	Load to be lifted (N)
Θ	Inclination Angle of the Road (^{o})
τ	Shear stress (N/mm^2)
φ	Friction angle (^{o})
α	Helix angle (^{o})
σ	Axial stress (N/mm^2)
σ_b	bending stress (N/mm^2)
σ_c	compressive stress (N/mm^2)
μ	Coefficient of friction between the tires and road surface

ABSTRACT

Driving by drunk drivers is one of the main causes of road traffic accidents, the number of which is increasing drastically, affecting the economy of society and the country as a whole. To minimize the collisions due to drunk drivers, a system is designed which detects the alcohol content in the air exhaled by the driver in the vehicle and automatically controls the accelerator and the brake pedals when the driver's blood alcohol level exceeds the limit. Designing the system involves, developing hardware and software programming as device modules. The hardware includes an alcohol sensor, Arduino Uno board, liquid crystal display, light emitting diode, stepper motor, motor driver, and buzzer. The program was developed by the Arduino C program and embedded into the microcontroller which receives the analog data from the alcohol sensor, analyses it and controls the car pedal system (accelerator and brake). The microcontroller compares the data it receives from the alcohol sensor and compares it with threshold limit the blood alcohol level. If the value exceeds the limit, it takes appropriate measures, such as depressing down the brake pedal and lifting the accelerator pedal to avoid the driver from driving the vehicle. Based on the recorded values, the system alerts drunk drivers and other road users with buzzer alarms and light emitting diode show warning lights. The system design considers three conditions. First, if the driver's blood alcohol concentration is less than 0.5g /l, the liquid crystal display shows the driver "NORMAL DRIVE". The pedals are operated by the driver. The buzzer and light emitting diode are off. The second is when the driver's blood alcohol concentration is greater than 0.5 mg/L and less than 0.8 g/L. The liquid crystal display the message "ALCOHOL WARNING" and the yellow light-emitting diode will continue to flash to alert the driver. Third, when the driver's blood alcohol concentration exceeds 0.8 g/L, the liquid crystal display the message "OVER DRUNK" and the stepper motor controls the pedal. The red light-emitting diode flashes continuously and the buzzer beep to alert the surrounding drivers. Global Positioning System receives the vehicle's position and Global System for Mobile sends the vehicle's position to the vehicle owner or police. Electronic design and simulation of hardware and software components modeled and simulated by Proteus software. By using LS-DYNA, the vehicle's safe speed is determined at which stopping the vehicle doesn't cause injury to the driver and passenger. When the vehicle brakes from 36 km/h, Head injury criteria, maximum chest deflection, and maximum force exerted on the femur are 983.9, 47.1 mm, and 5.42 kN, respectively. These values are below the Federal Motor Vehicle Safety Standard injury criteria limit. Finally, the developed model successfully demonstrated the functionality of the system according to expectations.

Keywords: Alcohol detection, Alcohol Sensor, Arduino Uno, Global Positioning System, Global System for Mobile, LS-DYNA,

CHAPTER ONE

INTRODUCTION

1.1 Background of the Study

Globally road traffic incidents cause 1.25 million fatalities and up to 50 million disabilities every year. About 90% of the deaths occur in low and middle-income countries even though these countries have less than half the share of the world's registered vehicles (Wegman, F. 2017). Among African countries, Ethiopia has a relatively high burden of road traffic injuries (RTI). According to the National Road Traffic Office data, 18,309 road traffic injuries occurred in Ethiopia in 2015-2016 amongst which 4,352 were fatal. It is challenging to accurately estimate the public health burden and causes of a road traffic crash in Ethiopia and other sub-Saharan African countries (Gebremichael et al., 2017). According to Ethiopia's National Road Safety Council, 81% of crashes in Ethiopia are attributed to driver error. Driver impairment is rarely recorded as a contributory factor and the traffic police have virtually no equipment to measure drug use. Drunk driving increases the likelihood of road traffic crashes and, as a result of that, fatality and serious injury. One-quarter of all road accident deaths are associated with alcohol. One-tenth of all road traffic injuries are associated with driving under the influence of alcohol (Gebremichael et al., 2017). Most of the time drivers break the prohibit rule "don't drink drive" as shown in Figure 1.1 and cause the fatality of people and loss of property.

Figure 1.1: Don't Drink Drive
(https://www.pngitem.com/middle/imhRmRx_clipart-don-t-drink-and-drive-images-png/)

A road traffic crash results from a combination of factors related to the components of the system comprising roads, vehicles, and road users, and the way they interact. The most causes of vehicle road accidents, crashes, loss of money, and death of people globally all over the world drunk driving. More often, people consume alcoholic drinks and drive vehicles. The major accidents have a common reason behind them is drunken driving. Traffic police to test the drivers whether the person is alcoholic are using nowadays breath analyzers or not. In those types of analyzers, only the level of alcohol is represented and that information is not stored for further communication (Shafi et al., 2016). Car accidents become the eighth leading cause of death, causing 1.35 million fatalities worldwide, with a rate of 18.2% per 100,000 inhabitants (Jain, A., Goyal, V., & Varma, C. 2021).. It has been widely reported that the driver had consumed alcohol increases both the risk of car accidents and the risk that they will cause severe injury or death. Globally, 21.8% of all deaths from vehicular accidents are related to alcohol, resulting in approximately 306,002 deaths (García-Echalar, A., & Rau, T. 2020). Due to drunken drivers, there are not only deaths people but also there is loss of property as shown in Figure 1.2.

Figure 1.2: Road accident
(https://www.alcoholproblems and solutions.org/geography-of-alcohol-and-drinking)

Drink-driving laws should be based on a blood alcohol concentration (BAC) limit of no more than limit. Many countries have implemented drunk driving laws to reduce alcohol-related car crash deaths. In the world, there is different standard for legal blood alcohol concentration (BAC) limit while driving. A 0.05g/dL BAC legal limit is the most common in most Western European countries. Ethiopia has 0.05- 0.08g/dL BAC legal limit as shown in Figure 1.3 (WHO, 2015).. Effective enforcement of drink driving laws is crucial in reducing the global burden of excessive road traffic accidents (Wali, B., et al., 2017).

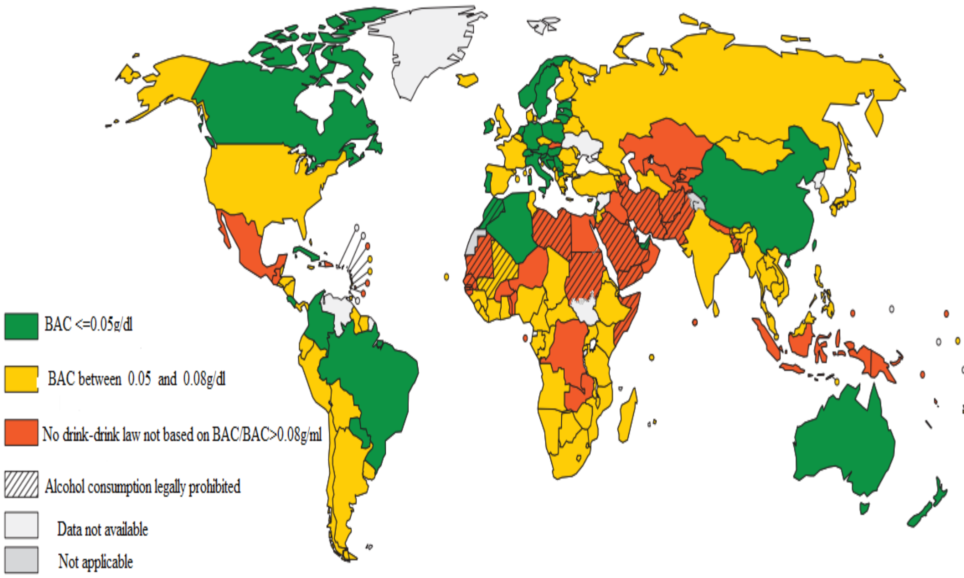

Figure 1.3: Drink-driving laws by country (WHO, 2015)

1.1.1 The effects of alcohol on driving

Alcohol negatively affects people's ability to drive immediately after drinking. When the driver is intoxicated, which endangers the lives of the driver and passengers. The following are the effect of alcohol on driving: Increases the risk of speeding up, not wearing a seat belt and recklessness, false sense of confidence and being in control, difficulty maintaining a constant speed and trajectory, and decreased attention and impaired judgment i.e. altered vision and hearing, decreased concentration, slower reaction times, poor physical coordination (Alonso, F., et al., 2015). It also increases the drowsiness of the driver as shown in Figure 1.4.

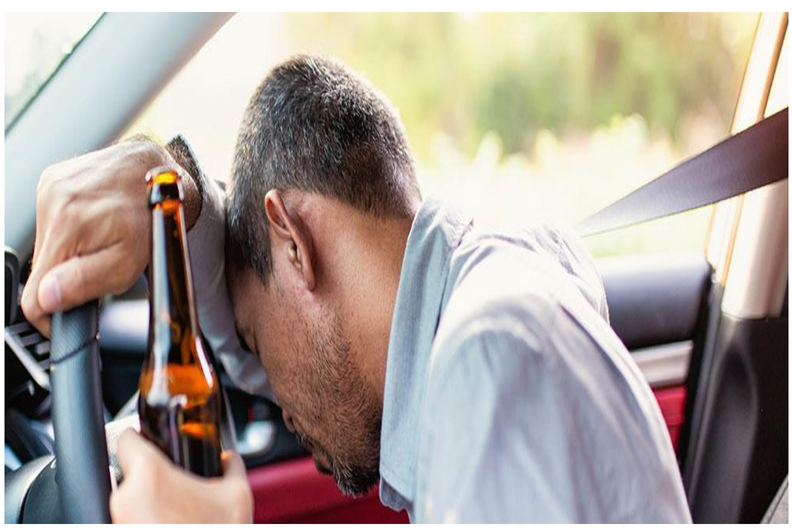

Figure 1.4: Effect of alcohol on drivers (https://www.freepik.com/premium-photo/man-drinking-alcohol-while-driving car_5444975.htm/)

1.2 Statement of the Problem

Most of the time drivers break the prohibit rule “don’t drink drive”. To control alcohol drunk drive on the road, technological innovation for alcohol detection systems is implemented in a cost-effective, efficient, and legal manner. The manual breath alcohol detection device is used by police officers to analyze the driver's alcohol level becoming more and more difficult for control drunk drivers and the breath alcohol tester increases the spread of COVID 19. The alcohol detection and engine locking system by cutting off the fuel supply and turning off the ignition. The driver can bypass the engine lock systems while starting the vehicle, because breath alcohol concentration reaches the highest level after about 45 minutes after alcohol consumption (Vukovic et al., 2015). While driving up or downhill road, the vehicle cannot be stopped by shutting off the engine. When the engine is stopped on an uphill road, the vehicle slide back and on the downhill, it accelerates due to its inertia, causing the vehicle to collision.

The main problem of instant engine shutdown by cutting off the fuel or the ignition interlock causes damage to turbocharged engines, including thermal shutdown, which leads to complete engine failure. When the engine is turned off immediately during high vehicle speeds, the steering wheel and braking system become harder because the pump has no power-assisted steering and vacuum booster driven by the engine. When the vehicle is stopped and the driver lost control, it has to stay all night on the road. Hence, it is necessary to implement GSM and GPS vehicle management systems to indicate the location of the vehicle to the vehicle owner or police station. In order to solve these problems, an automatic pedal control system for alcohol drunk drivers with GPS and GSM tracking systems was designed and developed.

1.3 Objectives

1.3.1 General Objective

The general objective of this thesis work is to develop an automatic vehicle pedal lock system with GPS and GSM for controlling the vehicle driving by drunk drivers.

1.3.2 Specific Objectives

The main objective of this thesis work is achieved through the following specific objectives:-

- To design vehicle pedal control system components
- To model the pedal control system using SOLIDWORK software.
- To study driver injuries during automatic pedal control by LS-DYNA.

- To develop GPS and GSM vehicle tracking system
- To design electrical circuits using PROTEUS software.
- To develop an Arduino program
- To develop a model for demonstration

1.4 Significance of the Thesis

The significance of this thesis work is to control drunk drivers automatically from driving of the vehicle. The implementation of this system has the following significance:

- Increases the life of the turbocharger
- Gives better maneuverability
- Improves safe driving
- Prevents traffic chaos
- Reduces the number of accidents
- Provides quick response
- Provides automated operation

The government organizations, non-governmental organizations, car owners, as well as society, and the country as a whole benefit from this work.

1.5 Scope of the Thesis Work

The scope of this thesis work is to stop the vehicle when the drunk driver tries to drive the vehicle and focuses on development of automatic pedals locking system with GPS and GSM tracking for drunk driving. This includes analysis of diver injury by using LS DYNA software during automatic pedal controlling, design of the Pedal Control components in SOLIDWORKS, develop Arduino programming code, design and simulate electric circuit by using Proteus software and finally develop a model for demonstration. The system controls the brake pedal and prevents the driver from depressing the accelerator. It also sends the location of the car to the owner or the police.

1.6 Limitations

During the execution of this thesis work, one of the main problems encountered was obtaining the specification of the output pulse of the wheel speed sensor relative to the speedometer readings. This specification is only known programmers of automotive manufacturing companies and it is a big challenge to integrate the real pulse output from the wheel speed sensor to vehicle speed.

The other problem is that the GSM module which cannot send messages due to the bandwidth of the GSM900A module which is not suitable for Ethiopia and requires additional registration with Ethio-Telecom and Information Network Security Agency (INSA) to connect to the network. However, due to the conflict in Ethiopia, Information Network Security Agency (INSA) restricted the registration of these wireless GSM modules. For experimental investigations, a fully equipped laboratory is required to verify the driver injury analysis results obtained from LS-DYNA simulations. Laboratory setup is not available for model testing. The effect of this system on the ergonomics of the driver is not studied due to a shortage of time. In Ethiopia, due to the lack of computerization and well-documented data on drunk driving accidents, identifying vehicles mainly involved in drunk driving accidents has become a difficult task. Due to the lack of laboratories, tests could not be carried out on real vehicles. The designed system cannot be applied to all types of vehicles. It must be modified according to the specifications of the selected vehicle.

1.7. Organization of the Thesis

This thesis consists of six chapters. **Chapter One** is an introduction to research. This includes research background, problem description, purpose, research importance, scope, limitations, and thesis report structure. **Chapter Two** focuses on various types of literature with a focus on research on the effects of alcohol on driving, automatic engine locking systems, driver injuries during emergency braking, GPS and GSM vehicle tracking systems. **Chapter Three** describes the materials and methods used to complete this paper. **Chapter Four** described the design and numerical analysis of pedal-controlled electric actuator components for vehicles. **Chapter Five** presents the results and considerations of software simulation. Finally, the conclusions and recommendations are included in **Chapter Six**.

CHAPTER TWO

LITERATURE REVIEW

2.1. Dynamics of Road Traffic Accidents

Globally road traffic accidents-the leading cause of death by injury and the tenth leading cause of all deaths globally. Altaf et al., 2017, estimated 1.2 million people are killed in road crashes each year, and 50 million are injured, occupying 30 percent to 70 percent of orthopedic beds in developing countries' hospitals. Road traffic accident injuries are predictable and preventable, but good data are important to understand the ways in which road safety interventions and technology can be successfully transferred from developed nations where they have proven effective. Alcohol affects the driving skills already at low levels cause for the road traffic accident. The effect is gradual, there is no sudden transition from unimpaired to impaired driving capability. An extensive review of the existing literature has been carried out, leading to the following conclusions. The fatality risk increases exponentially with the blood alcohol content (BAC) level of the driver (Altaf et al., 2017).

2.1.1 Crash rate and BAC level

The crash rate is calculated based on epidemiological studies. To estimate the relative rate for drink drivers of getting involved in a crash, the distribution of BAC levels in the entire driver population (measured in random roadside breath tests) is compared with the distribution of BAC levels among drivers involved in crashes (El Nagar & A. Y. 2017). With the aid of modern techniques, it is possible to control for even more confounding factors than in the Grand Rapids study (Safety Net Alcohol, 2009). Alcohol detection tests can measure alcohol in the blood for up to 6 hours, on the breath for 12 to 24 hours, urine for 12 to 24 hours (72 or more hours with more advanced detection methods), saliva for 12 to 24 hours, and hair for up to 90 days (Scot T, 2021). The relationship between crash rate and BAC level is graphically expressed in Figure 2.1.

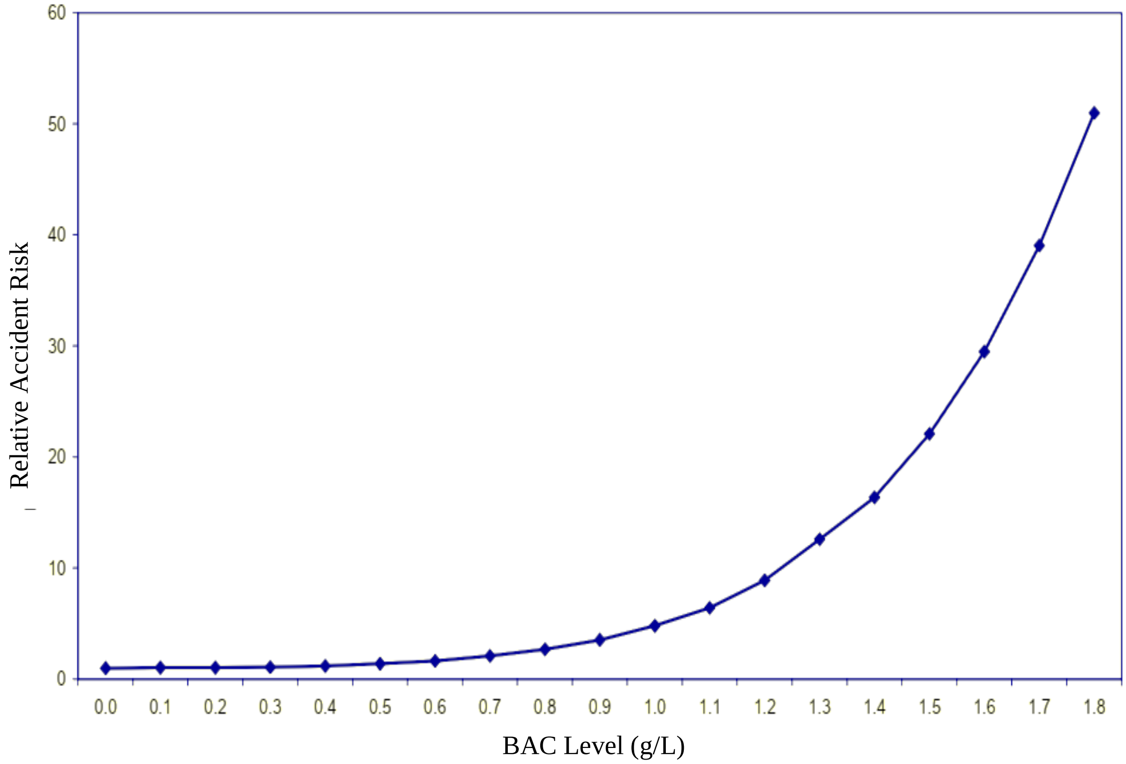

Figure 2.1: Relative accident risk rate crash Vs BAC-level (Safety Net Alcohol, 2014)

Ethiopia is one of the worst countries in the world where road transportation kills and injuries are in a large number of road users every year. In Ethiopia, traffic police reports are the official sources of data for road-related incidents. In Ethiopia, the rate of road traffic accidents is very high; because road transport is the major transport mechanism along with poor road infrastructure, poor enforcement of traffic laws, and other factors (San Hlaing et al., 2019). Like other low-income countries, the traffic controlling system is not that much supported by modern technological instruments in Ethiopia. Currently, the Ethiopia almost uses relatively simple and outdated control methods that have been in place for decades. Poor law enforcement drunk driving is the main causes of failure in Ethiopia's transport system (Ramani et al., 2013).

2.1.2 Absorption and Peak Blood Alcohol Concentration after Drinking

In many countries, before BrAC measurements can be legally performed, a waiting time of 15 minutes must be observed. Fifteen minutes between consumption of alcoholic beverage and BrAC measurement is not enough time to make the BrAC results reliable. The results show that BrAC and BAC values for all subjects have reached maximum values around 45 minutes after alcohol intake (Vukovic et al., 2015).

Under heavy intoxication resulting from drinking big amounts of alcohol has an impact on every human organ depending on blood alcohol concentration in a given time unit. After being swallowed, alcohol is quickly absorbed into the bloodstream (20% through the stomach, 80% through the small intestine), which can be observed already 5 to 10 minutes after the consumption and reaches the highest level after 30 to 90 minutes when it passes to all organs 90% of ethanol undergoes the process of detoxification in the liver (however, it concerns a given amount per hour), where it is metabolized into water and carbon dioxide the reminder is exhaled (through lungs), excreted in urine and process of perspiration (Nowak, A., & Nowak, I. 2017).

2.2 Impact of drunk driving in Ethiopia

In Ethiopia, road traffic crashes represent a major public health challenge. Driving under the influence of alcohol (drink driving) is a risk factor for road traffic crashes. Mass media campaigns can reduce the prevalence of drunk driving. Drink driving is an important factor contributing to the city's road safety crisis. From September 2013 to August 2014, analysis of road traffic crash data in Addis Ababa suggest that over half of fatal road traffic crashes are due to "reckless driving behaviour" (53.8%) and <1% are due to drink or drugged driving (0.6%) (Kebede et al., 2019). However, other studies have suggested that the prevalence of drink driving cases is as high as 9% and drink driving is significantly associated with road traffic crash injury and death in Addis Ababa (Negi, N. et al., 2020).

"Never Drink and Drive" campaign was launched in collaboration with the Addis Ababa city administration, with traffic police on the streets conducting sobriety checks and random 'blood alcohol concentration' (BAC) tests that 5.9% of the drivers stopped at sobriety checkpoints in Addis registered BAC above the legal limit (Beyene, N. 2019).

2.2.1 Alcohol Drunk Driving and BAC Limit in Ethiopia

Impairment by alcohol is a critical road safety problem as it significantly increases the risk of severe road crashes. Driving under the influence of alcohol alters both driving ability and driving behavior, and the risk of being involved in a fatal crash or incurring serious injuries also increases significantly. The risk of fatal collision could be four or five times higher among drunken drivers. In Ethiopia, the maximum alcohol level regulated by law is 0.04g/dl for breath alcohol and 0.08g/dl for blood alcohol and it is applied for all age groups. Drink-driving enforcement is implemented in Addis Ababa and to a limited extent in the Oromia Regional State. In the rest of the regions and city administration, there is no enforcement for drunk driving, due to a lack of breathalyzers and logistic and financial support. As a result, Addis Ababa has achieved more in curbing drink driving than other areas of the country, because of the Bloomberg Road Safety Initiative implemented since 2015. An assessment conducted in Addis Ababa indicates a significant reduction in drunk driving, from 9.7 percent in 2015 to 1 percent in 2019. This impressive achievement might be due to a consistent media campaign complemented by enforcement using a roadside random check. However, it is difficult to sustain the operation due to the failure of alcohol-detecting devices (breathalyzers) and calibration issues (United Nations economic commission for Africa, 2020).

2.2.1.1 Breath Alcohol Testing

There are numerous advantages of breath alcohol testing compared to blood or urine as follows:

- Breath alcohol testing is non-invasive, no needles are required as for blood samples,
- No privacy or human dignity issues, as in the collection of urine samples
- Breath samples cannot be tampered with, unlike urine samples
- Breath test results are known immediately, rather than days or weeks for blood

For these reasons, several tens of millions of breath alcohol tests are conducted globally each year, primarily by the police for enforcement of traffic safety, however also increasingly for testing of alcohol in the workplace. Therefore, this thesis work used breath alcohol testing for an automatic pedal controlling system and to reduce alcohol-impaired traffic accidents. When you drink alcohol, it goes into your stomach and small intestine. It gets absorbed into your blood, which carries it through your body and into your brain and lungs. A breath alcohol test measures how much alcohol is in the air you breathe out. The device uses that measurement to estimate how much alcohol is in your blood. That number is known as your BAC, or blood alcohol content. It may go up as soon as 15 minutes after drinking. BAC is usually highest about an hour after you drink (Wigmore J. G., 2014).

2.2.2 Measures to control alcohol drink-drive

A measure is effective when it leads to either a substantial reduction of the crash rate associated with alcohol consumption or to a substantial reduction of the number of kilometers driven while the driver is drunk (the prevalence). There is no treatment for drunk drivers that will cure them of their acute impairments. Some drivers erroneously believe that drinking coffee or drinking water after having consumed alcohol helps them to sober up. As there is no treatment possible, all measures are aimed at reducing the prevalence of drunk driving (Safety Net Alcohol, 2009).

The measures to reduce drunk driving are categorized into four separate groups. These groups:

a) **Reducing the availability of alcohol**
   - Limiting selling points, raising prices, and raising the minimum drinking age

b) **Separating drinking from driving**
   - Alcohol ignition interlocks and designated driver programs

c) **Police enforcement**
   - Legal limits and amount of (random) roadside breath tests and Sanctions

d) **Education and information**
   - Education programs on alcohol in schools and driver training, driver improvement courses (rehabilitation courses) and public campaigns and promotion of safety culture

From the above categories used to reduce drink driving separating drinking from driving most drastic measure in this category would be to make drink driving impossible for all drivers.

2.2.3 Separation of drinking and driving

a) Alcohol ignition interlocks

The most drastic measure in this category would be to make drunk driving impossible for all drivers. Such a measure is not as futuristic as it may sound. This means that drivers can only start the engine after having completed a breath test that has indicated that they are sober. It is tempting to see the installation of alcohol ignition interlocks in all cars as the panacea for the drink-driving problem. Unfortunately, there are still some technical drawbacks and inconveniences. Especially when it is cold, first performing a breath test before one can start a car; will mean that it will take several minutes before one can drive off. So far alcohol ignition interlocks are only used in rehabilitation programs for drivers with serious alcohol problems (Safety Net Alcohol, 2009).

b) Designated driver programmes

Another possibility to separate drinking from driving is not offering alcohol to drivers in restaurants, discos, pubs, bars, etc. A possible way of doing this is the so-called 'designated driver programme'. While the others drink the designated driver has to abstain from alcohol. To compensate for this inconvenience, the designated driver is very often offered free soft drinks. (Safety Net Alcohol, 2009).

2.3 Automatic Engine Locking System

This system detects the presence of alcohol in the vehicle and immediately locks the engine of the vehicle. The gas sensor measures the alcohol particles in the breath and if its concentration is found to be high, the message is displayed on LCD. If a customer sends back “STOP” message, then the microcontroller gives a signal to the motor drive, which is responsible for working with DC motors, thus the car will stop (Shivam, 2016). The system uses an MQ-3 alcohol sensor to continuously monitor the blood alcohol content (BAC) to detect the existence of liquor in the exhalation of a driver. By placing the sensor on the steering wheel, the system can continuously check alcohol levels from the driver’s breath. The ignition will fail to start if the sensors detect the content of alcohol in the driver’s breath. In case the driver got drunk while driving, the sensor will still detect alcohol in his breath and stop the engine so that the car would not accelerate any further and the driver can park by the roadside (Sahu et al., 2017). On detection of such situation, on-vehicle siren/audio alarm is activating to warn the persons on road, and vehicle control system is a trigger to lock ignition or stop the fuel inflow to the vehicle (Monisha et al., 2018). The other system which efficiently checks the accidents occurs or not and drunken driving. The system will detect alcohol through the driver's breath and stop the vehicle by interrupting the ignition, instead of directly stopping the vehicle. Implement a mechanism to cut off fuel supply instead of stopping ignition system directly because direct stop of ignition system on detecting alcohol may be dangerous as a driver driving a vehicle at a high speed and it may lead to a chance of an accident, so after cutting off fuel supply driver will place at a proper position (Altaf et al., 2017).

2.4 Effect of Automatic Braking on Driver and Passengers

When we brake a vehicle from high speed with automatic brake system occupants can be thrown against each other or against the vehicle's interior. In this condition, if an active safety system such as an anti-lock brake system (ABS) is not applied, the tire stopped rotating rapidly and the vehicle skidded. The skidding phenomenon also can be occurred during panic and emergency braking. When the driver pushes a brake pedal firmly, the speed of the tire decreases rapidly due to the inertia, and the vehicle is skidding (Liu, Y. P., 2013). The skidding phenomenon also can be occurred during panic and emergency braking. When the driver pushes a brake pedal firmly, the speed of the tire decreases rapidly due to the inertia, and the vehicle is skidding. ABS is used to initiate the pumping action, brake, and release in a split of seconds for a period of time, when triggered to avoid wheel lockup during braking which caused skidding (Zulhilmi et al., 2019). Therefore to prevent wheel locking this project work must be implemented on the vehicle with an ABS system. The anti-lock brake system is required to avoid wheel locking during braking, during emergency braking, or braking by an operational mode on the iced road, all wheels of the vehicle or some of them can be locked. ABS allows avoiding wheel locking (Nerijus Kudarauskas, 2017).

2.4.1 Injury of Driver and Passengers

Understanding human injury in automotive crashes has a significant effect on improving transportation safety. A key step to study the injury mechanism under automotive crashes is to determine the mechanical parameters such as loading conditions, stress state, and strain state that may cause injuries to the human body. Different parts of the body have different injury mechanisms; injury criteria for specified body regions have been documented and proposed for assessing the restraint system in automotive crashes (Li. N., 2014).

Head injury: which mainly concerns skull fracture and brain injury, is among the most considered injuries. Although the head skull can safely sustain a relatively large acceleration within a short period of time, compressive and shear loading due to pressure gradients may cause pain and damage to the human brain.

Neck injury: usually refers to its spinal cord fracture. Injuries of the neck spinal cord typically result from a combination of axial and bending loads. In practice, the neck could be treated as a slender column or beam and its axial force and bending moment should be carefully monitored.

Thorax injury: especially the rib cage and thoracic spine, is critical to protecting the internal organs. Fracture of the ribs or spines and impact waves could damage those thorax housed tissues. In automotive crashes, chest compression is largely due to seat belt loading.

2.4.2 Injury Mechanism

The primary cause of dysfunction and structural failure as a result of external forces acting on the human body is the relative displacement of adjacent body tissues and this, in turn, causes their deformation. Head injuries can be divided into three categories based on the type of load application and its time history (Ricci, P., 2018).

- **Impact load:** It is a collision of the head and a solid object at a high velocity. A "hard" impact will last about 1 - 3 milliseconds. A less hard impact will last about 5 - 15 milliseconds and a softer impact will last about 20-30 milliseconds.

- **Impulsive load:** The head is set in sudden motion without direct physical contact. Such a load may be in the range of 50-200 milliseconds.
- **Compressive load:** A particular load has a duration higher than 200 milliseconds. Such a load may be denoted static or quasi-static and consequences due to speed of load application may be totally neglected.

2.4.3 Injury criteria and thresholds

Previous literature has shown that the head, neck, and chest are the most frequently injured body regions injuries that are potentially life-threatening and cause a high risk of disability or even death. Explaining the proposed injury criteria and injury thresholds for these three body regions is important. The criteria adopted to evaluate the security capability are the Injury criteria of the dummy which is prescribed in the rule of CMVDR294 and the chest acceleration criteria which are prescribed in occidental regulation (Li. N., 2014).

Table 2.1: Injury Criterions (Li. N., 2014)

Injury criterions	Requirement
HIC_{15}	$\leq$700
HIC_{36}	$\leq$1000
Chest deflection	$\leq$63 mm
Neck force	Axial tension <400 N, axial compression, 3300 N, and shear 3200 N
Femur force	10 kN

HIC_{15} and HIC_{36}

For any two points in time, t_1 and t_2, during the event which are separated by not more than a 15 millisecond time interval and where t_1 is less than t_2, the head injury criterion (HIC_{15}) shall be determined using the resultant head acceleration at the center of gravity of the dummy head, $a_{(t)}$ expressed as a multiple of g (the acceleration of gravity) and shall be calculated using equation (2.1). The US National Highway Traffic Safety Administration (NHTSA) final specifies the maximum time for calculating the HIC value (t_2-t_1) as 15 milliseconds (HIC_{15}) and HIC value (t_2-t_1) 36 milliseconds (HIC_{36}) (Mihradi et al., 2017).

$$HIC=\left\{\left[\frac{1}{t_2-t_1}\int_{t_1}^{t_2} a(t)dt\right]^{2.5}(t_2-t_1)\right\} \qquad \text{Eq. 2.1}$$

$$a(t)=\sqrt{a_x^2+a_y^2+a_z^2} \qquad \text{Eq. 2.2}$$

Where: a(t) is the resultant linear acceleration time history (G's) of the center of gravity of the head, and t_1 and t_2 is the interval between every 36 milliseconds or 15 milliseconds of the crushing process which produced the maximal HIC. C3ms is the 3ms criterion of chest acceleration.

A dummy equivalent of the HIC value, denoted by HIC (d), is given as

$$HIC(d)=166.4+0.75446\times HIC \qquad \text{Eq. 2.3}$$

2.5 GPS and GSM Vehicle Tracking System

When the alcohol-drunk driver tries to drive a vehicle after the consumption of alcohol, the engine of the vehicle will be automatically locked. Using the GPS module, we can track the position of the vehicle and it sends a message by using GSM to the registered number (Ranjani et al., 2018). A system that incorporates GPS and GSM for providing accurate locations. The coordinates of the location of the vehicle are sent via GPS. Vehicle tracking and locking system installed in the vehicle, to track the place and locking engine motor. The place of the vehicle was identified using the Global Positioning System (GPS) and Global system mobile communication (GSM). When a vehicle gets locked the detailed location of the vehicle is sent immediately to the concerned authorities (N. Shankar & B.Indurani, 2018).

2.6 Effect of engine shut-off from running on engine system and components

The previous works on automatic engine locking system by ignition interlock or fuel cut off valve mostly works for the driver who drinks alcohol outside of the vehicle and tries to start. However, the automatic engine locking system did not allow to start of the vehicle and it will also work if the alcohol sensor detects the presence of alcohol and suddenly shut off the engine from running. This sudden shut-off of the engine will cause damage to engine components, especially for turbocharged engines. Immediate hot shut down of the engine is a common cause of oil starvation or lack of oil. In lack of lubrication, extreme wear will tend to scoring on the internal bearing surfaces. The turbine shaft will typically show signs of discoloration and even metal transfer from the bearing to the shaft (Miller J. K., 2018). The typical symptoms of a lack of lubrication failure during a hot shut-off engine include:

- Severe shaft discoloration
- Journal bearing discoloration

- Journal bearings seized to the turbine shaft
- Journal bearing hammered out
- Thrust bearing wear and discoloration
- Shaft fracture, typically at the turbine end
- Sludge or coke buildup in bearing housing from hot shutdowns

Another problem with turning off the engine is that the power-assisted braking system becomes stiff and difficult to stop the vehicle (James D. & Mitchell C., 2019). The brakes of modern passenger cars are equipped with hydraulic boosters. The brake fluid is pressurized with a pump driven by the car engine. When the engine is stopped, the pressure in the chain drops rapidly, so the braking force is only generated by the pedal. Therefore, the brake works, but it is less effective, and the pedal feels heavier when the engine is off. Most vacuum-operated brake boosters draw a vacuum from the engine's intake manifold. The engine is essentially a large air pump. This is because the piston moves up and down in the cylinder to deliver air and fuel and release exhaust gas. The vacuum booster uses the pressure difference to increase the braking force. A typical booster has a force chamber, which is divided into two small chambers by a flexible diaphragm. (James D. & Mitchell C., 2019).

The shut-off engine while the vehicle is running has a problem of hard steerability. The power steering system mainly consists of a centrifugal pump to pump steering oil which gets power from the crankshaft of the engine. If the ignition is turned off, it means the crankshaft is not running, and hence the pump doesn't get power from the crankshaft, and there is no pumping of oil, whose pressure is used to steer the wheels. Then when we turn the steering wheel while the engine is not running (ignition turned off) our effort is only applied to steer the wheels and hence it becomes harder than when the engine is running (Owen C. and Erjavec j., 2018).

2.7 Arduino programming software

Arduino is an open-source programmable circuit board that can be integrated into a wide variety of maker space projects both simple and complex. This board contains a microcontroller that can be programmed to sense and control objects in the physical world. Because of its flexibility and low cost, Arduino has become a very popular choice for makers. Arduino was introduced back in 2005 in Italy by Massimo Banzi as a way for nonengineers to have access to a low-cost, simple tool for creating hardware projects (N. Shankar & B.Indurani, 2018).

Arduino programming has the following advantages

- Inexpensive and cross-platform
- a simple, clear programming environment
- Open source and extensible software and open source and extensible hardware.

2.7.1 Types of Arduino boards

There are different Arduino boards which are following

- Arduino UNO, LilyPad Arduino, Red Board, Arduino Mega, and Arduino Leonardo

From the above different types of Arduino boards, Arduino Uno is an inexpensive decent little microcontroller, with a simple (and simplistic) IDE, easy programming, and plenty of hobbyist support and add-on parts for experimentation than others. However, its processor is low, and several pins minimum than others.

2.8 Proteus Software

Proteus is a complete development platform from product concept to design completion. Its advantages are intelligent principle layout, hybrid circuit simulation, accurate analysis, single-chip software debugging, single-chip and peripheral circuit co-simulation, PCB automatic layout and wiring. Proteus software is a complete embedded system software and hardware design simulation platform. Proteus is very suitable for skill evaluation and electronic competition. It is necessary and difficult to evaluate the skills of a single-chip microcomputer. Proteus can provide all the resources needed for the test, directly evaluate the correctness of hardware circuit design, directly debug the software with hardware schematic diagram, verify the function of the whole design, and test controllable, easy to evaluate, and easy to implement. There are widely practical used cases from Proteus (Fan, C. et al., 2018). The following Table 2.5 explains the advantages of Proteus Virtual Laboratory.

Table 2.2: Advantages of Proteus Virtual Laboratory (Fan, C. et al., 2018)

Hardware experiment	Proteus VSM experiment
Different hardware devices are needed	Just a general computer
Needed to configure several expensive hardware.	Support a variety of CPU simulations.
It requires a lot of test equipment purchase	It contains 13 kinds of virtual instruments
Mistakes lead to equipment losses.	Proteus VSM secures a virtual environment.
It is not easy to configure	It is convenient and quick.

2.9 System Components

The automatic vehicle pedal controlling system of this thesis consists of the following electronic components that are integrated into the conventional brake system components to make an automatic brake system.

2.9.1 Arduino UNO Microcontroller

Arduino is a flexible, programmable hardware platform designed for artists, designers, artisans, and craft makers. Arduino is small; a blue board, the name of which is mythically derived from a local pub in Italy (Viral M et al., 2018). One of the most popular Arduino boards on the market. See Atypical Arduino Uno in Figure 2.3. While this was not the first board to hit the market, it remains the most widely used and widely documented on the market. Due to its extreme popularity, the Arduino Uno has many project guides and forums on the internet that can help you get in or out of traffic. Plus, it has great features and ease of use (N. Shankar & B.Indurani, 2018).

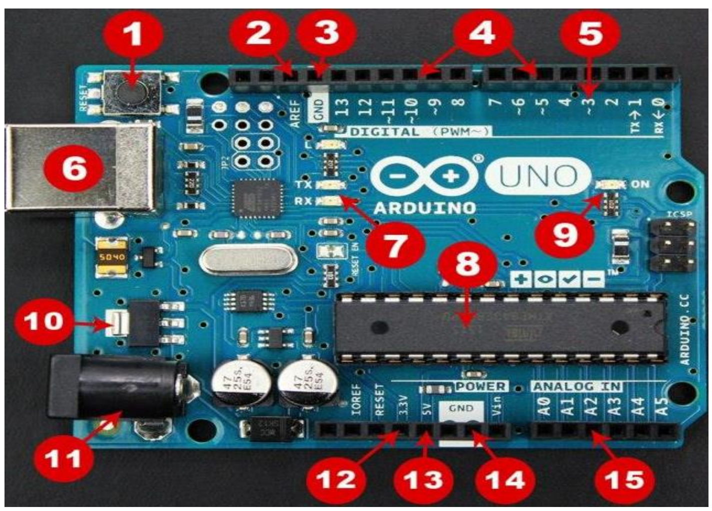

Figure 2.2: Arduino UNO board (Evans B., 2011)

2.9.2 Arduino Breadboard

Another very important component when working with an Arduino is a solderless breadboard. This device allows you to prototype an Arduino project without permanently soldering the circuit together. Using a breadboard allows you to create temporary prototypes and experiment with different circuit designs. Inside the holes (attachment points) of the plastic casing, there are metal clips connected to each other by strips of conductive material.

2.9.3 Alcohol Sensor

MQ3 alcohol gas sensor is made of SnO2 material, which has low conductivity in clean air. Whenever it is close to the alcohol gas, it will begin to conduct highly according to the gas concentration. Therefore, the user can use any microcontroller to sense the difference in output voltage and detect the presence of alcohol. See the typical MQ3 alcohol gas sensor in Figure 2.4.

Figure 2.3: MQ3 Alcohol sensor (Gbenga et al., 2017)

2.9.4 GSM Module

It is a device, which can be used to make a computer or any other processor communicate over a network. It can accept any GSM network operator SIM card as a mobile phone with its unique phone number. Whenever alcohol consumption is detected then the message will be sent to relatives and police stations with car numbers as well as location using GPS. A GSM modem is a special type of modem. It accepts the SIM card and operates the user's mobile phone number through the network, such as a mobile phone (Ramani et al., 2013). See typical GSM as shown in Figure 2.5.

Figure 2. 4: GSM module (Ramani et al., 2013)

2.9.5 GPS Module

This is a global positioning system used to locate a vehicle by latitude and longitude. When alcohol consumption is detected, the vehicle's location is tracked. The Global Positioning System (GPS) is a satellite-based navigation system consisting of a network of 24 satellites in orbit. GPS is suitable for any weather around the world. Under normal circumstances, there is no subscription fee or system fee for using GPS. The GPS receiver must acquire the signals from at least three satellites to estimate the 2D position (latitude and longitude) and to track the movement. When four or more satellites are visible, the receiver can determine the 3D position of the user's latitude, longitude, and height (Ramani et al., 2013). See typical GPS as shown in Figure 2.6.

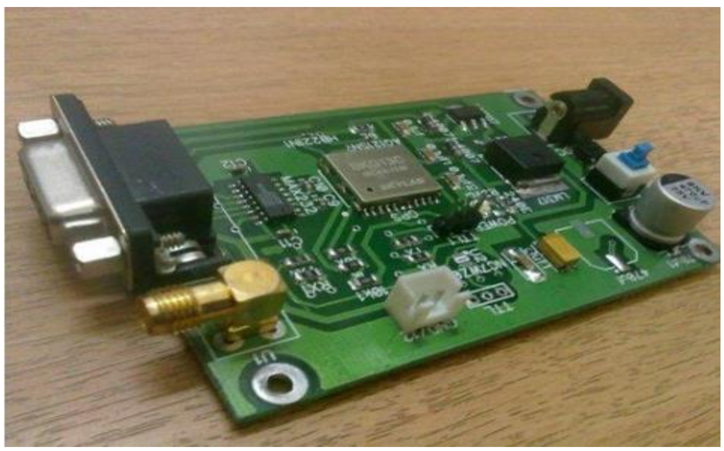

Figure 2.5: GPS module (Ramani et al., 2013)

2.9.6 LCD Display

It acts as an indicator to the driver and for the passengers. It indicates that the driver has drunk; it also displays a warning message to stop the vehicle. The LCD display is fitted inside the car and this LCD display acts as an indicator to the driver and other people who are sitting inside the car. As shown in Figure 2.7, the LCD displays the alcohol level detected by the alcohol sensor and also warns the driver to stop the car or vehicle for a certain amount of time after the car stops automatically, and indicates that smoke/gas is detected in the car (Shivam, 2016).

Figure 2.6: LCD display (Shivam, 2016)

2.9.7 Buzzer

A buzzer is used in the system to alert the people nearby so that they can analyze the situation and take necessary action accordingly. It is activated whenever the MQ3 sensor detects alcohol. Its frequency and tone can be changed and used according to the requirements. Hence, it is an easy and cheap way to alert people and grab attention to point out that something is wrong (Shinde et al., 2018). See the typical buzzer as shown in Figure 2.8.

Figure 2.7: Buzzer (Shinde et al., 2018)

2.9.8 A4988 Stepper Driver Module

The stepper motor unit controls the operation of the stepper motor. Stepper motors send current to a stepper motor through different phases. The A4988 NEMA 17 stepper motor is a small stepper driver unit that is used to control bipolar stepper motors. This driver unit has a built-in compiler so you can control the stepper motor with a few pins from the controller (Ashish C, 2019). See typical A4988 Stepper Driver Module as shown in Figure 2.9.

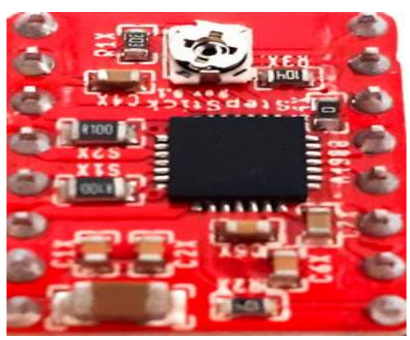

Figure 2.8: A4988 Stepper Driver Module (Ashish C, 2019)

3.9.9 Light Emitting Diodes (LED)

LED is a small lamp (it stands for "light-emitting diode"), and its working power is relatively small. The LEDs have polarity, which means they will only light up when you position the legs correctly. The long leg is usually positive and should be connected to a digital pin. Arduino board. The short leg is grounded; this side of the LED bulb usually also has a flat edge. It only takes a few lines of code to blink the LED (Yonas W, 2021).

These LEDs are used to notify the surrounding road drivers there is a problem within the vehicle. See typical LED in Figure 2.10.

Figure 2.9: Light Emitting Diodes (Yonas W, 2021)

2.9.10 Power supply of system components

For the real model, electricity from the vehicle battery is used to power the MQ3 alcohol sensors, microcontroller, LCD, buzzer, stepper motor, and other electronic circuit components. In this system, the stepper and buzzer need a 12V DC supply, while the microcontroller, MQ3 sensor, GSM, GPS module, and LCD use a 5V DC supply. The system is normally powered by the car battery when it is installed in the vehicles. For demonstration purposes, 9V DC is used by MAXDAY ALKALINE for stepper motor and buzzer instead of the car battery, and 5V DC is used by the laptop for the microcontroller, MQ3 sensor, and LCD.

2.9.10.1 Voltage Regulator

The 78xx series (L78xx, LM78xx, and MC78xx) is an independent series of integrated circuits with a fixed linear regulator. Replace xx with two digits to indicate the output voltage (for example, the output of 7805 is 5 V and the output of 7812 is 12 V). The LM7805, like most other regulators, has 3 pins (Mohammed M, 2016).

- **Pin 1 (input pin):** the input pin is the pin that accepts the incoming DC voltage, which the voltage regulator will eventually regulate down to 5volts.
- **Pin 2 (ground pin):** ground pin establishes the ground for the regulator.
- **Pin 3 (output pin):** the output pin is the regulated 5Volts DC. This is required for some components to operate with 5volts.

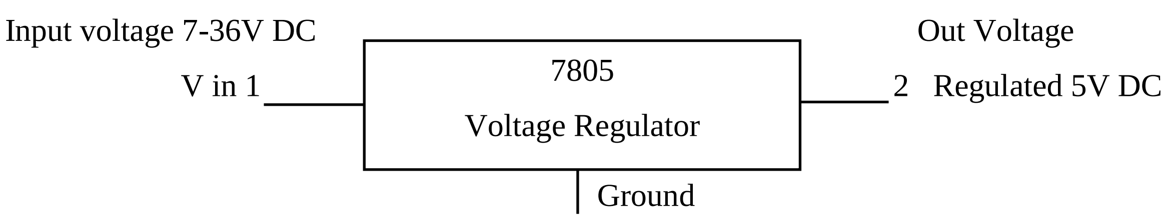

Figure 2.10: Voltage Regulator pins

This voltage regulator can accept an input voltage of 36 Volts, it is recommended to limit the voltage to 2-3 Volts higher than the output regulated voltage. For a 5-Volt regulator, no more than 8 volts should be applied as the input voltage. The difference between the input and output voltage appears as heat. The greater the difference between the input and output voltage, the more heat is generated. See the typical L7805 Regulator as shown in Figure 2.12.

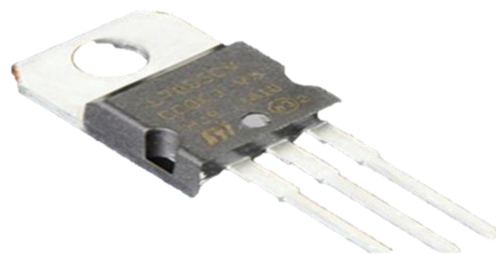

Figure 2.11: L7805 Regulator (Mohammed M, 2016)

2.9.10.2 Transistor

Transistors are semiconductor devices used to amplify and switch between electronic signals and power. NPN transistors can be used in two different modes: forward bias mode and reverse bias mode. In forward bias mode, the current can easily flow. Therefore, it acts like a closed switch. However, in reverse bias mode, the current through it is virtually zero, so it acts as an open switch. Therefore, in this project, the transistor is used in the relay driver circuit and acts as a switch to deactivate the relay as a result of the base current triggered by the alcohol sensor when alcohol is detected and the buzzer is activated (Mohammed M, 2016).

2.9.10.3 Resistor

A resistor is a passive two-end electrical component, and the resistor is implemented as a circuit component. Electronic circuits use resistors to reduce current, regulate signal levels, divide voltage, bias active components, and terminate transmission lines. High power resistors can dissipate watts of electrical energy in the form of heat and can be used as part of a motor control, power distribution system, or generator test load. The resistance of a fixed resistor varies slightly with temperature, time, or operating voltage. Variable resistors can be used to tune circuit elements (such as volume controls and dimmers) or as heat, light, humidity, force, or chemical activity detection devices.

2.9.11 Vehicle Speed Sensor (VSS)

The vehicle's sensors are driven by gears located on the transmission output shaft. The output gear always meshes with the drive gear located on the output shaft. The vehicle speed sensor generates a magnetic pulse in a waveform proportional to the vehicle speed. The power control module (also called the electrical control module) uses VSS frequency signals to control several electrical subsystems in the vehicle. VSS is connected to the speedometer cable and is located between the axle and the wheels of the vehicle. The most common VSS type uses a magnet attached to the back of the gearbox housing behind the speedometer. The top of the VSS captures the output of the transmission. Its opposite side is connected to a rotating magnet that creates a voltage. This voltage is then transmitted to a computing device that calculates the speed proportional to the moving vehicle (Crolla D, 2019).

Figure 2.12: Wheel speed sensor (https://www.apogeeweb.net/article/22.html)

2.10 General summary of literature review and research gaps

From the literature reviews the police use manual breath alcohol detectors to analyze breath alcohol levels, detect alcohol consumption and punish guilty drivers. However, it is becoming more and more difficult for the traffic police to control these drivers. An automatic fuel shutoff valve or ignition lock can also be used to automatically lock the engine to a drunk driver, thereby preventing the driver from starting the engine. However, breath alcohol and blood alcohol levels reach their highest levels in about 45 minutes and reach all organs after drinking (Vukovic et al., 2015). Due to this delay, the driver can pass this engine lock system when the vehicle starts. However, cutting off the fuel supply and switching off the ignition system (ignition lock) cannot stop the vehicle immediately and result in a collision or a rollover due to the inertia of the vehicle. On uphill and downhill roads, the vehicle cannot be stopped by turning off the engine. When the engine is turned off on an uphill road, the vehicle skids backward and accelerates forward down the hill. Nowadays, all mass-market vehicles come with oil-cooled turbine engines in which the oil dissipates heat and prevents bearing damage. The main problem of instantaneous engine shutdown by cutting off the fuel or ignition interlock causes damage to turbocharged engines, including thermal shutdown, causing complete engine failure (Miller J. K., 2018). When the engine is immediately turned off during high vehicle speeds, the steering wheel becomes stiff because there is no power to assist steering is driven by the engine. There is also another problem of brake becoming harder when the engine is turned off. So, a system is necessary to help solve these problems.

CHAPTER THREE

MATERIALS AND METHODS

3.1 Materials

The materials and equipment used in this thesis work are listed in Table 3.1 the detailed explanation of which is given in chapter two section 2.6.

Table 3.1: List of materials

Item	Unit	Quantity
Arduino Uno microcontroller	Set	1
GPS module	Pc	1
GSM module	Pc	1
Stepper motor	Pc	2
Motor driver	pc	2
Alcohol sensor	pc	1
LCD display	pc	1
Buzzer module	Pc	1
Resistor	pc	2
NPN transistor	pc	1
Light Emitting Diode(LEDs)	Pc	2
Wheel speed sensor	pc	1
Voltage regulator	pc	1
Circuit wires/jumper wire/	Pc	

3.2 Methods

The main data sources for this thesis work were primary and secondary data. Most of the thesis work data collection methods were based on the collection of secondary data. However, primary data observation and oral questions were used at some places where accidents occurred during the study. It motivated me for continuing with this work and collecting the secondary data. Secondary data was obtained from the Ethiopian federal Police commission, Addis Ababa police commission, and the Ethiopian Federal Transport Agency. Moreover, different books, journals, articles, and reports publications were also referred. Literature survey about the different types of automatic engine locking systems and vehicle tracking systems is the key step in the methodology of this thesis work. After reviewing the literature, the design of an appropriate automatic pedal locking mechanism was carried out by using SOLID WORKS and proto type for demonstration. The overall methodology followed in achieving the objectives of this thesis work is illustrated in Figure 3.1 in the form of a flowchart.

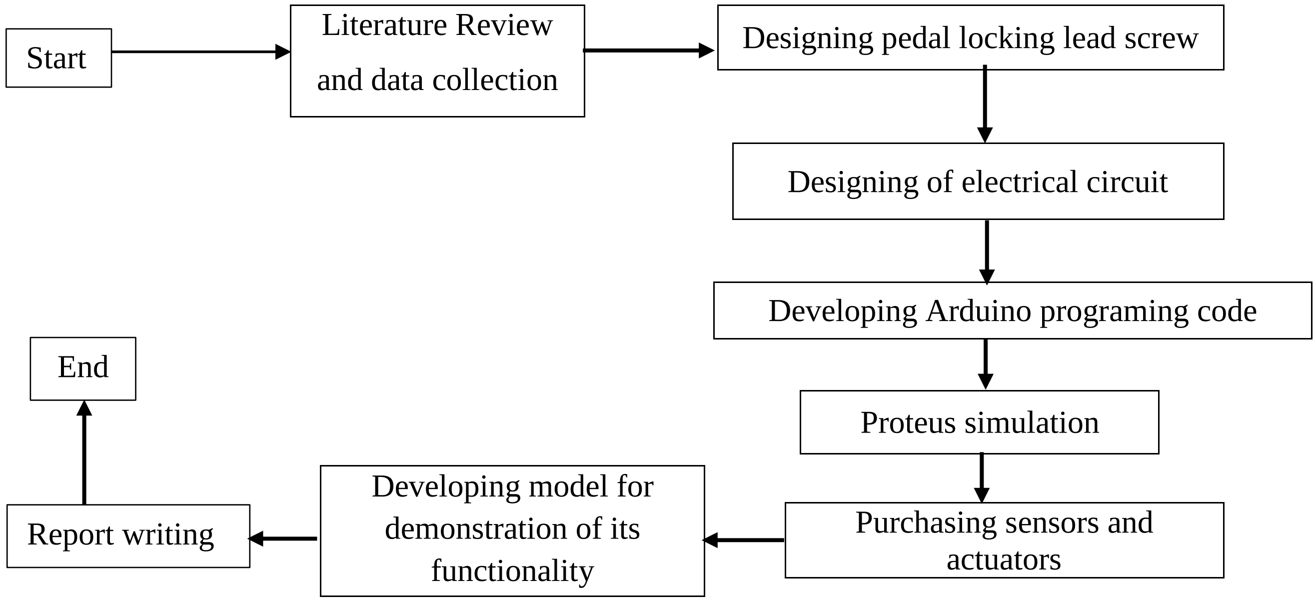

Figure 3.1: Methodology of the thesis work

3.2.1 Working principle of the system

The system consists of hardware parts controlled by software programming. The hardware is mainly composed of Arduino UNO microcontroller, MQ3 alcohol sensor, liquid crystal display, L293D motor driver, stepper motor, vehicle speed sensor, GPS module, and GSM module, as shown in Figure 3.2.

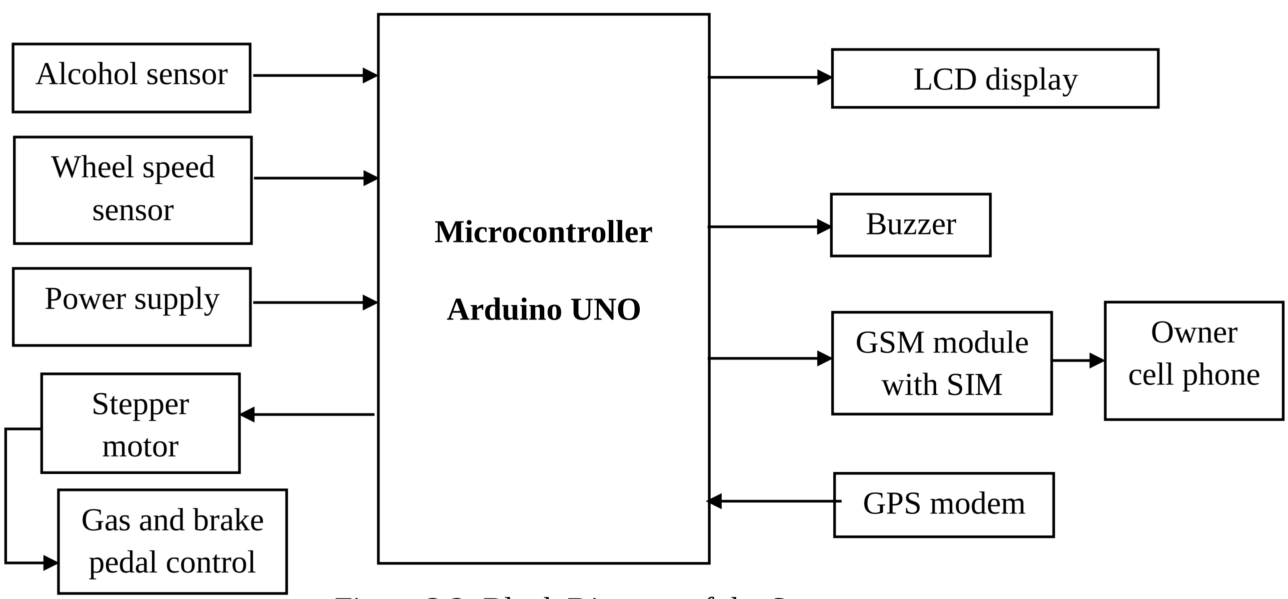

Figure 3.2: Block Diagram of the System

The working principle of the automatic pedal locking system is as shown in Figure 3.3.

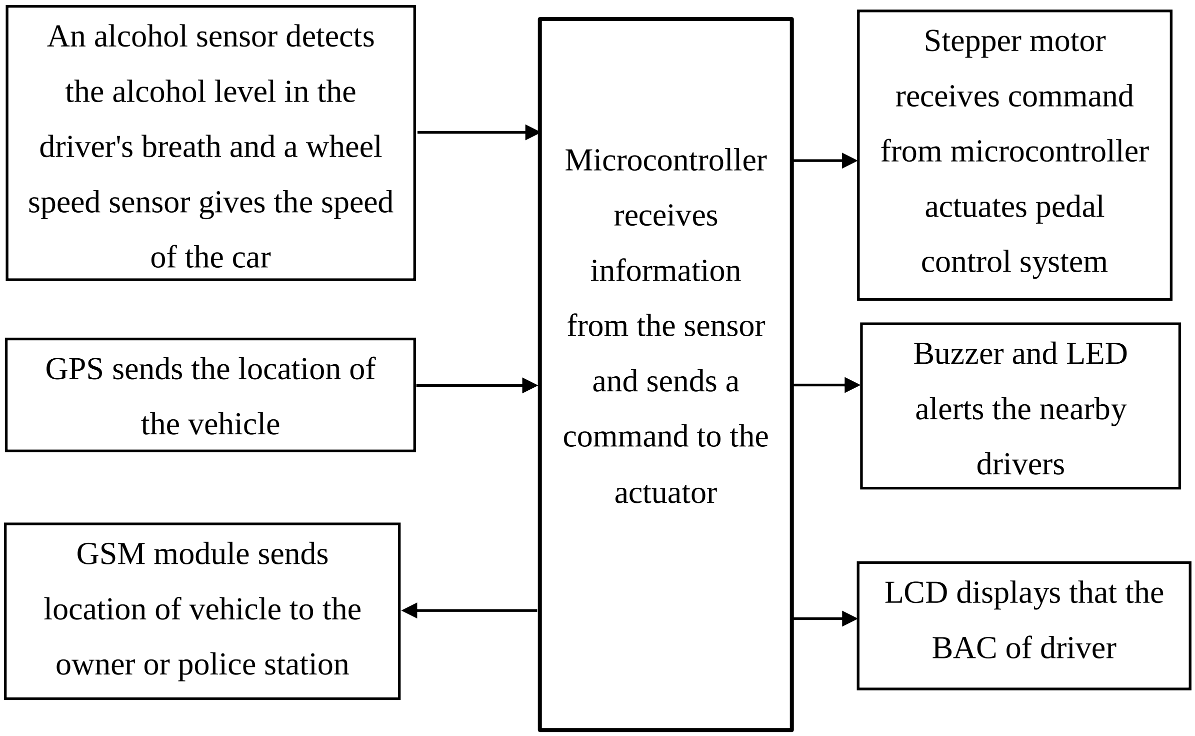

Figure 3.3: Working principle of the system

3.3 Analysis of Raw Data

3.3.1 Road accidents in Ethiopia

The study started with a compilation and review of existing literature on road safety in Ethiopia, as well as publications on road safety worldwide. In recent years, the number of deaths and serious injuries in road traffic accidents has increased annually. Trends show that road accidents have become an economic, social, and health burden for the country. Ethiopia's Federal Police Commission reported 2,161 fatalities nationwide in 2007, and more than doubled to 4,597 in 2018. Motor vehicle-related pedestrian road traffic collisions are a major road safety challenge. According to the World Health Organization, they cause nearly a quarter of all road traffic-related deaths. Accidents are 70 times more likely to occur in developing countries than in developed countries. Moreover, the vast majority of road traffic deaths are from vulnerable road users, such as pedestrians and drivers. In Africa, pedestrian deaths are also a major problem, with road traffic accidents accounting for an estimated 39% of all deaths in Tanzania, 75% in Côte d'Ivoire, and 85% in Ethiopia (Liu, Y. P., 2013).

According to the total traffic accident statistics of the Ethiopian Federal Police Commission for the past eight years, traffic accidents are serious and cause a gradual increase in deaths, seriously injured, slightly injured, and property damage. As per the eight years report, the aggregated summary is shown in Figure 3.4.

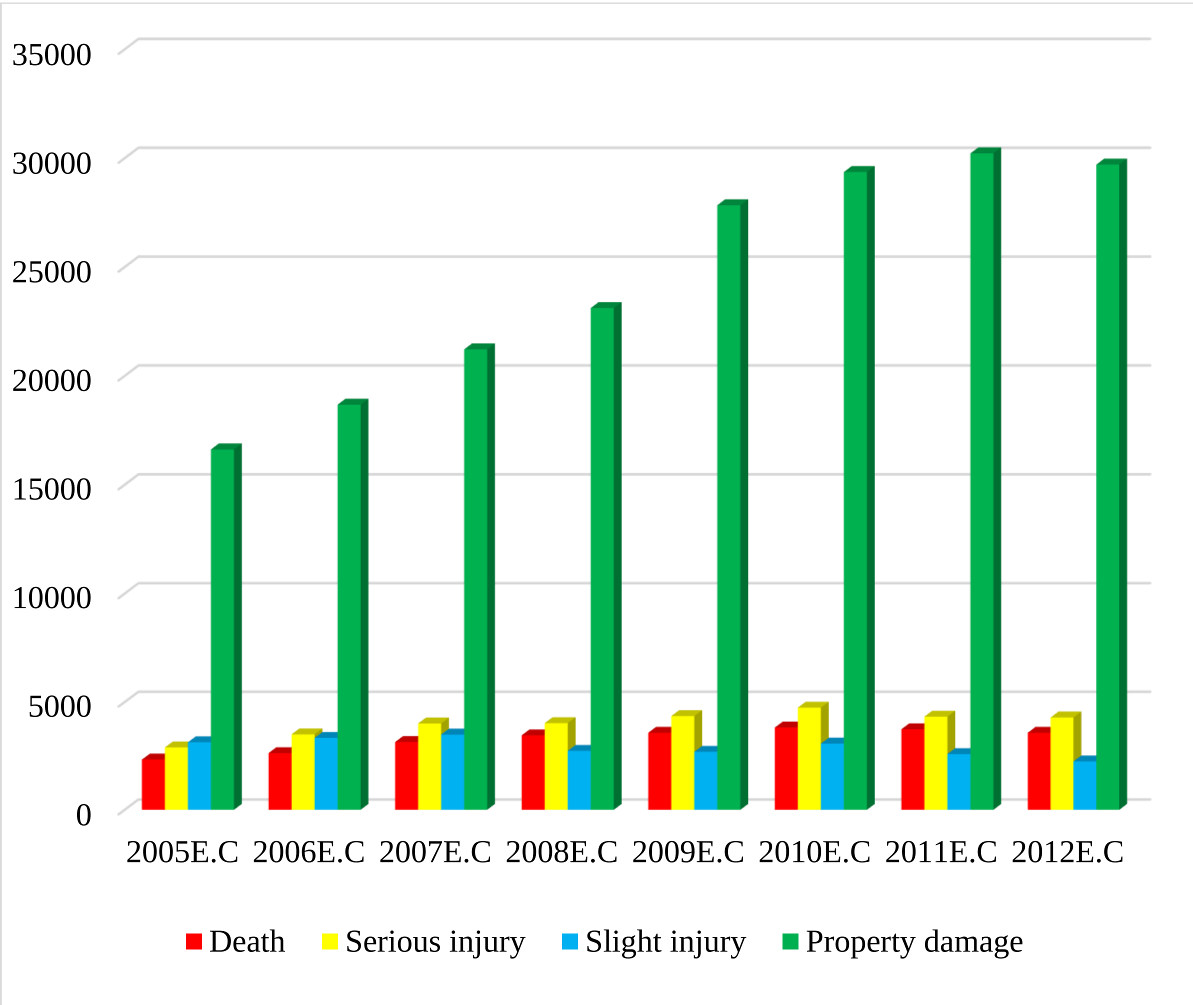

Figure 3.4: Eight years aggregate traffic accident report analysis in Ethiopia (Ethiopian Federal Police Commission, 2021)

According to the report, all parameters are increasing year by year. This shows that the traffic accident in Ethiopia is very serious and needs to be taken seriously. According to the Ethiopian Federal Police Commission's annual static data report on total road accidents, road accidents are serious and cause increasing property damage. As a result of these accidents, Ethiopia has lost millions of dollars in property. The type of vehicle needs to be identified, and the frequency of its involvement in traffic accidents is increasing rapidly year by year. According to the Federal

Police Commission's report, Figure 3.5 provides a summary of road traffic accidents over the past seven years by vehicle type.

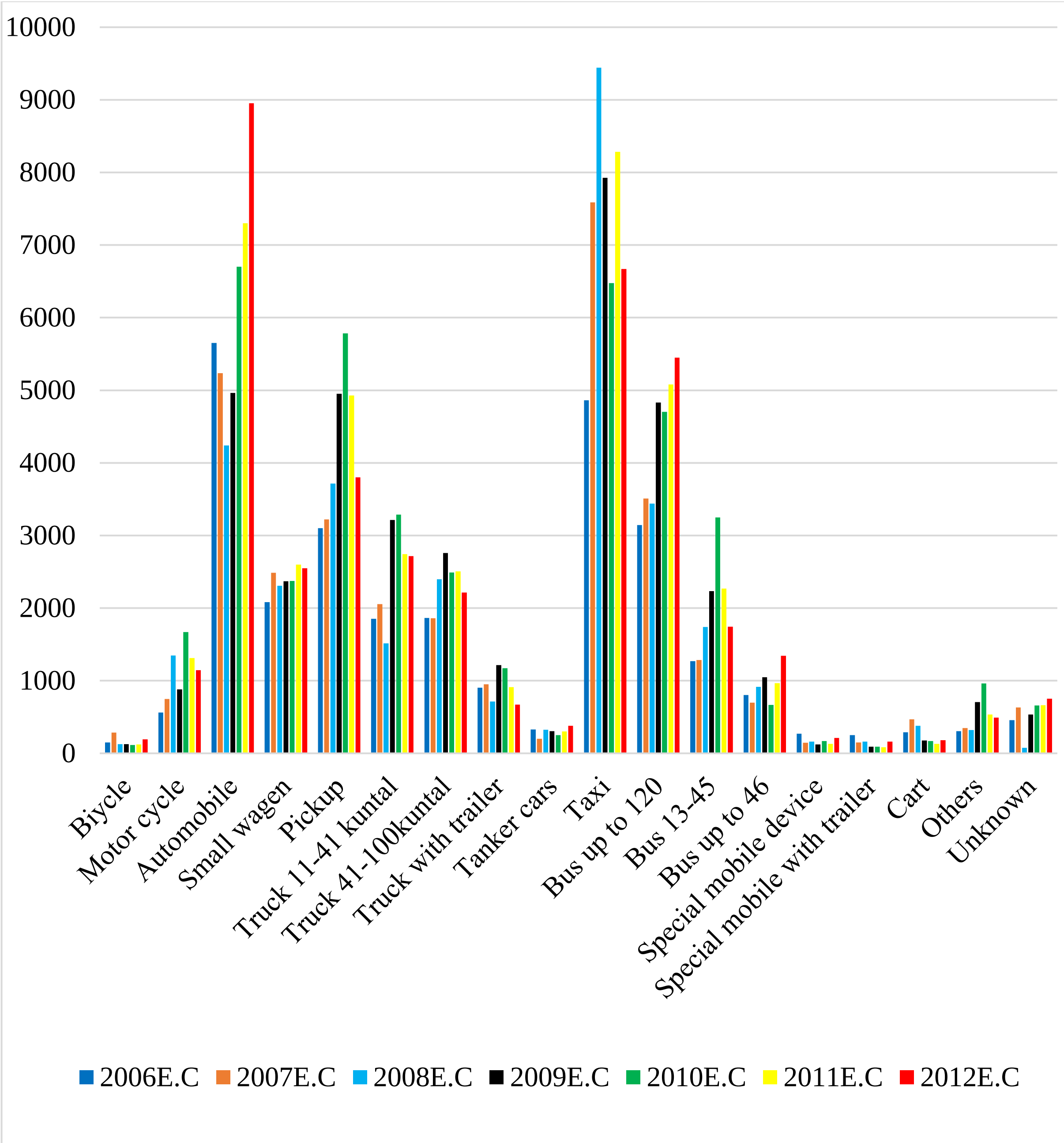

Figure 3.5: Seven years aggregate traffic accident report based on the types of vehicles in Ethiopia (Ethiopian Federal Police Commission, 2021)

Figure 3.5 shows that the proportion of automobiles and taxis has been high over the last seven years, with pickups and buses with up to 120 seats accounting for a significant proportion of road accidents. Between 2007 and 2008, there were more taxi accidents than car accidents.

However, over the last three years, car accidents have increased and taxi accidents have decreased. According to traffic police observations, most drunk driving accidents occur at night. According to seven years of statistical data, the proportion of deaths, serious injuries, minor injuries, and property losses in the automobiles category is higher than that of other types of vehicles. It is also necessary to prove traffic accidents based on the number of deaths, injuries, and property damage caused by automobiles in Ethiopia. According to the Federal Police Commission's report, Figure 3.6 shows a summary of automobiles accidents over the past nine years. It shows that in the past nine years, automobiles have been largely involved in road traffic accidents. Therefore, there is a need to find ways to reduce automobile traffic accidents.

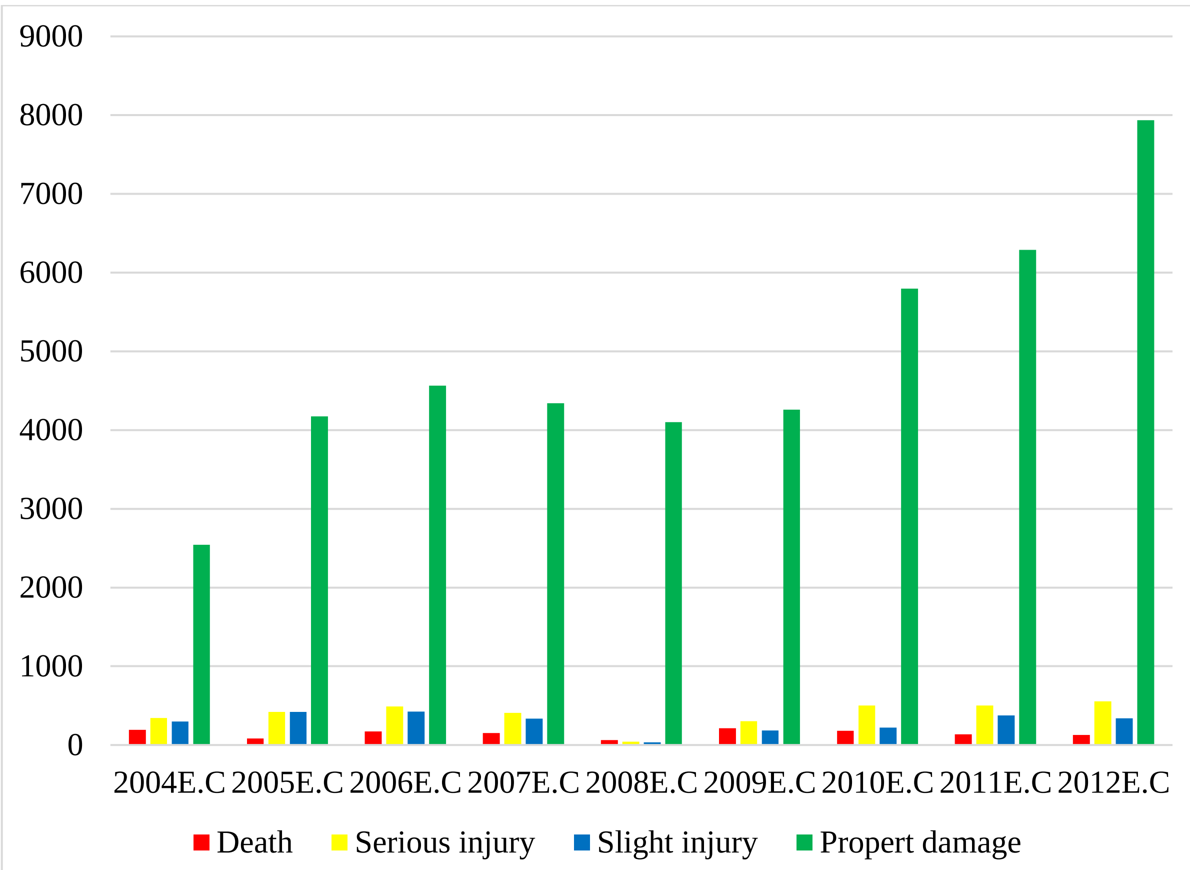

Figure 3.6: Ten years Automobile cars traffic accident report analysis in Ethiopia (Ethiopian Federal Police Commission, 2021)

Figure 3.7 given shows the maximum number of automobiles were registered in Addis Ababa. Therefore it is necessary to study drunk driver accidents in a state of intoxication in Addis Ababa more feasible than in other regions.

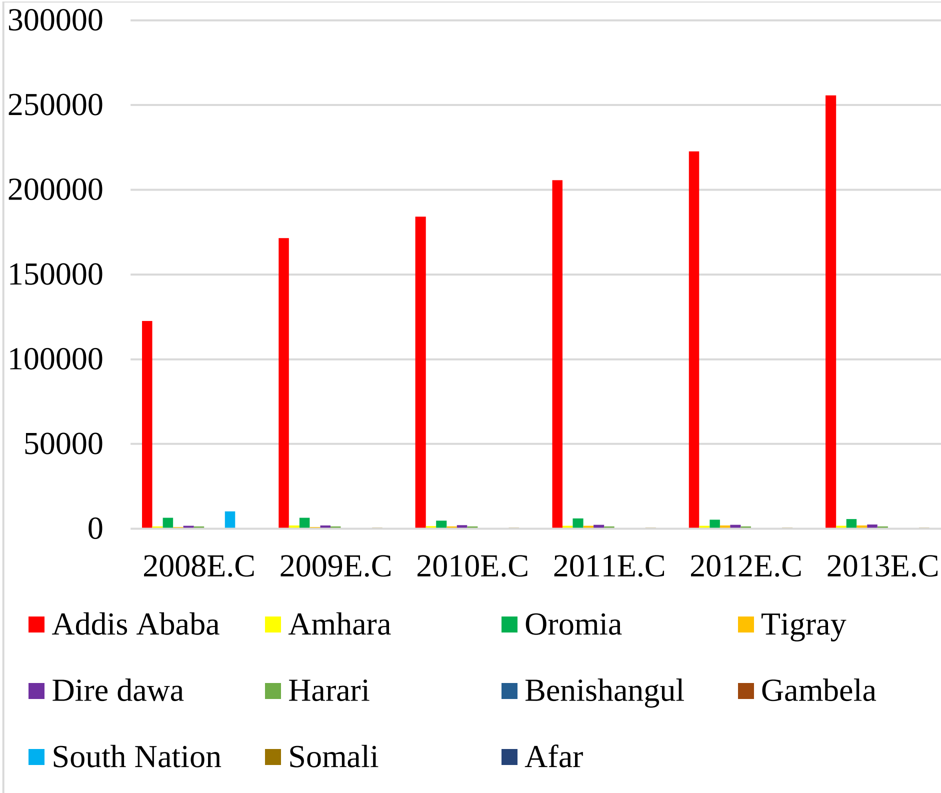

Figure 3.7: Number of automobiles registered by region in Ethiopia (Ethiopian Federal Police Commission, 2021)

3.3.2 The Breath Alcohol Testers in Addis Ababa city

In most countries, 0.08 grams of alcohol per 100 ml of blood (BAK 0.08 g/dL) (Beyene, N. 2019). It is the legal limit that a driver would be considered if they legally exceeded it while intoxicated. Any driver with a concentration greater than 0.08 g/dL may be considered a driver under the influence or the influence of alcohol and should not be allowed to drive. The level of alcohol in the blood can be determined with the help of an alcohol tester (Beyene, N. 2019). According to the Addis Ababa Police Commission report, the police routinely conduct breath alcohol tests on drivers in different sub-cities of Addis Ababa. It is necessary to display the number of drivers who attempt to drive while under the influence of alcohol. The Addis Ababa Police Commission reported that there was an aggregated summary of drunk drivers in various Addis Ababa sub-cities for a period of three years as shown in Figures 3.8, 3.9, and 3.10.

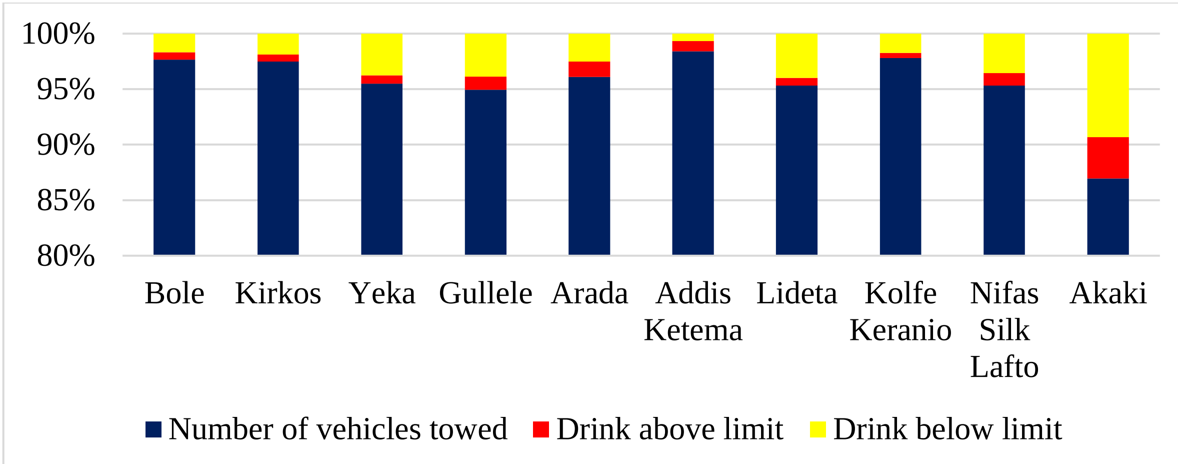

Figure 3.8: Traffic police alcohol breath test report analysis in Addis Ababa in 2010E.C (Addis Ababa Police Commission, 2020)

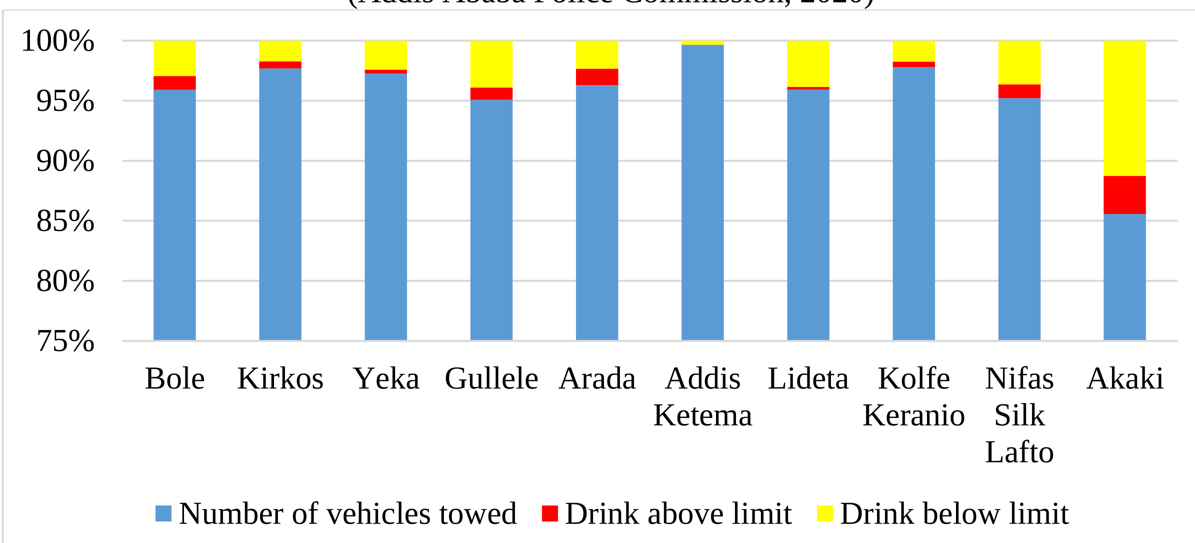

Figure 3.9: Traffic police alcohol breath test report analysis in Addis Ababa in 2011E.C (Addis Ababa Police Commission, 2020)

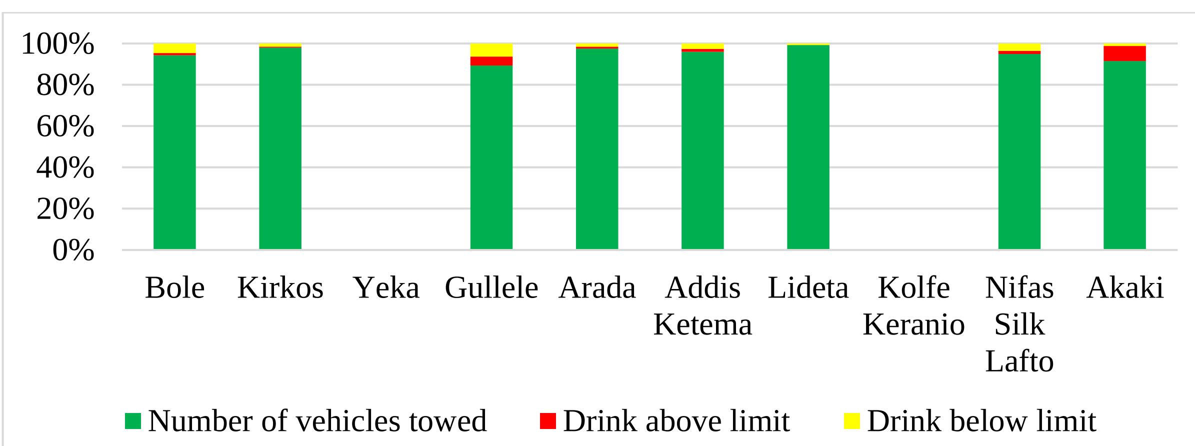

Figure 3.10: Traffic police alcohol breath test report analysis in Addis Ababa in 2012E.C (Addis Ababa Police Commission, 2020)

In 2010, 2011, and 2012 E.C for three years, alcohol breath tests were conducted in Addis Ababa. During the COVID-19 pandemic and now, breath testers are not used by traffic police and no data are available. However, the Addis Ababa Police Commission stated that they did not have a sufficient number of breath alcohol testers, nor did they have well-organized documents on drunk driving. From the graph in Figure 3.10, there is no record data for the two sub-cities of EC (Yeka and Kolfe Keranio) in 2012E.C. According to the Addis Ababa Police Commission, due to the COVID 19 pandemic, none of the sub-cities have recorded data because the breath alcohol tester increases the spread of COVID 19. Therefore, automatic pedal control for drunk driving is the best solution to the above-mentioned problems.

3.3.3 Traffic accident due to alcohol drunk driver in Ethiopia

According to the Ethiopian Federal Police Commission, no blood alcohol measuring device was used during the traffic accident inspection. However, there is little evidence that drunk driving accidents have occurred in the past three years, as shown in Figure 3.11.

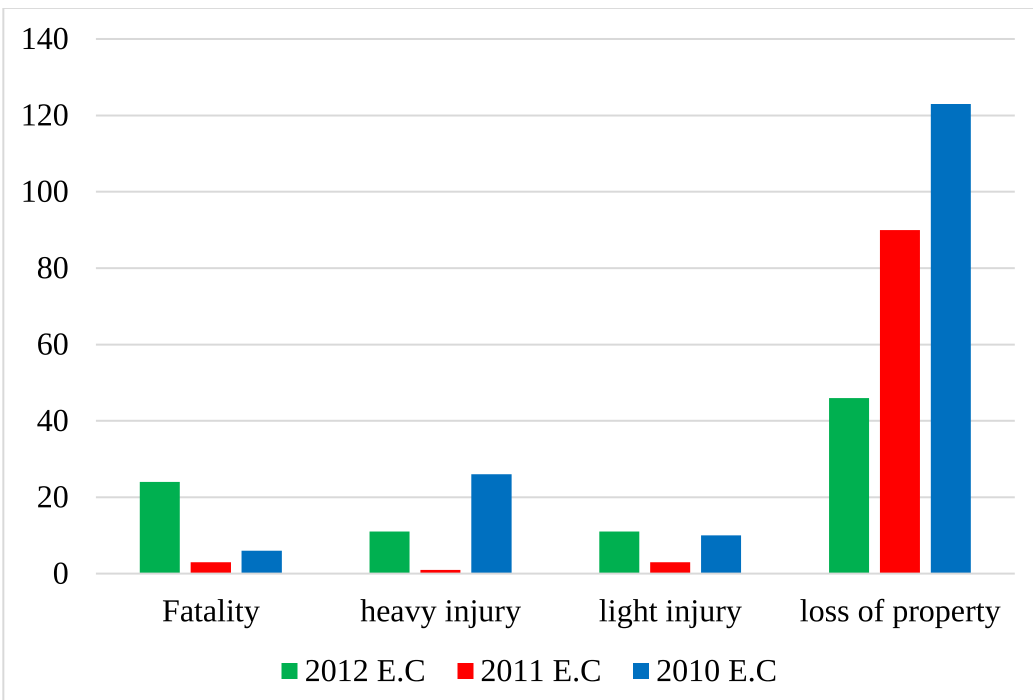

Figure 3.11: Three years traffic accident by an alcohol drunk driver (Addis Ababa Police Commission, 2020)

3.4. LS-DYNA Software Procedures

LS-DYNA software used to study dynamic behaviour driver during automatic vehicle braking (i.e. driver injury and vehicle stability). Simulation of the model in LS-DYNA includes three steps: pre-processing, solver, and post-processing.

A) Preprocessing

LS Pre Post is particularly capable of importing, editing, and exporting LS-DYNA keyword files for generating LS-DYNA input files. In pre-processing

- Import of Nastran, IGES, and Step-files possible
- Mesh generation
  - ✓ 2Dmesh Sketch board, n-Line Meshing, Tet-Meshing
  - ✓ Automatic surface meshing
  - ✓ Meshing of simple geometric objects (Plate, Sphere, Cylinder)
- Special applications
  - ✓ Airbag folding, dummy positioning, seatbelt fitting
  - ✓ Metal forming, roller hemming
  - ✓ ALE
  - ✓ Model check (element quality, contact)

B) Solver

LS-solver is used to start LS-DYNA simulations with either SMP or MPP versions.

C) Post-processing

After simulation, post-processing help us to get the output of our simulation and plotting graphs

- 3D animation
- BINOUT processing
- X-Y plots
- Time History Plotting
- ASCII plotting

3.4.1 Modelling of Toyota Yaris 2010 sedan

The finite element (FE) model of the Toyota Yaris 2010 passenger car was developed through a reverse engineering process at the National Crash Analysis Center (NCAC) of George Washington University (GWU), as shown in Figure 3.12. The model is a part of a series of finite element models developed to support collision simulation. The model has passed the National

Highway Traffic Safety Administration (NHTSA) Frontal New Car Assessment Program (NCAP) to verify the corresponding vehicle test. The finite element model has been validated and verified in a variety of ways to ensure that it is an accurate representation of the actual vehicle. This model was created for use with the LS-DYNA nonlinear explicit finite element code. Since the purpose of this work is to study the driver's injury during automatic emergency vehicle braking, the finite element model was downloaded from the NHTSA crash simulation vehicle models.

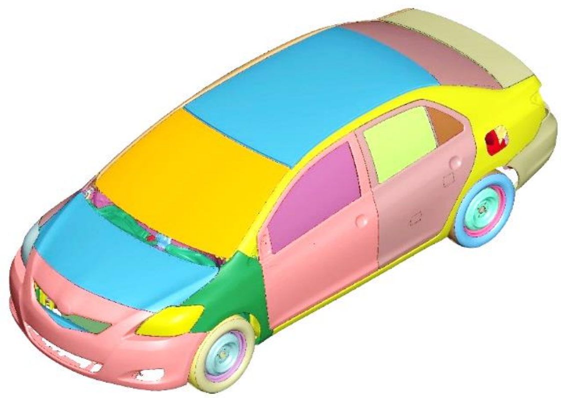

Figure 3.12: FE Toyota Yaris sedan 2010 Model [NHTSA]

The mass, moments of inertia, and center of gravity (CG) locations of the actual vehicle, as measured at the SEAS, Inc. lab, and vehicle model were compared. The weight pitch, roll, and yaw inertias; and x, y, and z coordinates for the CG were found to be similar and within acceptable limits. The location of the center of gravity and moment inertia of the full vehicle is given in Table 3.2.

Table 3.2: FE moment inertia of the full vehicle

FE Model	
Properties (unit)	value
Weight (ton)	1.25303
Pitch inertia (ton-mm^2)	425003
Yaw inertia (ton-mm^2)	1552710
Roll inertia (ton-mm^2)	1741260
Vehicle CG X (mm)	-1843.88
Vehicle CG Y (mm)	-2.2305
Vehicle CG Z (mm)	548.187

3.4.1.1 Design of Sled Model

In order to simplify the simulation process, only the main components of the car were extracted from the complete model. The mass distribution of the car is given in the center of gravity, which represents the mass of all components. During the sled test, it is not necessary to use the complete FE model because it requires a lot of simulation time. Simply take the components that are critical to our study and apply the mass moments of inertia (pitch, roll, and inertia) to the vehicle's x, y, and z coordinates on a sled model. The simplified sled model developed from the complete Toyota Yaris sedan 2010 model is shown in Figure 3.13. The sled model consists of the driver's occupant space and the dashboard, steering wheel, seat belt, and lower floor. The components of the sled model are designed with the characteristics of original materials. The speed pulse was applied through the "PRESCRIBED MOTION RIGID" condition to the sled model to resemble the actual movement of the vehicle and driver. Sled testing is of great use in testing vehicle components, occupant injuries, and the performance of occupant restraint systems.

Figure 3.13: Simplified sled model [LS-DYNA]

3.4.1.2 Hybrid III 50th percentile human model

In the sled tests, a Hybrid III 50th percentile male dummy is used to study injury responses. All injury reactions during the impact are collected by the sensors in the dummy. A displacement sensor in the chest measures the dummy thorax deflection. The dummy is placed on the seat in a normal driving position and secured with a seat belt. The dummy hands are positioned on the steering wheel. Automobile manufacturers are required to build cars that meet or exceed these minimum safety requirements. Hybrid III dummies are the most frequently used test devices for assessing "injuries" in crash tests. The basic measurements designed to provide these dummies include head and neck acceleration, chest acceleration, chest deflection, and femur load.

A 50th percentile hybrid III representing an average 50th percentile male occupant was used in this study and downloaded from Livermore Software Technology (LSTC) from the LSTC model download section web page, as shown in Figure 3.14.

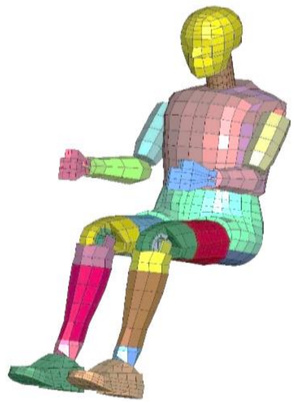

Figure 3.14: Hybrid III 50th Percentile Dummy [LS-DYNA]

The Hybrid III 50th Percentile Male Dummy Finite Element Model used to study the severity of driver injuries during automatic braking of a vehicle contains the following characteristics as shown in Table 3.3.

Table 3.3: Characteristics dummy

Number of Parts	128
Number of Nodes	7448
Number of Shells	66
Number of Beams	6
Number of Springer Damper	35
Number of Solids	63
Number of Elements	4333

The keyword *CONSTRAINED provides a way of constraining degrees of freedom to move together in some way. The keyword cards used in this dummy section are;

- *EXTRA_NODES_NODE
- *EXTRA_NODES_SET
- *JOINT_LOCKING
- *JOINT_SPHERICAL
- *JOINT_TRANSLATIONAL
- *JOINT_STIFFNESS_GENERALIZED
- *RIGID_BODIES

Accelerometers are used to measure the deceleration response and velocity of the vehicle are represented by Node IDs as shown in Table 3.4.

Table 3.4: Location accelerometers in dummy

Location Accelerometer	Node ID
Head	1008011
Neck	1000039
Chest	1008023
Chest deformation	1000003
Pelvis deformation	1000010

3.4.1.3 Seatbelt Model

The dummy is constrained by a three-spot style seatbelt, as shown in Figure 3.15. The seatbelt finite element models include seatbelt, slip ring, pre-tensioner, retractor, and the sensor element that can make pre-tensioner and retractor work.

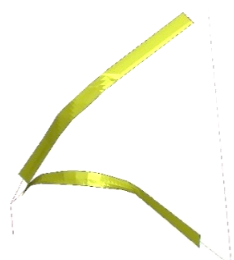

Figure 3.15: Seat belt model (LS-DYNA)

3.4.2 Positioning of Dummy

There are many ways in which dummies can be positioned and included in an LS-DYNA analysis. However, this study will focus on the following common approach:

- Load vehicle/structure into LS Pre-Post (File > Open > LS-DYNA Keyword File)
- Import dummy model (File > Import > LS-DYNA Keyword File)
  - ✓ Click “Import No Offset” or
  - ✓ Click “Setting Offset” in the Import File dialog (Offset the entity
  - ✓ Enter Default Offset
  - ✓ Click “Set” and click “Import”
- Position dummy
- Write out a positioned dummy as a separate file
- Setup dummy contacts
- Write out vehicle/structure as a separate file (with contacts)

The final positioned dummy with vehicle structure looks like as shown in Figure 3.16.

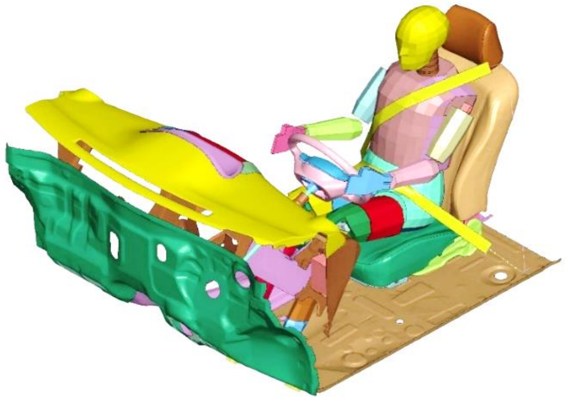

Figure 3.16: Position 50th hybrid dummy [LS-DYNA]

After finishing the positioning of the dummy create a combined LS-DYNA key file. Note that the combined file is the master file in which the vehicle, belt, and dummy are included. Editing the combined file will reveal the following:

KEYWORD

- INCLUDE
    - ✓ Vehicle Model
    - ✓ Dummy Model and Driver Belt Model
- BOUNDARY
    - ✓ Prescribed motion rigid for vehicle
- CONTACT
    - ✓ Automatic surface to surface between dummy and belt
    - ✓ Automatic surface to surface between dummy and vehicle
- CONTROL
    - ✓ Termination
    - ✓ Time setup
- INITIAL
    - ✓ Velocity generation (give initial velocity for dummy)
- Database
    - ✓ ASCII
    - ✓ D3plot
- DEFINE
    - ✓ Curve

3.4.2.1 Define curve

The keyword *DEFINE provides a way of defining boxes, coordinate systems, load curves, tables, and orientation vectors for various uses. Define a curve for example load (ordinate value) versus time (abscissa value) often loosely referred to as a load curve. For the simulation of this simulation, there are different curves that the vehicle can follow (i.e. speed curve).

3.4.2.2 Simulation time

During the automatic braking of a vehicle, the head is set in sudden motion without direct physical contact. It is an Impulsive load injury mechanism type. Such a load may be in the range of 50-200 milliseconds (Ricci, P., 2018). The total duration of the simulation was taken an average of 125 milliseconds to capture the braking and rebound of the dummy.

3.4.3 Post-Processing

These post-processing instructions are based on the Node/Element/Joint IDs that exist in the dummy model.

Head Injury Criteria (HIC)

- Load your d3plots in LS Pre-Post (File > Open > LS-DYNA Binary Plot)
- Go to Post > Setting
- Select "Hic/Csi const."
- Select Time units: sec
- Select Gravity constant: 9810 mm/s^2
- Go to Post > ASCII
- Select "nod-out *" from the upper list and Click "Load"
- Select node "1000001" in the middle list
- Select "hic$_{15}$" or "hic$_{36}$" in the bottom list for HIC$_{15}$ and HIC$_{36}$ respectively
- Click "Hic/Csi" Check "Apply pre-filter"
- Select Filter: SAE, Select C/s (Hz): 108, and Click "Plot" or "New"

During applying of pre-filter for HIC and CSi select "SAE" for the filter. Because most of the time the recommended filter is an "SAE-108 filter" for all curves being processed from the Dyna Dummy. This consistently gives reasonably smooth curves without loss of vital data. In my opinion, this is a very good choice of filter. One more thing to notice here is that our acceleration is in the units "mm/sec/sec". In the MKS unit, acceleration due to gravity is 9.81 m/sec/sec. Converting this into our units, therefore, gives "g=9810 mm/sec/sec". To convert our plot to units in terms of Acceleration due to Gravity, we have to divide the Plot Curve by 9810 (which can be done in the “Scale” panel of this box) (1/9810 = 0.000102). Then go to “Scale”, apply the “Y-scale” factor of 0.000102 and then Apply.

3.4.3.1 Chest Deflection

- In a physical dummy, the deflection is measured from the rotation of the chest potentiometer arm. The arm is connected to a potentiometer at the base which is calibrated for different rotation angles. This rotation is then multiplied by a "linearizing factor" (or "transfer function") which results in the chest deflection.
- In my dummy model, the chest potentiometer arm is represented by PIDs 1000094 and 1000095. The arm is connected to a rotary spring of very low stiffness (ID 1000003). The linearizing factors are 158.0 mm, 145.0 mm, and 96.0 mm for the 95th, 50th, and 5th percentile dummies respectively.
    - ✓ Load your d3plots in LS Pre-Post (File > Open > LS-DYNA Binary Plot)
    - ✓ Go to Post > ASCII
    - ✓ Select “deforc *” from the upper list and Click “Load”
    - ✓ Change “Trans” to “Rotat” in the drop-down menu.
    - ✓ Select “1000010-R” in the middle list (base of the potentiometer)
    - ✓ Select "Relative Rotation" in the bottom list
    - ✓ Click “Plot” or “New” (plots angular spring rotation in rad/ms)
    - ✓ Click "Scale”, Enter Y-scale: 145 (for the 50^{th} percent dummy)
    - ✓ Click “Apply”, “Auto-fit”, “Title”, Enter Y-Axis Label: Chest Deflection (mm)
    - ✓ Click “Apply”

3.4.3.2 Femur Forces

- Load your d3plots in LS Pre-Post (File > Open > LS-DYNA Binary Plot)
- Go to Post > ASCII
- Select “jntforc *” from the upper list and Click “Load”
- Select "Jt-1000024" (left femur) or “Jt-1000025” (right femur) from the middle list
- Select "Z-force" from the bottom list
- Click “Plot” or “New” (plots axial femur force in kN)
- Click "Filter" in the Plot Window
- Select Filter: SAE, Select C/s (Hz): 108 and click “Apply

3.4.3.3 Upper Neck Forces

- Load your d3plots in LS-PrePost (File > Open > LS-DYNA Binary Plot)
- Go to Post > ASCII, Select "jntforc *" from the upper list, Click "Load" load "Jforc"
- Select "Jt-1000039" from the middle list
- Select "X-force" (Shear Force, F_x) or "Z-Force" (Tensile Force, F_z) from the bottom list
- Click "Plot" or "New" (plots upper neck force in k-N)

3.5 Arduino programming code

Arduino programming code used to controll the sensors and actuators. The basic structure of the Arduino programming language is very simple and consists of at least two parts.

void setup (), {statement;} and void loop () {statement;}

when setup () is ready, loop () is running. Both functions are required for the program to work. The customization function must obey the variable declaration at the beginning of the program. The setup () function is called once when the program starts. Used to initialize output mode or start serialization. Even if there are no statements to execute, they must be included in the program. After calling the setup () function, the loop () function runs exactly as its name suggests and loops continuously to allow the program to modify, react, and control the Arduino board.

3.5.1 Conversion of breath alcohol content to blood alcohol concentrations

Several studies have been conducted on the variables that affect the absorption, distribution, and elimination of alcohol. Some of these studies included measurements of exhaled alcohol concentration (BrAC). The measured value is less invasive than blood draw and is considered to have a good correlation with blood alcohol content (BAC). To avoid the need to convert BrAC to BAC on a case-by-case basis, it was practical to establish and enforce a threshold for BAC limits along with the existing BAC limits. Breath analysis with an Alco scale gives an estimate of BAC by using a breath-to-blood conversion factor known as the blood/breath ratio. This blood/breath factor was used to calibrate the breath analyzer and the value 2100:1 has become generally accepted for legal purposes to produce direct readings in BAC units (Vukovic J et al., 2015). According to the Ethiopian blood alcohol concentration BAC legal limit, the threshold for drinking alcohol while driving is 0.08 g/dl or 0.8 g/L (Beyene, N. 2019). The written code Arduino code and the flowchart of the hardware components are shown in Figure 3.17.

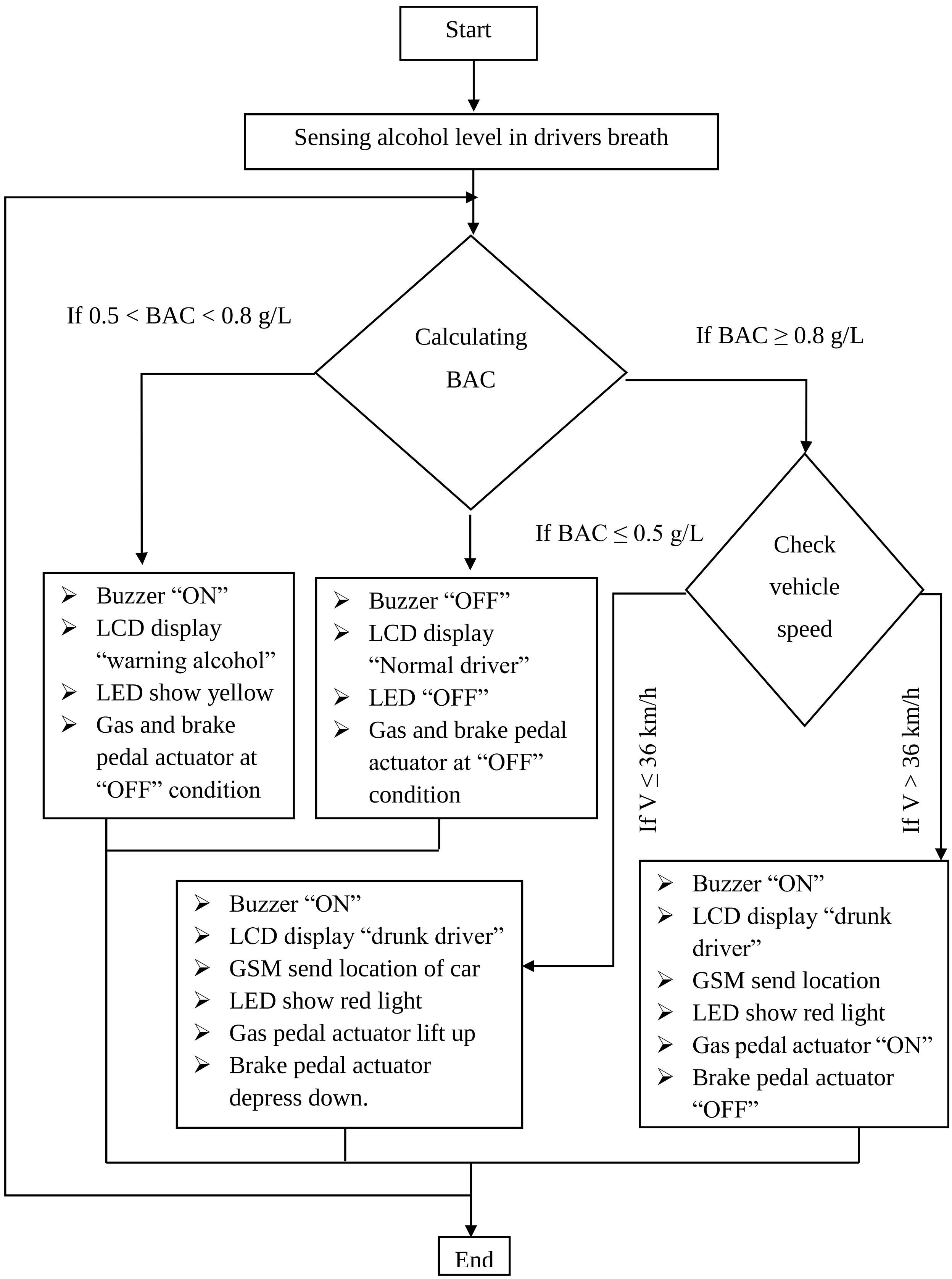

Figure 3. 17: System programing flowchart

3.5.2 Connect Arduino board to the computer

After finishing writing a code, it is necessary to connect the Arduino board to the computer and upload a sketch. Therefore, an Arduino Uno board and a standard USB cable are required first. Then connect the Arduino board to a computer with the USB cable. Sketch uploaded after these steps.

- Connect Arduino with the USB cable
- Select Tools → Board → Arduino Uno to find a board in the Arduino menu.
- Choose the correct serial port of the board.
- Click the Upload button and if the upload is successful, "Upload Complete" message.

3.5.3 Selection of GPS and GSM modules

The GSM module is a specific type of module, which accepts the user identity module card and operates by registering with the telephone operator (same as a mobile phone). The GPS module is used to obtain regional data, that is, the geographic direction of the vehicle at a specific time. According to researchers, the best GPS and GSM modules for vehicle tracking systems are GPS receiver NEO 6M and GSM 900A, respectively. GSM SIM900A is an instant application for many mobile phones and personal digital assistants. GSM SIM900A is a dual-frequency general packet radio service motor designed for the high-frequency extension of GSM 900 MHz and distributed control system 1800 MHz. It is also very cheap, dual-frequency, and configurable baud rate (Tummanapally S., & Sunkari S., 2021). The GPS NEO 6m module is a kind of independent GPS receiver, which is characterized by its high performance as a location device. With optimized architecture, power supply and memory, this module is very suitable for devices that use batteries as a low-cost and space-limited resource. It has high positioning accuracy, capture sensitivity, tracking sensitivity, and can accelerate Time-To-First-Fix (TTFF) in less than 1 second (Satria et al., 2017). See a typical GPS NEO 6M and GSM 900A in Figure 3.18.

Figure 3. 18: GPS NEO 6M and GSM 900A (Satria et al., 2017)

3.6 Proteus Simulation

3.6.1 Creating schematic circuit of the electronic system

To start the program, click the "Start" button and select "Programs", "Proteus 8 Professional". The main application is loaded and launched, and the Proteus home page is displayed.

- Specify the name and path of the project on the first page of the wizard.
- On a schematic so check the box at the top of the next step and choose the default.
- Similarly, the layout at the top of the layout page and again choose the default.
- The next screen allows us to define the layer stack for PCB.
- The project opens in two tabs. One is for schematic and the other is for PCB layout.
- Click the Schematic tab to bring the Schematic module to the front.
- The largest area of the screen is called the editing window and acts as a window in the drawing this is where we place and wire components.
- The smaller area in the upper left of the screen is called the overview window.
- The blue box shows the edge of the current sheet and the green box the area of the sheet that is currently displayed in the editing window.
- A new object is selected from the object selection. The overview window is used to preview the selected object.
- The first thing we need to do is get the parts from the libraries that need in our schematic.

3.6.1.1 Selecting Parts from the Library

There are two ways to select parts from the library:

- Click the P button in the upper left of the object selector
- Browse the Library icon on the keyboard shortcut for this command (by default, this is the P key on the keyboard).
- There are several ways to find components from the libraries and import them into the schematic. For parts that know the part name, it's usually best to start the search with it.
- Try typing the name in the keyword field in the device library browser dialog box.
- Now place the objects on the schematic and selected the parts the next thing to place them on the drawing area of the editing window and connect them.
- After placing objects on the schematic, the necessary components must connect them.

3.6.1.2 Wiring up microcontroller to sensors and actuators

- The alcohol sensor output is connected to an analog pin on Arduino (A0).
- Buzzer is connected to Arduino pin D13.
- Connect the TX and RX pins of the GPS to D3 and D4 of the Arduino pin.
- Serial software to communicate with GPS. So connect the TX of the GPS to D4 of the Arduino board. RX to D3 of the Arduino board.
- Connect TX and RX of the GSM module to RX and TX of the Arduino board
- Connect the LCD to the D8 through D13 of the Arduino Board (LCD - Arduino) pin connectors (RS – D7, EN – D6, D4 – D5, D5 – D4, D6 - D9, and D7 - D2)

After wiring up all necessary components it is necessary to add Arduino library for proteus alcohol sensor library (GasSensorTEP.HEX) to the alcohol sensor

- GSM module library (GSMLibraryTEP.hex) to GSM module
- GPS library (GpsTEP.HEX) to GPS
- Add '.hex' file of Arduino code and Finally simulate

The final Proteus schematic design of automatic alcohol detection system for alcohol drunk driver which is ready to develop prototype is shown in Figure 3.19.

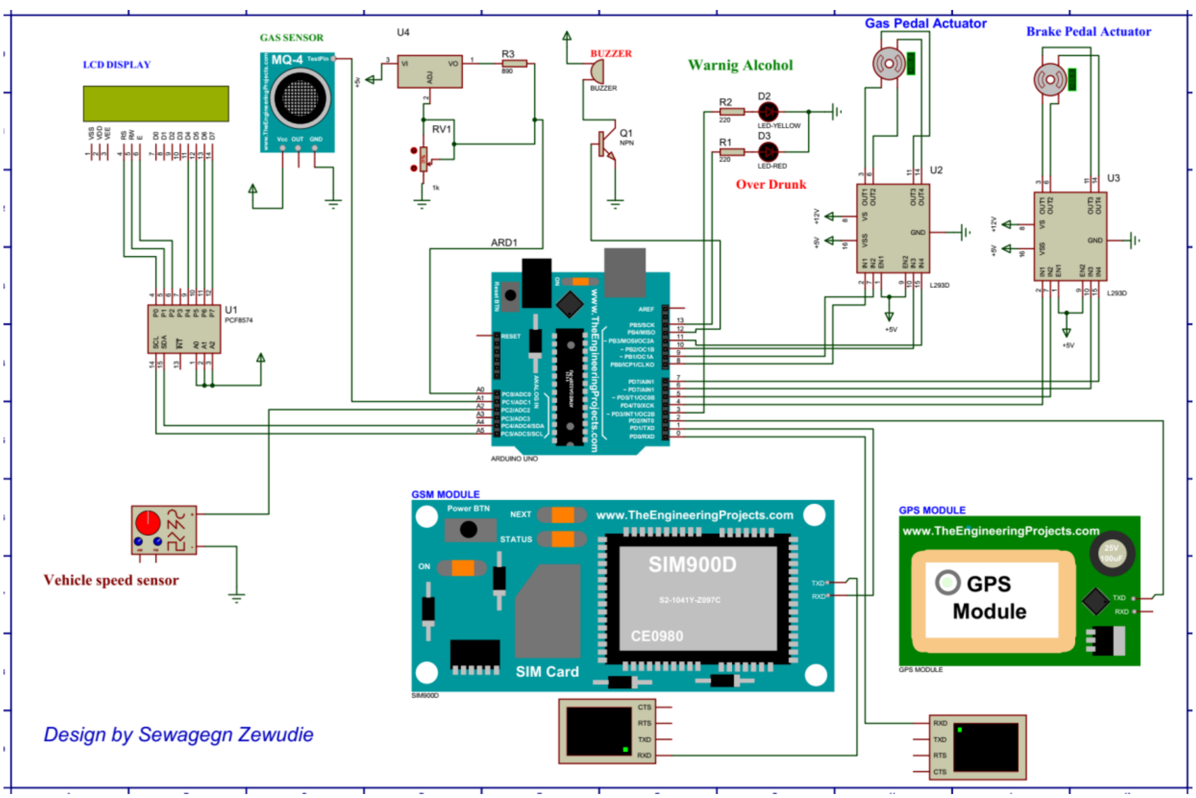

Figure 3.19: Proteus schematic design

The final proteus schematic design contains hardware components includes

- LCD display
- Alcohol sensor
- Microcontroller
- Stepper motor
- LED light
- GSM module
- GPS module
- Buzzer
- NPN transistor
- Stepper motor driver

3.7 Selection of appropriate pedals controlling actuators

The primary function of an operating system is to influence the controlled system to obtain the desired movement or action. There are three main types of power with which operating systems operate: electric power, hydraulic power, and pneumatic power.

3.7.1. Comparison of Electric, Mechanical and Hydraulic actuator

Hydraulic cylinders, known for their great force at an affordable price, have been widely used in factory automation equipment and other specialty automation equipment for decades. The hydraulics are robust, relatively easy to use, and offer a low cost per unit of force. A variety of factors affect the performance and cost of any technology, including (Dietrich, A. 2016).

- Motion control capabilities
- Force capabilities
- Speed capabilities
- Life and maintenance of devices
- Efficiency/utility costs;
- Leaks and environmental concerns

a) Motion control capabilities

The main reason why engineers choose electric actuator systems instead of hydraulic cylinder systems is the flexibility of their motion control capabilities: position control (multi-position, precision), speed acceleration and deceleration control, and output force control. Standard hydraulic systems are well suited for end-to-end position applications, but mid-stroke positioning is more complicated and requires control valves and operator assistance. Finally, the position, speed, and force repeatability of the hydraulic cylinder are affected by seal wear, leakage, pressure drop, and pump spikes, as well as other maintenance factors (Dietrich, A. 2016). See motion control comparison as shown in Figure 3.20.

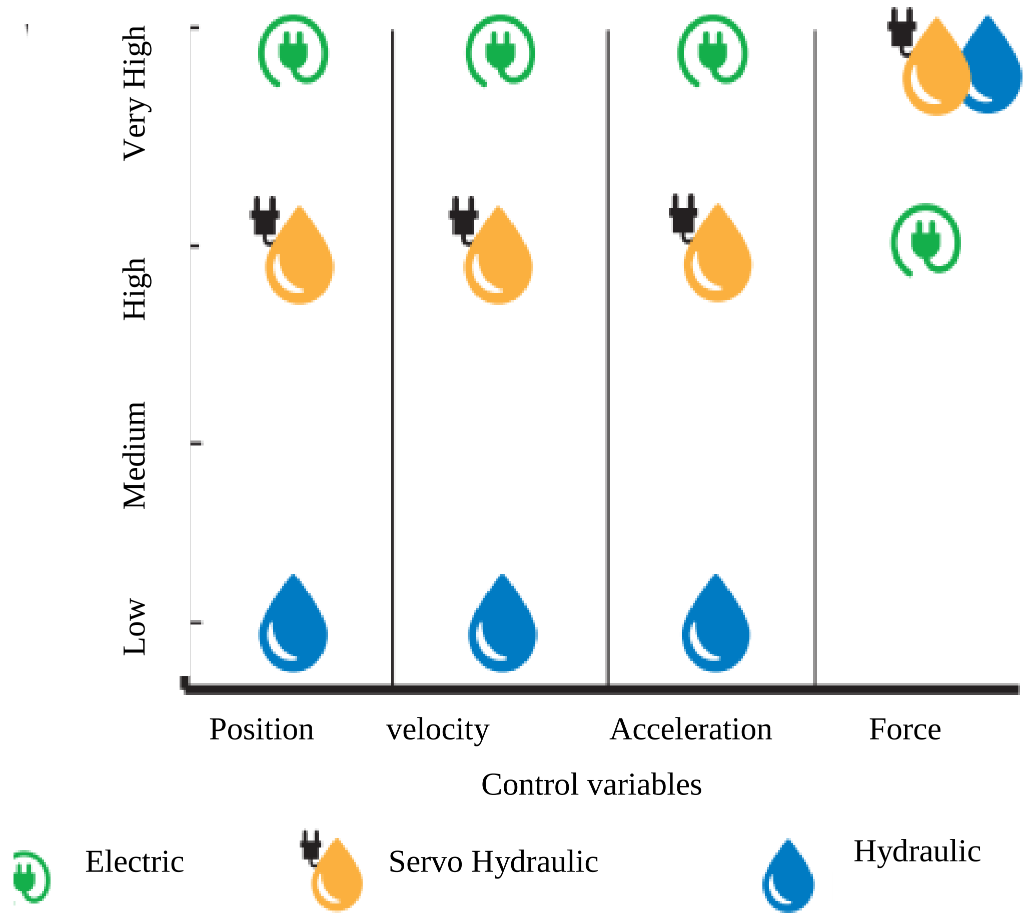

Figure 3.20: Motion control comparison (Dietrich, A. 2016)

b) System components

The number of components and the overall space required by the hydraulic system are much larger than that of the electrical system. The hydraulic system requires an oil cylinder; a power unit that provides oil pressure; control valves and auxiliary valves, filters, hoses, accessories, and additional components. The overall area of the electric rod-type actuator is smaller.

c) Service life and maintenance

Hydraulics require frequent maintenance and attention to achieve the desired performance over the life of the system. Maintaining the integrity of the rod and piston seals is key to repeatability as these are the main elements that contain the pressure required to move and force. Electric actuators designed for the life of an application do not require maintenance. The main drive elements of an electric actuator are the drive screw and other thrust bearing elements. These factors include dynamic load assessment (DLR), which can be used to estimate the amount of work (force over distance) that an electric actuator can perform. Electrical systems require little or no maintenance compared to hydraulic systems (Dietrich, A. 2016). See maintenance comparison as shown in Figure 3.21.

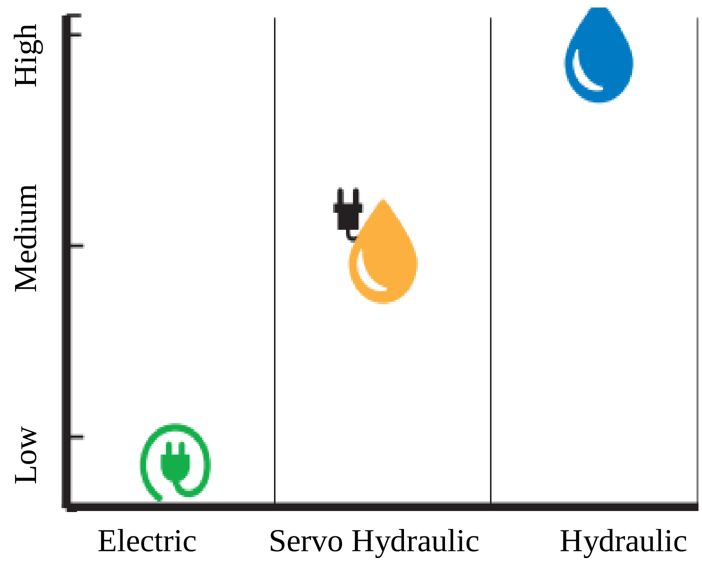

Figure 3.21: maintenance comparison (Dietrich, A. 2016)

d) Efficiency and electric utility costs

Electric actuator systems usually operate in the 75-80% efficiency range of the work they complete; hydraulic actuator systems usually operate in the 40-55% efficiency range. Another factor in the power utility cost equation is that the electric starter only needs to provide current to the motor when needed. When electric actuators are at a standstill, they do not require any current or very low amount of current to maintain their position (Dietrich, A. 2016). See operation efficiency comparison as shown in Figure 3.22.

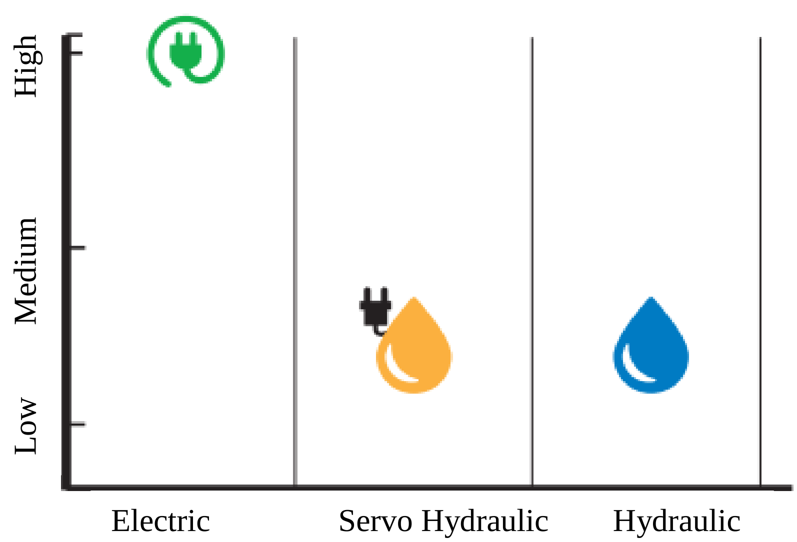

Figure 3.22: Operation efficiency comparison (Dietrich, A. 2016)

e) Leaks and environmental concerns

Many hydraulic leaks create messes in the manufacturing environment and also present a safety hazard. Leaking oil in the surrounding environment can be a major concern for communities. Electric actuator technology is one of the cleanest linear motion technologies that can be actively and easily deployed. The high-quality seals used on the electric actuator rod retain the grease inside the actuator, almost eliminating contamination problems. Unlike hydraulic systems, electric systems present minimal environmental risk (Dietrich, A. 2016). See environmental risks comparison as shown in Figure 3.23.

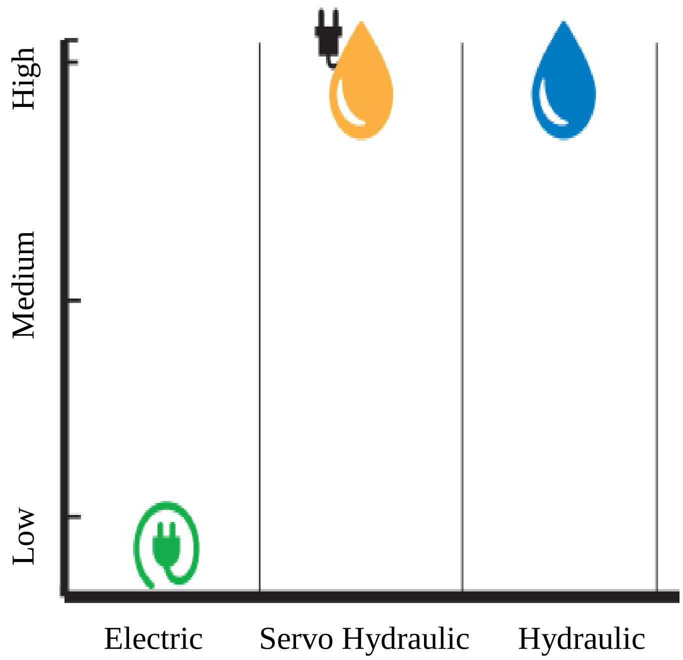

Figure 3.23: Environmental risks comparison (Dietrich, A. 2016)

Summary

Hydraulic systems are usually less expensive to implement than electrical servo systems in terms of purchase costs. These drawbacks include a larger space footprint, regular maintenance, and manual system adjustments for optimal system performance. Hydraulic systems are sensitive to temperature fluctuations, are prone to leaks, and operate in an open-loop environment, making data collection challenging. Hydraulics do offer a long service life, but they are not as efficient operators as electric systems. Electric systems offer smaller space requirements and provide precise position, velocity, and speed control with more efficient operation. Therefore electric actuators are preferable for this thesis work.

3.8 Selection of electric motor

3.8.1 Stepper motor vs servo motor

An electric motor is a machine, which converts electric energy into mechanical energy. Most electric motors operate through the interaction between the motor's magnetic field and electric current in a wire winding to generate force in the form of torque applied on the motor's shaft. Its action is based on the principle that when the current-carrying conductor is placed in the magnetic field (Theraja B. L. & Theraja A. K., 2010).

Table 3.5: Comparison between stepper motor and servomotor (Gill, H. 2016)

Characteristics	**Servo Motor**	Stepper motor
Cost	The cost for a servo motor higher	Steppers are generally cheaper
Versatility	Servo motors are very versatile in their use for automation.	Stepper motors are also very versatile in their use for automation.
Reliability	This is a toss-up because it depends on the environment and how well the motor is protected.	The stepper takes this category only because it does not require an encoder which may fail
Setup Complexity	Servo motors require tuning of the (PID) closed-loop function.	They require only the motor wires to be wired to the stepper motor driver.
Motor life	The brushes on servo motors must be replaced every 2000 hours of operation.	The bearing on stepper motors is the only wearing part. That gives stepper motors a slight edge on life.
Speed and Torque	Servo motors will do fine with low-speed applications	Stepper motors provide most torque at low speed (RPM).
Repeatability	Servomotors can have very good repeatability if set up correctly.	Have very good repeatability with little or no tuning required.

Both technologies are a clear choice in today's mechatronics mechanical design. However, once the strengths and weaknesses of servo and stepper motor systems are clearly understood. Stepper motors are a convenient solution due to their low cost, versatility, ease of setup, long motor life, high torque at low speeds, high overload safety, and simplicity of motors.

3.8.2 Stepper motor vs DC motors

The brushed DC motor is better than the stepper motor in terms of controllability, and it is easy to control two machines at the same time. The DC motor only needs to provide the input voltage for its two leads. However, a Stepper Motor is better than DC motors to the applications that require accurate positioning and repeatability with a fast response to starting, The stop, reverse, speed control, and another major advantage of a stepper motor is its ability to stabilize the load once the desired position is achieved. This thesis needs more applications of this stepper motor. So the best motor used for this thesis is a stepper motor. See the comparison of brushed motors vs stepper motors as shown in Table 3.6.

Table 3.6: Comparison of brushed motors vs stepper motors (Christian C, 2021)

Characteristics	Brushed DC Motors	Stepper Motors
Control characteristics	Simple; no extras needed	Simple; microcontroller needed
Speed Range	Moderate (depends on type)	Low (200-2000 RPM)
Reliability	Moderate	High
Efficiency	Average	Low
Torque/speed	High torque at low speeds	Maximum torque at low speeds
Cost	Low	Low

3.8.3 Stepper motor

A stepper motor is a special brushless DC electric motor that divides a complete rotation into several equal steps (movement in separate steps). Stepping is controlled by a computer for highly accurate positioning and speed adjustment. Computer-controlled stepping can be used to achieve highly accurate positioning and velocity regulators (Ahmed M. T. & Ibraheem Al-Naib, 2019). See a typical stepper motor as shown in Figure 3.24.

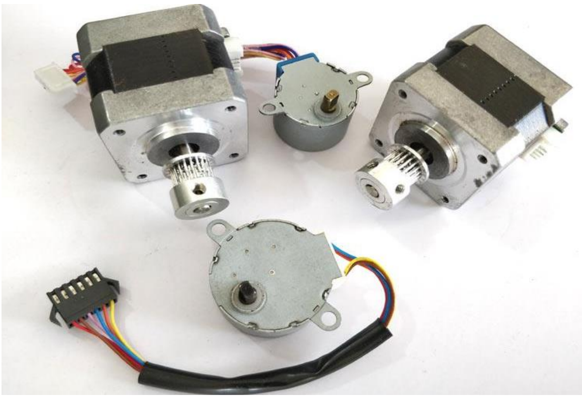

Figure 3.24: Stepper motor (Ahmed M. T. & Ibraheem Al-Naib, 2019)

Stepper motors are excellent for many precision motion control applications. Stepper motors are used in an array of precision moving and measuring devices such as nuclear power plants, aeronautics, robotics, automotive, medicine, manufacturing, etc.(Ahmed M. T. & Ibraheem Al-Naib, 2019).

Features of Stepper Motor

- Stepper motors do not have brushes.
- Can be effectively controlled by the open-loop method
- Stepper motors can hold the shaft stationary.
- Excellent response to start / stop / reverse
- Stepper motors are relatively inexpensive and low maintenance
- Stepper motors are relatively inexpensive and low maintenance

3.8.4 Type of stepper motor

By construction, the step motors come into three broad classes.

- Permanent Magnet Stepper
- Variable Reluctance Stepper
- Hybrid Step Motor

3.8.4.1 Permanent Magnet Stepper

The magnetic poles of the rotor and stator of a permanent magnet stepper motor have no teeth. In contrast, the rotor has alternating north and south poles parallel to the axis of the rotor shaft. When the stator is energized, an electromagnetic pole is generated. The magnetic rotor is aligned with the stator magnetic field. Then the other stator in the sequence is powered, and the rotor moves to adapt to the new magnetic field. Therefore, when the stator is energized in a certain order, the stepper motor rotates at a certain angle (Nikhil Agnihotri, 2011).

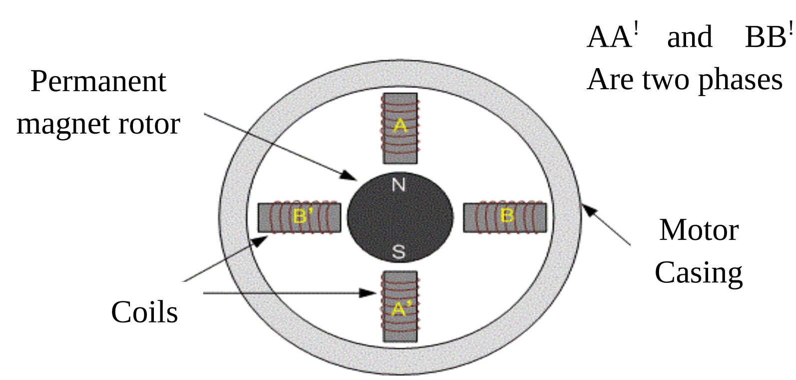

Figure 3.25: Two-phase permanent magnet stepper motor (Nikhil Agnihotri, 2011)

3.8.4.2 Variable reluctance stepper

The variable resistance stepper motor has a non-magnetic soft iron toothed rotor. When the stator coil is energized, the rotor moves to have a minimum clearance between the stator and its teeth. Note that the teeth on the rotor are designed so that when aligned with a phase, they will be misaligned.

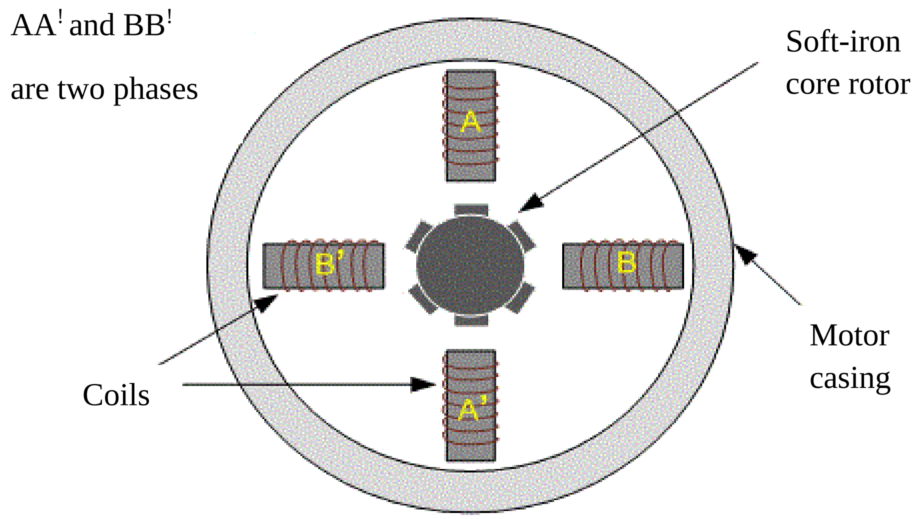

Figure 3.26: Two-Phase Variable Reluctance Stepper Motor (Nikhil Agnihotri, 2011)

a) Hybrid stepper

A hybrid stepper motor is a permanent and variable combination. It features a rotor with magnetic teeth that better guide the magnetic flux to a preferred position in the air gap. The magnetic rotor has two cups. One for the north poles and the second for the south poles. The rotor cups are designed so that the north and south poles are arranged in an alternative manner.

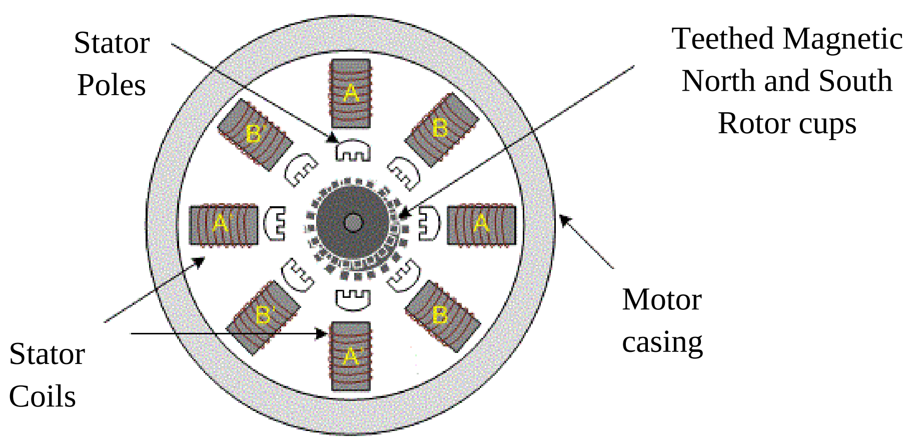

Figure 3.27: Construction of Two-phase Hybrid Motor (Nikhil Agnihotri, 2011)

Comparison of Hybrid Stepper Motor with other Motors

- Hybrid motors have a minimal step angle of 1.80 when compared with others
- It has increased output torque whereas for variable reluctance motors it is low and for permanent magnets it is moderate
- The pulse rate and speed of hybrid stepper motors
- Hybrid stepper motors have quick acceleration and response
- It produces quite less noise when compared with variable reluctance motors

A) Unipolar and Bipolar Motors

Unipolar SMs are collected of two windings; everyone has a center tap. The center taps are either carried outside the motor as two individual wires or coupled to each other inside and carried outer the motor as a single wire. A bipolar stepper motor has one winding per stator phase. A two-phase bipolar stepper motor has 4 leads in a bipolar stepper we don't have a common lead like in a unipolar stepper motor. A bipolar stepper motor has an easy wiring arrangement but its operation is a little complex.

Comparison between unipolar and bipolar

The current runs through the whole coil instead of the only half coil as in a unipolar motor. As a result, the Bipolar motor will produce more torque than a unipolar motor of the same size. Compared to unipolar motors, the bipolar motor is uncomplicated in structure but necessitates a positive and negative source and extra complex switching electric circuit. Therefore, bipolar stepper motors are selected for the automatic pedal controlling system.

3.9 Selecting the Best Type of Screw

The threading mechanism provides a means of generating linear motion by rotating either the screw or the nut in the assembly. A screw is a cylindrical element with a thread formed on it. The nut is the component that matches the screw. There are three main types of screw technology used in linear actuators: acme, ball, and roller. The difference lies in the design and operation of the matching nut, as well as the design of the shape of the screw (Tolomatic excellence, 2019).

3.9.1 Acme Screws

The Acme screw has a thread form having a trapezoidal tooth shape that is typically rolled into a steel shaft. The thread form itself is very strong and linear force is transmitted to a solid nut from the sliding surfaces on the flanks of the thread form.

The efficiency of a solid nut system is determined by the nut material and the lead, it can range from 20% to 40% and is relatively low compared to other screw technologies. However, the disadvantage of the low system efficiency is the increased motor torque input required in comparison to other screw technologies. The Acme screws are threaded with a trapezoidal tooth shape that is typically rolled into a steel shaft. The thread form itself is very strong and the linear force is transmitted from the sliding surfaces on the flanks of the thread form to a solid nut. The efficiency of a massive nut system is determined by the nut material and the slope, it can be between 20% and 40% and is relatively low compared to other screw technologies. The disadvantage of the low system efficiency, however, is the increased motor torque input required compared to other screw technologies. Common nut materials include brass, bronze, self-lubricating plastics, resins, and metals (Tolomatic excellence, 2019). See a typical Acme power screw as shown in Figure 3.28.

Figure 3.28: Acme power screw (Tolomatic excellence, 2019)

Acme Screw Advantages:

- Low cost, quiet operation, reduce or remove back driving
- Ideal for applications with:
    - ✓ slow to medium speeds
    - ✓ low duty cycles
    - ✓ low to medium force capacities

Acme Screw Limitations:

- Solid nut design may wear, increasing backlash, and affect the positioning
- Lower efficiency ratings require higher input torque
- Unpredictable service life
- External factors such as environment can affect screw life

3.9.2 Ball Screws

The ball screw utilizes the shape of a circular arch thread. Since the nuts have the same shape as the thread, the balls that fit between the grooves. It can transmit force and relative motion very efficiently. Usually about 90% depending on the diameter of the screw and the lead of the screw. Ball bearings can roll and recirculate in one or more circuits in the nut when rotational and linear motion occurs (Tolomatic excellence, 2019). See ball-type screw as shown in Figure 3.29.

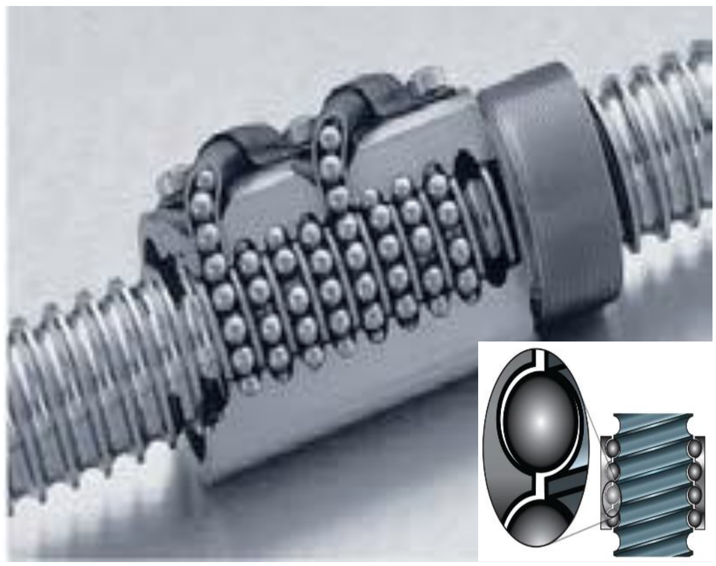

Figure 3.29: Ball type screw (Tolomatic excellence, 2019)

Ball Screw Advantages:

- Higher force capabilities, longer life, and increased efficiency (~90%)

Ball Screw Limitations:

- It May easily be back-driven depending on lead, higher initial cost vs Acme screw, and increased operational noise vs Acme screw

3.9.3 Planetary Roller Screw

Threads are usually triangular in shape and transmit force through a set of matching rollers with multiple threads connected to the nut. These rollers rotate inside the nut and make contact with the threaded shape of the screw. The roller nut has a pre-numbered roller that provides significantly more points of contact with the screw in the same space compared to ball nuts, resulting in very high force transfer capacity and longer life than ball screws of the same diameter (Tolomatic excellence, 2019). See a typical planetary roller screw as shown in Figure 3.30.

Figure 3.30: Planetary Roller Screw (Tolomatic excellence, 2019)

Roller Screw Advantages:

- Very high force capabilities, Extremely long life, High speed and acceleration rates possible, Low maintenance and High efficiency

Roller Screw Limitations:

- Highest cost of three screw technologies, In vertical applications, the screw can be back-driven or free fall, Nut assembly has a larger outside diameter vs, ball screw

Summary

For most applications that require high force, repetitive cycles, and long expected life a roller actuator and ball screw are used. The most common applications of the ball and roller actuators include robots and aircraft. Acme screws provide a more reliable design for common applications. With no back drive and low cost, this design is a very flexible solution for most automated linear motion applications. From the above explanation, the automatic vehicle pedal locking electric linear actuator use an Acme type screw because this linear electric actuator works with lower force and low repetitive duty cycle and it is low cost, quiet operation, reduce or remove back driving.

3.10 Selection of Appropriate Alcohol Sensor

3.10.1 How is alcohol measured?

The amount of alcohol in the blood can be measured by testing a small sample of blood or urine, or by analyzing the exhaled air (WHO, 2008). The amount of alcohol in the bloodstream is described in terms of BAC. BAC level is usually measured as:

- grams of alcohol per 100 milliliters of blood (g/100 mL)
- grams of alcohol per deciliter (g/dL)
- milligrams of alcohol per deciliter (mg/dL)

Increasing the level of alcohol concentration in the exhaled breath increases the conductivity of sensitive substances. Alcohol levels are calculated as BAC (Blood Alcohol Concentration) levels. Breath and blood alcohol levels differ by a factor of 2100. That is, for every 1 mg of alcohol you breathe, your blood contains 2100 mg of alcohol.

The formula for calculating BAC from the alcohol measured in the breath is:

$$\% \text{ BAC} = X \times 0.21$$

- Where, %BAC= Blood alcohol concentration in percentage and X= alcohol concentration in breath in mg/L.

3.10.2 Sensitivity Substances and Detection range of different gas sensors

These MQ series gas sensors contain a built-in heater and an electrochemical gas sensor. Different sensors have different gas detection ranges and chemical sensitivity. Table 3.7 the best alcohol sensor for this thesis MQ-3 alcohol sensor because it mainly detects alcohol rather than other chemicals.

Table 3.7**:** Sensor types, gas detection range, and chemical sensitivity (Rasekhet al., 2021)

Sensor Name	Detection Ranges (ppm)	Main Applications (Gases Detected)
MQ3	10–300	Alcohols
MQ4	300–100	Urban gases, methane (CH_4)
MQ8	100–1000	Hydrogen (H_2)
MQ9	10–10,000	CO, combustible gases
MQ135	10–10,000	Ammonia, benzene, sulfides
MQ136	1–200	Sulfur dioxide (SO_2)

Features of MQ-3 Alcohol Sensor

- Compatible with most of the microcontrollers
- Low-power standby mode
- Requires heater voltage
- Good sensitivity to alcohol gas
- Fast response and High sensitivity
- Long life and low cost
- Requires simple Drive circuit

The MQ-3 gas sensor is extremely sensitive to alcohol and has excellent resistance to interference from gasoline, smoke, and steam (Mohammed M, 2016). The alcohol sensor (MQ-3) is suitable for detecting alcohol concentration because it is sensitive, has a fast response time to small BAC values, and provides an alcohol-based analog resistance output. The sensor is made of tin dioxide (SnO_2) sensitive layer.

The sensor is configured to have high sensitivity to alcohol and low sensitivity to benzene. It has a simple drive circuit with fast response, stability, and long life (Gbenga et al., 2017). The recommended value of load resistance is 10K to 47K.

3.10.3 Working principle of MQ3 alcohol sensor system

MQ3 is a metal oxide semiconductor (MOS) type sensor and a widely used sensor in the MQ sensor series. Metal oxide sensors are also known as chemical resistors, as the sensor system is based on the change in resistance of the sensor material when it is exposed to alcohol. By inserting it into a simple voltage divider network, alcohol concentrations can be detected. This alcohol sensor system uses an MQ3 alcohol sensor that acts as a breath analyzer.

Calculations for alcohol content (John Searle, 2015).

- According to the MQ3 datasheet, alcohol in clean air is 0.04 mg/L.
- The output voltage of the MQ3 sensor gives 0.60 v in the clean air then alcohol 0.04 mg/L.
- Now find a multiplier by dividing alcohol by output voltage in clean air and we get:
- Multiplier = 0.040/0.60 = 0.067
- Now the formula for calculating alcohol:
- Alcohol = 0.067×v
- Where v is the output voltage of the alcohol sensor.

Table 3. 8: Complete specifications MQ3 sensor specification (Mohammed M, 2016)

No.	Parameter	Values
1	Time taken for sensor to stabilize	15 to 20 second
2	Operating temperature	Room temperature=290C
3	Heater temperature	450C to 60^{o}C
4	Input voltage	5V
5	Output voltage range	0 to 4.75V
6	Saturated output voltage value	4.75V
7	Normal atmosphere detected value	1.85v to 2.5V
8	Human's breath without alcohol detected value	0.50v to 1.84V
9	Detected BAC%	0.00% to 0.06% - Normal
		0.08% to 0.20% - High

3.10.4 Best installation position of the alcohol sensor in the vehicle

The sensor must have been integrated within the casing above the steering column and positioned at the side door. Cabin air is continuously drawn from the sensor inlet through the optical cavity. The sensor signals allow continuous monitoring of the CO_2 and alcohol concentrations. The distance between the sensor at the steering column and the driver's head is typically 40-70 cm. The exhaled breath will thus be highly diluted when entering the sensor, calling for exceptional demands on signal resolution (Ljungblad et al., 2017). The sensor system may be integrated into suitable parts of the vehicle cabin as shown in Figures 3.31 and 3.32.

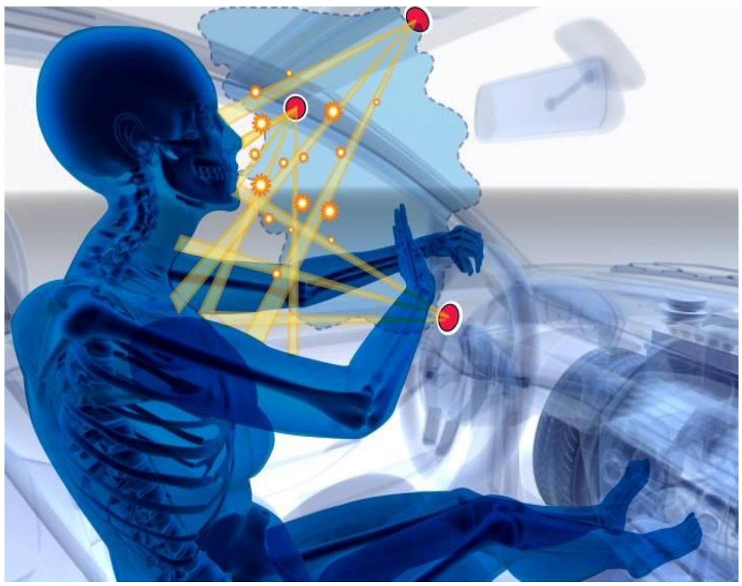

Figure 3. 31: Breath alcohol sensor mounting places (Maria Vegega, 2010)

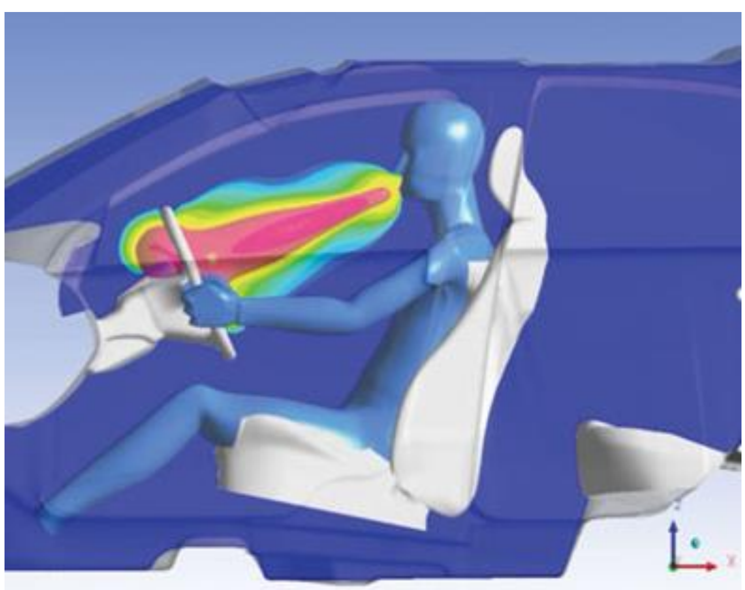

Figure 3. 32: Driver exhale gas striking area in the vehicle (Ljungblad et al., 2017).

CHAPTER FOUR

DESIGN ANALYSIS

4.1 General Vehicle Specification

The number of deaths and serious injuries in road accidents recorded by the Ethiopian Federal Police Commission shows that most of the accidents can be traced back to automobiles and taxis. Due to the dramatic increase in the number of nightclubs and bars in Addis Ababa, drivers are often exposed to alcoholic traffic accidents. Toyota Yaris 2010 Yaris Sedan model car is selected. See the general specification of the Toyota Yaris as shown in Table 4.1.

Table 4.1: General specification of Toyota Yaris Sedan (Yaris service & repair manual, 2010)

Engine	
Model	1.5L 4 cylinder (1NZ-FE)
Type	4 cylinder inline
Bore and stroke	75.0 mm and 84.7 mm
Horsepower	106 hp @ 6000 rpm
Transmission	4 Automatic
Max torque	140 Nm @ 4200 rpm
Maximum allowable speed	174 km/hr
Dimensions and weights	
Overall length, width, height	4300 mm, 1690 mm, 1460 mm
Wheelbase	2460 mm
Vehicle weight and carrying capacity weight	1043-1083 kg and 383 kg
Brake pedal	
Minimum pedal reserve distance when depressed with the pressure of 294N	With ABS greater than 73 mm Without ABS 70 mm
Pedal free play,	1-6 mm
Pedal height	107.3 – 117.3 mm
Accelerator pedal	
Pedal reserve distance	40mm(measured value)
Pedal free play	1-5 mm
Pedal height	65 mm (measured value)
Weight distribution front vs. rear is 59:41 (SAE)	

4.1.1 Pedal free play, reserve distance, and height

The brake pedal height is the travel distance between the brake pedal seat and the floor. The free stroke of the brake pedal is to measure the distance traveled by the pedal before the master cylinder starts to act for the first time. Depress the pedal until you feel a slight resistance. The brake pedal reserve is the measured value from the floor of the vehicle to the top of the brake pedal when the brake is applied. Pedal stroke is also called pedal displacement or pedal stroke. The maximum pedal resistance should not be greater than the maximum pedal resistance. The resistance of the pedal should be within the range of 36 to 53N for the accelerator pedal, and the resistance of the brake pedal should be less than 400N (Xi Yubin, 2015). The average maximum brake pedal force under ABS conditions is 383 N, while the average maximum brake pedal force of conventional brakes is 436 N (Fitch et al., 2010). From the Toyota Yaris Sedan 2010 service manual, the maximum brake pedal force is equal to 294N. Researchers have concluded that the maximum active pedal force varies from 136.3 N to 387 N (Macuzic et al., 2017).

From the research of the above researchers, the maximum pedal force applied to this automatic pedal control system is about

- The maximum force required to step on the brake pedal is 294N.
- The maximum force the driver can apply to the accelerator pedal is 387N.

Therefore, the total force required by the linear electric actuator is 294 N to depress the brake pedal and 387 N to lift the driver's foot off the accelerator pedal. The components should be designed based on these forces.

4.2 Center of Gravity and Maximum Gradient

Toyota Yaris Sedan 2010 is a four-wheel vehicle with brakes and front-wheel drive. SAE said the second-generation 2010 Toyota Yaris has a front-to-rear weight distribution of approximately 59:41. Then the longitudinal position of the center of mass C is computed from the following equations.

Longitudinal distance of the center of mass from front to rear

$$a_1=\frac{\text{weight distribution on rear}}{\text{total weight of the vehicle}}\times\text{wheelbase}$$

$$a_1=\frac{6010.6}{14660}\times 2460\text{mm}=\mathbf{1,008.6mm}$$

Longitudinal distance of mass center from the rear

$$a_2 = \frac{\text{weight distribution onfront}}{\text{total weight of vehicle}} \times \text{wheelbase}$$

$$a_2 = \frac{8649.4}{14660} \times 2460\text{mm} = \mathbf{1{,}451.4mm}$$

Thomas D. Gillespie summarized the typical values center of gravity height of different vehicles as shown in Table 4.2.

Table 4.2: Typical values center of gravity height of different vehicles (Jazar, R. N. 2017)

Vehicle Type	C.G Height (inches)
Sports car	18-20
Compact car	20-23
Luxury car	20-24
Pickup truck	30-35
Passenger van	30-40

Toyota Yaris 2010 model is a kind of compact car then takes the center of gravity height from the Table above 20-23 inches or 508-584.2 mm. Note that the average value of the center of gravity height is h = 541.1 mm. Hwan K. et al. 2017 Summarize the coefficients of friction of four road conditions: dry asphalt, gravel, wet as shown in Table 4.3.

Table 4.3: Road friction coefficient and road surface condition (Kim et.al, 2017)

Road Surface Conditions	Friction Coefficients
Dry Asphalt	0.8
Gravel	0.6
Wet	0.4
Snowy	0.3

Remark: Most of the times road surface condition in Ethiopia is dry asphalt and the value coefficient of friction is taken as 0.8. Different vehicles have different climbing capacities. The following is a list of maximum gradients for different means of transport.

Table 4.4: Maximum gradients for different means of transport (Hassen, M. A. 2015)

Means of transport	Maximum Gradient
Train	2%
Ordinary cars	25%
4 wheel drive cars	30%
Man–walking up Without support of hands	45%

Toyota Yaris is in the group of ordinary cars that can maximum climb up about 25% gradient. Then maximum inclination angle that can climb up to be

$$\tan\phi=0.25$$

$$\phi=\tan^{-1}(0.25)=14^{0}$$

4.2.1 Maximum achievable deceleration of a vehicle

To determine the maximum force required to stop the car, it is necessary to study the science of car dynamics. In a simplified study of braking, the aerodynamic resistance and rolling resistance can be neglected because they are usually much less than the braking forces. When studying car braking, we must take into account three conditions. The first condition is when the car accelerates on a flat road, the second condition is that the car accelerates on an uphill road, and the third condition is when the car accelerates on a slope. The inertial force is equal and opposite of the braking force (Khurmi, R. S., & Gupta, J. K. 2014).

Let

α = Angle of inclination of the plane to the horizontal,

m = Mass of the vehicle in kg (such that its weight is mg newton),

h = Height of the C.G. of the vehicle above the road surface in meters,

x = Perpendicular distance of C.G. from the rear axle in meters,

L = Distance between the centers of the rear and front wheels (also called wheelbase)

R_A = Total normal reaction between the ground and the front wheels in newton,

R_B = Total normal reaction between the ground and the rear wheels in newton,

μ = Coefficient of friction between the tires and road surface, and

a = Retardation of the vehicle in m/s^2

F_B = Total braking force on rear wheels and F_A = Total braking force on front wheels.

When the vehicle moves the level road, therefore retardation of the vehicle (maximum possible deceleration) (Genta, G., & Morello, L. 2019).

$$a = \mu \times g \qquad \text{Eq. 4.1}$$

$$a = 7.848\ {}^{m}/_{s^2}$$

When the vehicle moves down the inclined plane, therefore retardation of the vehicle (maximum possible deceleration) (Genta, G., & Morello, L. 2019).

$$a = g(\mu \times \cos\alpha - \sin\alpha) \qquad \text{Eq. 4.2}$$

$$a = 9.81\ {}^{m}/_{s^2}\left(0.8 \times \cos 14^{\circ} - \sin 14^{\circ}\right)$$

$$a = 5.24\ {}^{m}/_{s^2}$$

When the vehicle moves up the inclined plane, therefore retardation of the vehicle (maximum possible deceleration) (Genta, G., & Morello, L. 2019).

$$a = g(\mu \times \cos\alpha + \sin\alpha) \qquad \text{Eq. 4.3}$$

$$a = 9.81\ {}^{m}/_{s^2}\left(0.8 \times \cos 14^{\circ} + \sin 14^{\circ}\right)$$

$$a = 9.035\ {}^{m}/_{s^2}$$

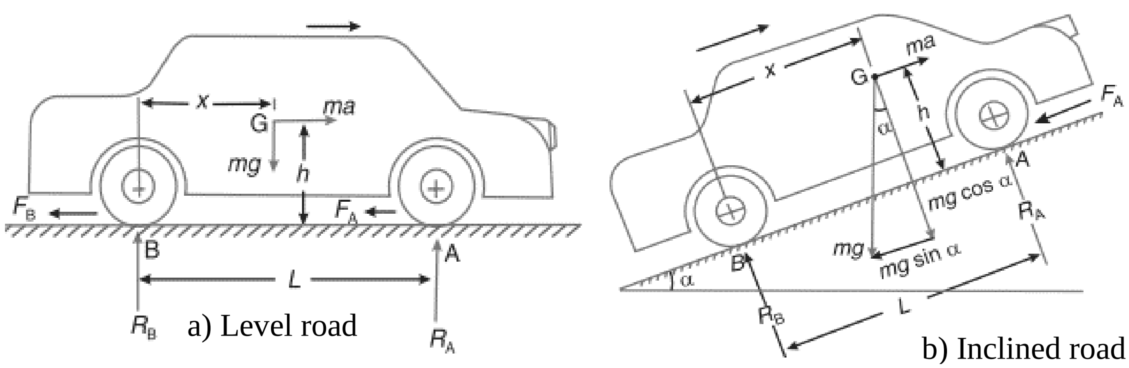

Figure 4.1: Accelerated car (Khurmi, R. S., & Gupta, J. K. 2014)

4.2.2 Vehicle stopping distance

Vehicle stopping distance is the sum of driver reaction distance and vehicle braking distance. The distance covered by the vehicle during full braking is called the braking distance, the longest braking distance depends on:

- The initial speed of the vehicle
- The type of surface
- The condition of the surface and the state of repair of the vehicle.
- Reaction time

4.2.2.1 Driver Reaction Times

The driver's response time includes recognizing that the lights have changed, deciding to continue driving or braking, and when you stop applying the brakes (take your foot off the accelerator and apply the brake). One controlled study found that the driver's average reactive braking time was 2.3 seconds. The study included all types of drivers, the tests were carried out on a controlled route and in a driving simulator (McGehee et al., 2010). The United Kingdom Highway Code and the ACPO Code of Conduct for the Operational Use of Police Commissioners' Association of Road Police Enforcement Technology use 3.0 seconds for the driver's response time. The National Security Council (NSC) recommends a minimum of 3 seconds (3 second reaction time) between vehicles traveling in the same lane. Some states, including California, have introduced a default driver response time of 2.5 seconds (https://copradar.com/redlight/factors/). However, when the driver drank, the alcohol reaction time was significantly longer. The reaction time also increases with the amount of consumed alcohol. The reaction time for drunk drivers with a BAC value of 0.80 g/L or higher is approximately 5 or more seconds (Siliquini et al., 2015).

4.2.2.2 Reaction distance

$$S = v \times t \qquad \text{Eq. 4.4}$$

Where

S= reaction distance in metres

v = speed in m/s.

t = reaction time in seconds.

4.2.2.3 Stopping distance

The stopping distance is based on the maximum deceleration that can be achieved. The distance traveled by the vehicle while braking can be obtained from the following equation 4.5 of motion, assuming a braking efficiency of 100% (Khurmi, R. S., & Gupta, J. K. 2014).

$$v^2 = u^2 - 2aS \qquad \text{Eq. 4.5}$$

Where

S= braking distance in meters

v = final speed in m/s.

a= maximum possible deceleration and u=initial speed in m/s

The rotating parts of the vehicle are slowed directly by the brakes. These parts must be accounted for when assessing the required braking power of the brakes and the energy that must be dissipated. Aerodynamic drag and rolling resistance can be neglected in a simplified study of braking, since they are usually far smaller than braking forces. Also, rolling resistance can be considered as causing a braking moment on the wheel more than a direct braking force on the ground (Genta, G., & Morello, L. 2019).

If the vehicle comes to standstill due to application of the brake, the final velocity, V = 0 in the above equation 4.5, then stopping distance, S is given by equation 4.6.

$$S=\frac{u^2}{2a} \qquad \text{Eq. 4.6}$$

Total stopping distance for alcohol drunk driver obtained from equation 4.7.

$$S=u\times5+\frac{u^2}{2a} \qquad \text{Eq. 4.7}$$

Total stopping distance for automatic braking the stepper motor needs 3 seconds to full depress the brake pedal. Then stopping distance obtained from equation 4.8.

$$S=u\times3+\frac{u^2}{2a} \qquad \text{Eq. 4.8}$$

4.3 Design of electric linear actuators

4.3.1 Components of electric linear actuators

Electric linear actuators have various components as shown in Figure 4.2. The inner tube is also known as the extension tube or the motor tube. This tube is attached to the threaded drive nut and expands and retracts as the nut moves along the axis of rotation. Lead screw, rotary screw, or lifting screw. This part of the linear actuator rotates, extends, or retracts the inner tube nut/tube, creating a linear motion. The drive nut can be tapered or spherical, connected to the inner tube, and moving along the main shaft. A nut is a component that allows the inner tube to extend or retract. Use a gear to increase or decrease the speed between the drive of the drive mechanism and the speed of the inner tube of the driven parts. The motor is where all the power is generated for the electric linear actuator (Firgelli A., 2018). The motor housing contains all the internal parts of the gear motor without leaving anything exposed to external damage.

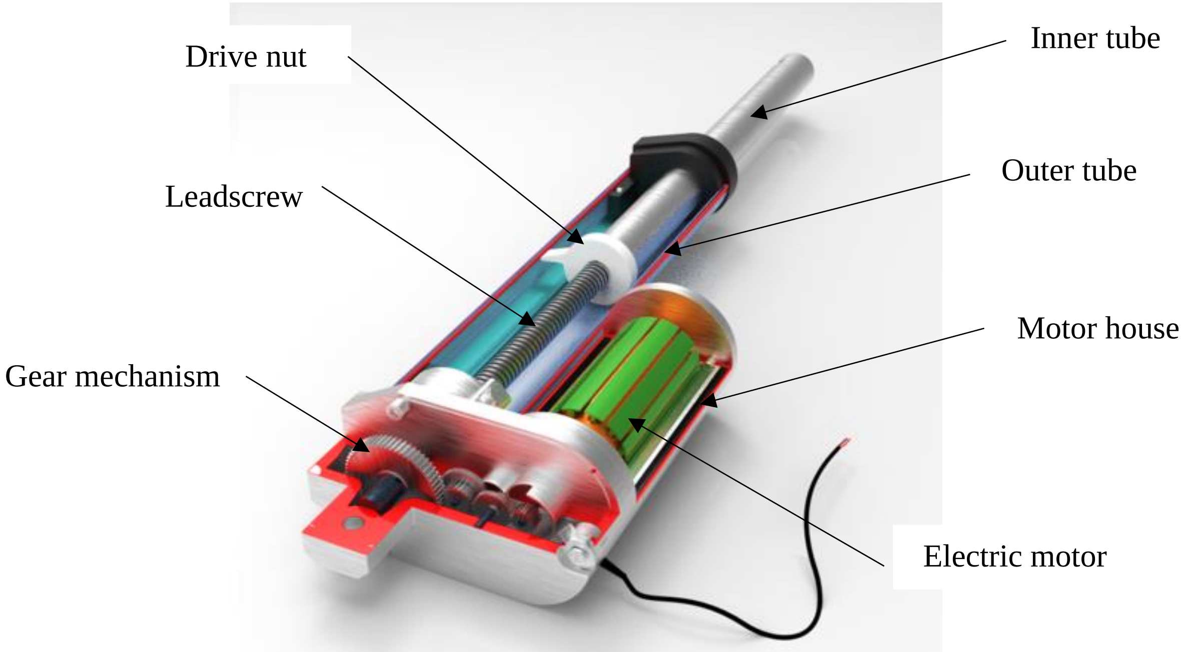

Figure 4.2: Components of electric linear actuators (Firgelli A., 2018)

4.3.2 Design of leadscrew (power screw)

A screw is a screw used as a coupling in a machine to convert rotational motion into linear motion. Threads are formed by cutting continuous spiral grooves on a cylindrical surface. Power screws have the following advantages (Juvinall & Marshek K., 2020).

- The power screw has a large carrying capacity.
- The power screw is small in size and compact in structure.
- The design of the power screw is simple.

a) Materials used for power screw

The screws are usually made from C30 or C40 steel. See the property of carbon steel in Table 4.5. Since the failure of the power propellers can lead to a serious accident, a higher safety factor is required. Nuts are made of a softer material than screws, so if they fail at all, the nut will fail, not the screw, which is more expensive and also difficult to replace. For the manufacture of nuts, plastic, bronze, or copper alloys are used. For steel screw and bronze nut. The value of the safety factor for the ultimate strength of soft materials and alloys is about six (Asmare, T., 2018).

Table 4.5: Mechanical properties of carbon steel (Juvinall & Marshek K., 2020)

Properties	Metric
Tensile strength	525 MPa
Yield strength	440 MPa
Bulk modulus (typical for steel)	140 GPa
Shear modulus (typical for steel)	80 GPa
Elastic modulus	200 GPa
Poisson's ratio	7872 kg/m^3

4.4. Design of accelerator and brake pedal actuator power screw

The maximum force required to depress the brake pedal is 294 N and the maximum force exerted on the accelerator pedal by the driver is 387 N (Macuzic et al., 2017). Suppose the material, coefficient of sliding friction, safety factor, and bearing pressure for the brake pedal force screw are similar to those of the Material used for accelerator power screw.

Let:

- p = Pitch
- μ = Coefficient of friction
- dc = Minor diameter
- d_o = Major diameter
- h = Thread depth
- d = Pitch diameter
- α = Helix angle
- W = Load to be lifted
- l = Lead
- φ = Friction angle
- σ = Axial stress
- n = Number of engaged thread

The axial stress σ in the body of power screw due to load W is

$$\sigma = \frac{W}{A} = \frac{4W}{\pi d_c^{\,2}} \quad \text{Eq. 4.9}$$

$$\sigma = \frac{\text{tensile stress}}{\text{FOS}} \quad \text{Eq. 4.10}$$

$$d_c = \sqrt{\frac{4 \times W}{\pi \times \sigma}} \quad \text{Eq. 4.11}$$

Take the value of the minor diameter of screw for accelerator and brake pedal power screw 4.582 mm and 4.001 mm respectively. Accelerator and brake pedal power screw minor diameter is approximate 4.77 mm and 4.02 mm respectively from the basic standard of basic dimensions of ISO metric screw threads as shown in Table 4.6.

Table 4.6: Basic dimensions of ISO metric screw threads (Juvinall & Marshek K., 2020)

Nominal or major diameter (d_o) in mm.	Minor or core diameter (dc) in mm	Pitch (p) in mm	Area of core (Ac) in mm^2
3	2.39	0.5	5.03
3.5	2.76	0.6	6.78
4	3.14	0.7	8.78
5	4.02	0.8	14.2
6	4.77	1	20.1

For minor dimeter of 4.02 mm accelerator pedal Acme tread screw the nominal see the Table 4.6. Nominal or major diameter meter d_o = 5 mm, Pitch (p) = 0.8mm, Thickness t = 0.37p = 0.296 mm and thread depth = h, for Acme screw h = 0.5p+0.25 = 0.65 mm and

Pitch diameter =d= d_o- $\frac{p}{2}$=4.6 mm, Helix angle $tan\ \alpha\ = \frac{p}{\pi\ d} = \frac{0.8mm}{\pi \times 4.6mm}$, α=3.17°, repeat the same procedure for brake pedal lead screw.

Ham and Ryan showed that the coefficient of friction in screw threads is independent of axial load, practically independent of speed, decreases with heavier lubricants, changes little with material combinations, and is best suited for steel on bronze (Budynas RG & Nisbett JK, 2011). Therefore the nut material chosen for this system is bronze. The friction coefficient for dry steel screw and bronze nut is 0.14-0.21, see Table 4.7.

Table 4.7: Coefficients of sliding friction pair materials (Budynas & Nisbett, 2012)

Screw material	Nut material			
	Steel	Bronze	Brass	Cast iron
Steel, dry	0.15–0.25	0.15–0.21	0.15–0.19	0.15–0.25
Steel, machine oil	0.11–0.17	0.10–0.16	0.10–0.15	0.11–0.17
Bronze	0.08–0.12	0.04–0.06	-	0.06–0.09

From the friction coefficient, we can find φ = the friction angle

$$tan\varphi = \mu, \varphi = tan^{-1}(0.18) = 10.20^{\circ}$$

Torque required to rotate the screw is

$$T=W \times \tan(\alpha+\varphi)\frac{d}{2} \qquad \text{Eq. 4.12}$$

Shear stress in the screw due to torque

$$\tau=\frac{16T}{\pi(d_c)^3} \qquad \text{Eq. 4.13}$$

4.4.1 Bearing pressure

To reduce the wear of the bolt and nut, the pressure of the bearing on the thread surfaces must be within the limits. In the design of power bolts, the bearing pressure depends on the materials of the bolt and nut, the relative speed between the nut and the bolt, and the nature of the lubrication (Tolomatic, 2019). See Table 4.8 for bearing pressure different materials.

Table 4.8: Limiting values of bearing pressures (Khurmi, R. S., & Gupta, J. K. 2014)

Application of screw	Material		Safe bearing pressure in N/mm^2	Rubbing speed at the thread pitch diameter
	Screw	Nut		
Hand press	Steel	Bronze	17.5 - 24.5	Low speed, well-lubricated
Lead screw	Steel	Bronze	1.05 – 4.25	High speed> 15 m / min

This power screw is used for lead threads and the screw nut combinations are steel and bronze respectively, so the safe surface pressure is 1.05 to 4.25N/mm^2. Suppose the load is evenly distributed across the threads it is in contact with. Number of meshes between threads and nuts;

$$n=\frac{W}{\frac{\pi}{4}\left(d_o^{\,2}-d_c^{\,2}\right)p_b} \qquad \text{Eq. 4.14}$$

4.4.1. Check bending, shear, compressive, and buckling stress

a) The maximum bending stress

The maximum bending stress occurs at the root of the thread. It is calculated by assuming the thread is a simple cantilever beam built-in at the root. The load is assumed to act at the mid-point on the thread (Gopinath R., 2014).

$$\sigma_b=\frac{3W\times h}{\pi\times d\times n\times t^2} \qquad \text{Eq. 4.15}$$

b) The maximum shear stress (Check the Threads for Shear)

Both the nut and screw threads are subject to traverse shear stress resulting from the bending forces. For a rectangular section, the maximums shear stress occurs at the neutral axis and equals (Gopinath R., 2014).

$$\tau=\frac{3W}{2\pi\times d_c\times n\times t} \qquad \text{Eq. 4.16}$$

c) Tensile /Compressive Stresses

A loaded power screw is subject to a direct tensile or compressive load. The tensile stress area is generally provided in a screw using a stress area based on the root diameter may be used for conservative design studies (Gopinath R., 2014).

$$A=\frac{\pi d^2}{4} \quad \text{Eq. 4.17}$$

Then Tensile /Compressive Stresses

$$\tau_{t/c}=\frac{W}{A} \quad \text{Eq. 4.18}$$

d) Combined Stresses

According to maximum shear stress theory, the maximum shear stress

$$\tau_{max}=\frac{1}{2}\sqrt{(\sigma)^2+4\tau^2} \quad \text{Eq. 4.19}$$

According to maximum normal stress theory, the maximum normal stress

$$\sigma_{max}=\frac{1}{2}\sigma_b+\frac{1}{2}\sqrt{(\sigma)^2+4\tau^2} \quad \text{Eq. 4.20}$$

4.5. Design of accelerator and brake pedal drive Nut

There is a relative motion between the screw and the nut and wear is also occurring. Bronze is an ideal material for nuts because

- Its excellent corrosion resistance.
- Higher tensile strength.
- It has excellent conformability and machineability and a low coefficient of friction

The nut material is bronze for which the elastic limit may be taken as 100MPa in tension, 90MPa in compression, and 80MPa in shear. For steel screw and bronze nut. The value of the factor of safety based on the ultimate strength of soft material and alloys is about six (Asmare, T., 2018). Let

- W = Load
- h = Axial length of nut
- D_1 = inner diameter nut
- D_2 = Outer diameter nut collar
- N = Number of thread engaged
- σ_t= Tearing strength
- σ_c= Compression strength
- t_1= Thickness of nut collar

The axial length of nut (h) is given by $h = n \times p$

a) Determine the inner diameter of the nut

The inner diameter D_1 is found by considering the tearing strength of the nut. We know that

$$W=\frac{\pi}{4}\left[D_1{}^2-d^2\right]\times\sigma_t \quad \text{Eq. 4.21}$$

$$D_1 = \sqrt{\frac{4w}{\pi \times \sigma_t} + d^2} \qquad \text{Eq. 4.22}$$

b) Determine the outer diameter of nut collar

The outer diameter D_2 is found by considering the crushing strength.

$$W = \frac{\pi}{4}\left[D_2^{\,2} - D_1^{\,2}\right] \times \sigma_c \qquad \text{Eq. 4.23}$$

$$D_2 = \sqrt{\frac{4w}{\pi \times \sigma_c} + D_1^{\,2}} \qquad \text{Eq. 4.24}$$

c) Determine the thickness of the nut collar

Considering the shearing of the collar of the nut, we have

$$W = \pi \times d \times t_1 \times \tau \qquad \text{Eq. 4.25}$$

$$t_1 = \frac{W}{\pi \times d \times \tau}$$

The shear stress at the root of the threads in the nut and screw is given by

$$\tau = \frac{3W}{2\pi \times d \times n \times t} \qquad \text{Eq. 4.26}$$

4.6 Design of coupling between the lead screw shaft and stepper motor shaft

A good shaft coupling should have the following requirements ((Juvinall & Marshek K., 2020).

- ➢ It should be easy to connect or disconnect.
- ➢ It should transmit the full power from one shaft to the other shaft without losses.
- ➢ It should hold the shafts in perfect alignment.
- ➢ It should reduce the transmission of shock loads from one shaft to another shaft.
- ➢ It should have no projecting parts.

4.6.1 Design of sleeve

The usual proportions of a cast iron sleeve coupling are as follows:

- ➢ Outer diameter of the sleeve, D = 2d + 13 mm, D = 2 × 5mm+13mm=23mm
- ➢ length of the sleeve, L = 3.5 d, L = 3.5 × 5mm =17.5mm

We know that torque transmitted by a hollow section

$$T = \frac{\pi}{16} \times \tau_c \left(\frac{D^4 - d^4}{D}\right) \qquad \text{Eq. 4.27}$$

Where

- τ_c = Permissible shear stress
- l = Length of key,

- T = Torque transmitted by the shaft,
- F = Tangential force
- d = Diameter of the shaft,
- w = Width of a key.
- t = Thickness of key, and
- τ and σ_c = Shear and crushing stresses

The safe value of shear stress for cast iron may be taken as 14 MPa (Khurmi, R. S., & Gupta, J. K. 2014). The induced shear stress in the sleeve is less than the shear stress value of cast iron. Therefore, the design is safe.

4.6.2 Design for key

The width and thickness of the coupling key are taken from the ratio. The length of the coupling key is at least the same as the length of the sleeve (that is, 3.5d). Table 4.9 shows standard parallel, taper, and Gib head key ratios in accordance with IS: 2292 and 2293-1974.

Table 4.9: Proportions of standard parallel, tapered keys (Khurmi. S., & Gupta, J. K. 2014)

Shaft diameter (mm) up to and including	Key cross-section	
	Thickness (mm)	Width (mm)
6	2	2
8	3	3
10	4	4
12	5	5
17	6	6

Since the diameter of the shaft is 5 mm, the length of key L=17.5 mm, Width of key w=2 mm Thickness of key t=2 mm. Let us now check the induced shear and crushing stresses in the key. First of all, let us consider the shearing of the key. We know that torque transmitted (T).

Considering shear stress

$$\tau = \frac{2\times T}{L\times w\times d} \qquad \text{Eq. 4.28}$$

Considering crushing stress

$$\sigma_c = \frac{4\times T}{L\times t\times d} \qquad \text{Eq. 4.29}$$

The permissible crushing stress for the usual key material is at least twice the permissible shearing stress. Therefore, we have w = t. In other words, a square key is equally strong in shearing and crushing. Since the induced shear and crushing stresses are less than the permissible stresses (14 MPa), therefore the design of the key is safe.

4.6 Determine motor Power

4.6.1 Maximum motor power to control accelerator and brake pedal

The maximum power required by a stepper motor to depress the automobile pedals can be determined by

$$P = T\omega_n \qquad \text{Eq. 4.30}$$

The distance that the drive nut travel to depress the pedals is equal to the maximum travel distance of the pedal. It is equal to maximum pedal travel of brake pedal (40mm) and accelerator pedal 30mm.

4.6.1.1 Speed of brake pedal motor

The driver's reaction time includes recognizing a change in the light signal, the decision to continue driving or to brake, and when stopping - applying the brake (remove the foot from the accelerator and apply the brake). A controlled study found that the average driver's response time to braking was 3 seconds and lift accelerator pedal is about 1.8 seconds (McGehee et al., 2013). Assume that the total time required to automatically depress the brake pedal of the vehicle is equal to 3 seconds.

$$v=\frac{s}{t}=\frac{0.04\text{m}}{3\text{ s}}=0.013\ {}^{\text{m}}/_{\text{s}}$$

Lead is the linear travel of the nut. The lead single start power screw is equal to the pitch of the screw and approximately equal to one revolution of the screw.

$$\text{lead(l)=pitch(p)}\approx 1\ \text{revolution}$$

$$\frac{v}{l}=n[\ {}^{\text{rev}}/_{\text{s}}\ ]$$

$$n=\frac{0.013\ {}^{\text{m}}/_{\text{s}}}{0.0008\text{m}}=16.66\ {}^{\text{rev}}/_{\text{s}}=1000\ \text{rpm}$$

Angular velocity

$$\omega=2\pi n=104.625\ {}^{\text{rad}}/_{\text{s}}$$

Then power required by the motor

$$P=0.1308\text{N.m}\times 104.625\ {}^{\text{rad}}/_{\text{s}}$$

$$P=13.68\text{watt}$$

4.6.1.2 Speed accelerator pedal motor

Assume the total time required to automatically lift the vehicle accelerator pedal equal to 1.8 seconds (McGehee et al., 2013).

$$v=\frac{s}{t}=\frac{0.03m}{1.8\ s}=0.0166\ {}^{m}/_{s}$$

Lead is the linear travel of the nut. The lead single start power screw is equal to the pitch of screw and approximately equal to one revolution of the screw.

$$\text{lead(l)=pitch(p)}\approx 1 \text{ revolution}$$

$$\frac{v}{l}=n[{}^{rev}/_{s}]$$

$$n=\frac{0.0166\ {}^{m}/_{s}}{0.001m}=16.66\ {}^{rev}/_{s}=1000\ \text{rpm}$$

Angular velocity

$$\omega=2\pi n=104.625\ {}^{rad}/_{s}$$

Then power is required by the motor

$$P=0.21156N.m\times 104.625\ {}^{rad}/_{s}$$

$$P=22.135\text{watt}$$

4.6.2 Selecting appropriate stepper motor

From the methodology part of selecting the best motor and the maximum power required to control vehicle pedals, the specification of the stepper motor should be within the following specification see Table 4.10.

Table 4.10: Required specification of stepper motor

Criteria's	Accelerator pedal motor	Brake pedal motor
Maximum power	22.135 watt	13.68 watt
Maximum torque	0.21156 N.m	0.1308 N.m
Maximum rpm	1000	1000
Type of stepper motor		
Based on construction		Hybrid
Based on the arrangement of stator windings		Bipolar
Input voltage		---

Table 4.10, the required data specification NEMA 17 bipolar stepper motor 24 V DC, 2A and this motor models can meet the requirements. Refer to the speed and torque curve in the black box in Figure 4.3. Since the vehicle has only a 12V battery it needs an additional 12V battery since 24V dc was selected for the work of this thesis. It has a 5 mm diameter shaft, which fits the screw diameter. This makes the coupling of the motor shaft and the lead screw easy. The required torque specifications are 0.21156 N.m and 0.1308 N.m, and the speed for both pedal actuators is 100 RPM, which are used for accelerator and brake pedal drive.

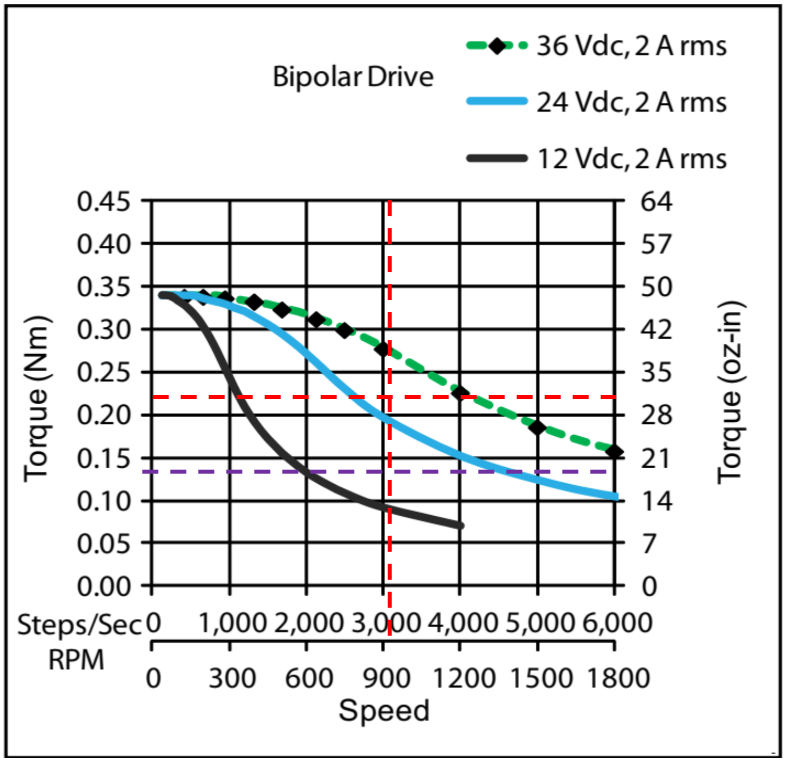

Figure 4. 3: Stepper motor torque vs speed
(http://www.pbclinear.com/Download/DataSheet/Stepper-Motor-Support-Document.pdf)

4.7 Design of brake and accelerator pedal actuating inner tube

Inner tubes are also known as extension tubes, drive tubes, translating tubes, or pistons. This tube is usually made of aluminum or steel. While retracted, the inner tube is where the spindle is located. This tube is attached to a threaded drive nut that expands and contracts as the nut moves along the rotating spindle. The inner tube is usually made of aluminum or stainless steel. For this task, the material chosen for the inner tube to reduce weight is aluminum.

Material properties of aluminum alloy Young's modulus (68.9 GPa), shear modulus (26 GPa), shear strength (207 MPa), tensile yield strength (276 MPa), compressive strength (280 MPa), and ultimate tensile strength are 310 MPa (Elsherif et al., 2019).

The inner tube is the hollow circular part of the linear electric actuator and is also considered a vertical rod subject to buckling and compressive stress, one end of which is free and the other end is fixed. The force on the inner tube, which is equal to the load required to operate the brake pedal, is 294 N with a rod length of about 40 mm (Macuzic et al., 2017). The force acting on the inner tube is equal to the load required to lift the driver's leg from the gas pedal, which is 387 N for a rod length of about 30 mm (Macuzic et al., 2017). The minimum inner diameter must be greater than the outer diameter of the screw shaft and there must be sufficient clearance between the screw shaft and the inner tube. Suppose the gap between the screw and the inner tube is 1mm.

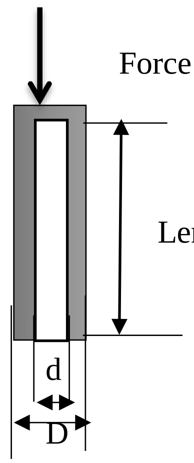

In order to calculate buckling stress use Euler's formula

Let

- E =elasticity modules
- A =area
- K =least radius of gyration
- C=end fixity coefficient (c=0.25 for one ended fixed
- Wcr=crippling force
- σ_{cr}=crushing stress
- L/k=slenderness ratio
- L =length

According to Euler's theory, the crippling or buckling load (W_{cr}) under various end conditions is represented by a general equation (Khurmi, R. S., & Gupta, J. K. 2014).

$$W_{cr}=C \times \pi^2 \times E \times \frac{I}{L^2} \quad \text{Eq. 4.31}$$

$$W_{cr}=C\pi^2 \times E \times \frac{A \times K^2}{L^2} \text{ where } (I=A \times K^2) \quad \text{Eq. 4.32}$$

$$W_{cr}= C \times \pi^2 \times E \times \frac{A}{\left(\frac{L}{K}\right)^2} \quad \text{Eq. 4.33}$$

And crippling stress

$$\sigma_{cr}=\frac{W_{cr}}{A} \qquad \text{Eq. 4.34}$$

$$\sigma_{cr}=\frac{C\times\pi^2\times E}{\left(\frac{L}{K}\right)^2} \qquad \text{Eq. 4.35}$$

In order to determine the vertical bar is short or long calculate the slenderness ratio by equating crippling stress to crushing stress. The inner tube is considered as a short bar if cylinder ness ratio ($\frac{L}{K}$) less than 80. Since $\frac{L}{K}$ less than 80 Euler's formula is not valid we must use Professor Johnson's formula for the short bar. Then we can determine the outer diameter of the inner tube (Juvinall & Marshek K., 2020).

$$W_{cr}=A\left[\sigma_y-\frac{2\sigma_y}{3\pi}\left(\frac{l}{k}\right)\sqrt{\frac{\sigma_y}{3\times C\times E}}\right] \qquad \text{Eq. 4.36}$$

$$W_{cr}=\left(\frac{\pi}{4}\left(D^2\text{-}d^2\right)\right)\left[\sigma_y-\frac{2\sigma_y}{3\pi}\left(\frac{l}{k}\right)\sqrt{\frac{\sigma_y}{3\times C\times E}}\right] \qquad \text{Eq. 4.37}$$

$$D=\sqrt{\frac{4\times W_{cr}}{\pi\left[\sigma_y-\frac{2\sigma_y}{3\pi}\left(\frac{l}{k}\right)\sqrt{\frac{\sigma_y}{3\times C\times E}}\right]}+d^2} \qquad \text{Eq. 4.38}$$

4.8 Design of brake pedal control motor mounting bar

The distance between the mounting tape point and the load applied by the motor is approximately 150 mm. The maximum force applied to the rod is 294 N (Macuzic et al., 2017). The material used for the engine mounting rod can be aluminum or steel metal. Steel is more suitable for rail installation because it has a higher resistance to bending, pressure, shear, and tensile strength than aluminum. The specified cross-section is a circular steel bar due to its higher resistance to bending than the sacred cross-section.

$$M=\sigma_b\times\frac{\pi}{32}\left(D^3\right) \qquad \text{Eq. 4.39}$$

Where

σ_b= allowable bending stress and M=maximum bending moment

$$\sigma_b=\frac{\sigma_{ultimate}}{FOS}=\frac{650MPa}{2}=325MPa$$

a) Determining maximum bending moment

Free body diagram

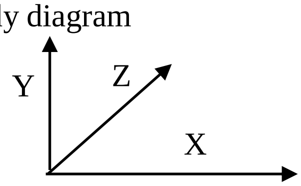

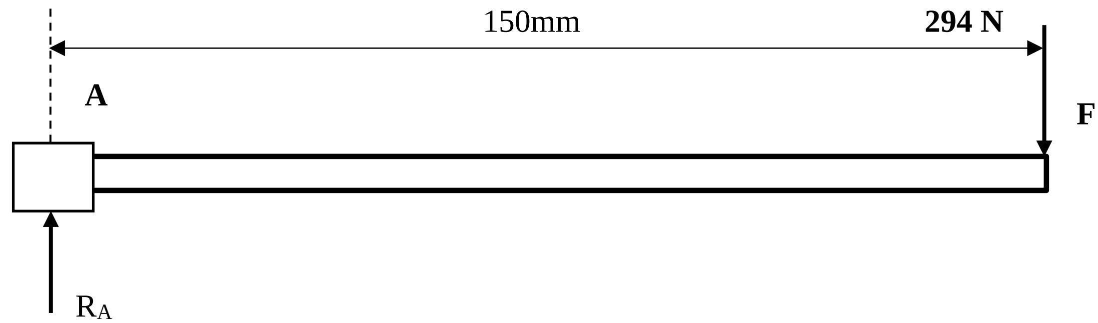

Maximum Reaction Force at the fixed end can be expressed as:

$$R_A = F = 294\text{N}$$

Bending moment at A

$$\sum M_A = 0,\ 294\text{N} \times 150\text{mm} = 44.1\ \text{N.m}$$

b) Shear force and bending moment diagram

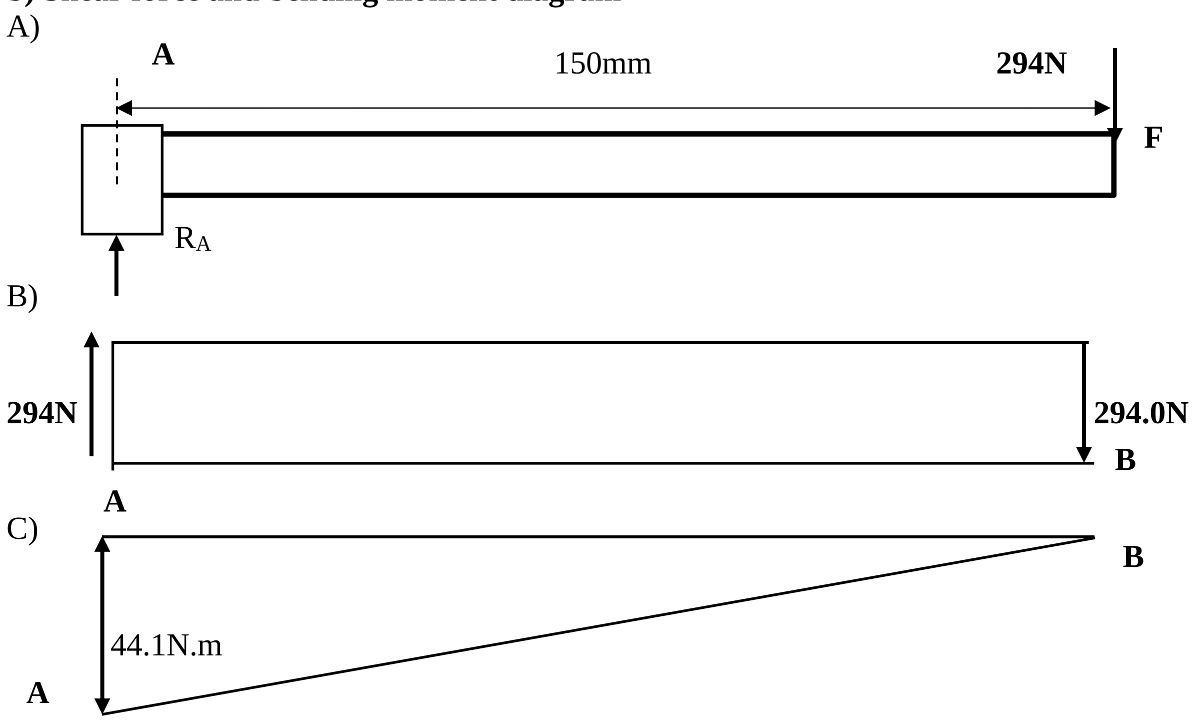

Figure 4.4: (A) free body diagram (B) Shear force diagram (C) Bending moment diagram

c) Shear force diagram

- Shear force at A, $F_A = R_A = +294\text{N}$
- Shear force between A and B is constant and equal to +294N
- Shear force at B, $F_B = -294\text{N}$

Bending momentum diagram

- B.M at A $M_A = 44.1\text{N.m}$

- B.M at B $M_B = 0$

Therefore, the maximum bending moment at D which is equal to 45,000N.mm. Then we can calculate the diameter of the bar from the maximum bending moment.

$$D=\sqrt[3]{\frac{M\times 32}{\sigma_b \times \pi}} \qquad \text{Eq. 4.40}$$

4.9 Vehicle Speed Sensor output Pulse

From LS DYNA software analysis the vehicle speed must be less than or equal to 36 km/h that we can apply the automatic brake without any injury to the driver and passengers. So it is very important to get the output pulse (frequency) of the vehicle speed sensor at 36km/h vehicle speed. The vehicle speed of the Toyota Yaris 2010 sedan automatic transmission vehicle has a HOL-2VSS0003 vehicle speed sensor as shown in Figure 4.5.

Figure 4.5: HOL-2VSS0003 vehicle speed sensor

4.9.1 Determine wheel speed sensor frequency from the vehicle speed

The sampled pulse frequency (f) is computed from measurements of the time of each low to high transition. The output of the speed sensor is a sequence of pulses at a frequency that is proportional to car speed.

Let

ω_g = Rotational speed of the gearbox output shaft speed (rad/s)

ω_d = Rotational speed of the differential crown wheel (rad/s)

ω_w = Rotational speed of the wheel (rad/s)

$v_w =$ Wheel linear speed (m/s)

$v_v =$ Vehicle linear speed (m/s)

i_0 = Gear ratio of the differential

r_w = Radius of the wheel (m)

Since both vehicle and wheel move together in a linear direction, the vehicle (linear) speed is equal to the linear speed of the wheel. Then calculate the wheel's linear speed, also give the vehicle's speed.

$$v_w = v_v \qquad \text{Eq. 4.41}$$

Wheel's linear speed is calculated function of rotational speed and radius as:

$$v_w = \omega_w \times r_w \qquad \text{Eq. 4.42}$$

The vehicle speed is 36 km/h or 10m/s. From Table 4.11 the tire size is P175/65R14.

Table 4.11: Gear ratio of Toyota Yaris 2010 (https://www.caranddriver.com/toyota/yaris/specs)

Automatic Transmission 4 Speeds	Ratio
First Gear Ratio (:1)	2.85
Second Gear Ratio (:1)	1.55
Third Gear Ratio (:1)	1.00
Fourth Gear Ratio (:1)	0.70
Reverse Ratio (:1)	2.34
Final Drive Axle Ratio (:1)	4.24
Tire Size	P175/65R14

Then wheel radius of the wheel can be calculated from tire size. From tire size

Aspect ratio (AR) = 65%

Tire width (W) = 175 mm

Rim diameter (D) = 14 inch = 0.3556 m

The aspect ratio (AR) is defined in percentage, as the ratio between tire sidewall height (H) and tire width.

$$AR\ (\%) = \frac{H}{W} \times 100 \qquad \text{Eq. 4.43}$$

$$H = 0.65 \times 175 = 113.75\ \text{mm} = 0.11375\ \text{m}$$

The wheel diameter d_w (m) is the sum between the rim diameter and twice the height of the tire:

$$d_w = D + 2 \times H \qquad \text{Eq. 4.44}$$

$$d_w = 0.3556\ \text{m} + 2 \times 0.11375\ \text{m} = 0.5831\ \text{m}$$

The (free static) wheel radius r_w (m) is half the wheel diameter:

$$r_w = \frac{d_w}{2} = \frac{0.5831\ m}{2} = 0.29155m$$

Wheel's angular speed is calculated function of linear speed and radius as:

$$\omega_w = \frac{v_w}{r_w} = \frac{10\ {}^{m}/_{s}}{0.29155\ m} = 34.299\ {}^{rad}/_{s}$$

The wheel speeds are equal with the differential speed:

$$\omega_w = \omega_d$$

The rotational speed of the differential crown wheel is also reduced, being equal gearbox output shaft speed divided by the differential gear ratio:

$$\omega_w = \omega_d = \frac{\omega_g}{i_0}$$

The rotational speed of gearbox output shaft:

$$\omega_g = \omega_w \times i_0 = 34.299\ {}^{rad}/_{s} \times 4.24 = 145.4296\ {}^{rad}/_{s}$$

The following formula is used to convert the angular frequency in radians per second to the frequency in revolutions per minute.

$$rpm = \frac{{}^{rad}/_{s}}{2\pi} \times 60$$

Then the rotational speed of gearbox output shaft:

$$\omega_g = 145.4296\ {}^{rad}/_{s} = 1389.45477\ rpm = 23.1576\ rps$$

The Frequency of the wheel speed sensor is the number of teeth passing the sensor every second in Hz. The speed sensor doesn't have teeth. The speed sensor is usually a magnetic pick-up type of (active or passive) that senses changes in magnetic density. However, it used a toothed wheel under the speed sensor for speed measurement. Most of the time a toothed wheel has 60 teeth to get the number of pulses per second generated is directly proportional to the speed in RPM. Therefore the wheel rotates at the wheel speed sensor frequency divided by the number of teeth.

$$\text{output shaft rotation (revs per second)} = \frac{\text{wheel speed sensor frequency (Hz)}}{\text{number of teeth}}$$

$$\text{wheel speed sensor frequency (Hz)} = 23.1576 \times 60 = 1389.45477\ \text{Hz}$$

This frequency of the wheel speed sensor is then used to write the Arduino code to control the brake pedal actuator.

CHAPTER FIVE

RESULTS AND DISCUSSION

5.1 Design Results

The design geometric dimensions of the accelerator gas and brake pedal actuation system components are shown in Tables 5.1 and 5.2. See Table 5.3 for maximum bending, shear, and bending stress.

Table 5.1: Accelerator pedal actuator dimensions

Actuating system	Components	Parameters (Unit)	Symbol	Values
Accelerator pedal actuator	Lead screw	Minor diameter (mm)	dc	4.77
		Major diameter (mm)	d_o	6
		Helix angle (°)	α	3.313
		Friction angle (°)	Φ	10.2
		Thread depth (mm)	h	0.75
		Pitch (mm)	p	1
		Thickness (mm)	t	0.259
		Pitch diameter (mm)	d	5.5
		Thread engagement with nut	n	9
	Drive nut	Inner diameter (mm)	D_1	7.7
		Outer diameter (mm)	D_2	8.5
		Thickness (mm)	t	2
		Axial length (mm)	L	9
	Inner tube	Outer diameter (mm)	D	8
		Inner diameter (mm)	d	7
		Length (mm)	L	30
Shaft coupling	Sleeve	Outer diameter (mm)	D_O	25
		Inner diameter (mm)	D	6
		Length (mm)	l	17.5
	Key	Length (mm)	l	17.5
		Width (mm)	w	2
		Thickness (mm)	t	2

Table 5. 2: Brake pedal actuator dimensions

Actuating system	Components	Parameters (Unit)	Symbol	Values
Brake pedal actuator	Lead screw	Minor diameter (mm)	dc	4.02
		Major diameter (mm)	d_o	5
		Helix angle (^{o})	α	3.17
		Friction angle (^{o})	Φ	10.2
		Thread depth (mm)	h	0.65
		Pitch (mm)	p	0.8
		Thickness (mm)	t	0.296
		Pitch diameter (mm)	d	4.6
		Thread engagement with nut	n	10
	Drive nut	Inner diameter (mm)	D_1	7
		Outer diameter (mm)	D_2	8.5
		Thickness (mm)	t	1.5
		Axial length (mm)	L	10
	Inner tube	Outer diameter (mm)	D	7
		Inner diameter (mm)	d	6
		Length (mm)	L	40
Shaft coupling	Sleeve	Outer diameter (mm)	D_O	23
		Inner diameter (mm)	D	5
		Length (mm)	l	17.5
	Key	Length (mm)	l	17.5
		Width (mm)	w	2
		Thickness (mm)	t	2

Table 5. 3: Maximum bending, shear, and bending stress for gas and brake pedal actuators

<table>
<tr><th>Components</th><th colspan="2">Parameter</th><th>Values (N/mm^2)</th><th>Remark</th></tr>
<tr><td rowspan="5">Brake pedal lead screw</td><td colspan="2">Maximum bending stress</td><td>32.78</td><td rowspan="10">Maximum bending, shear, and combined stress less than the ultimate tensile stress of screw material ($150\ N/mm^2$).</td></tr>
<tr><td colspan="2">The maximum shear stress (Check Threads for Shear)</td><td>8.22</td></tr>
<tr><td colspan="2">Tensile /Compressive Stresses</td><td>28.11</td></tr>
<tr><td rowspan="2">Combined Stresses</td><td>Maximum shear stress theory</td><td>18.34</td></tr>
<tr><td>Maximum normal stress theory</td><td>36.67</td></tr>
<tr><td rowspan="5">Accelerator pedal lead screw</td><td colspan="2">Maximum bending stress</td><td>45.87</td></tr>
<tr><td colspan="2">The maximum shear stress (Check Threads for Shear)</td><td>11.95</td></tr>
<tr><td colspan="2">Tensile /Compressive Stresses</td><td>19.72</td></tr>
<tr><td rowspan="2">Combined Stresses</td><td>Maximum normal stress theory</td><td>18.34</td></tr>
<tr><td>Maximum shear stress theory</td><td>36.67</td></tr>
</table>

5.2 Simulate Arduino code in Proteus

The coded alcohol detection program is uploaded to the microcontroller that controls via Arduino. The alcohol sensor detects the alcohol content exhaled by the driver, and the stepper motor controls the vehicle pedal. The Arduino code is compiled as a HEX file and uploaded to Proteus. Proteus software is used to test the circuit to check whether the system is working properly. In order to change the BAC value of the driver, the POT-HG in the Proteus library generates different input voltages for the microcontroller. POT-HG allows the resistance to be changed during the simulation run in Proteus. In order to vary vehicle speed sensor signal generator is used. Based on the program developed by Arduino and burned on the microcontroller, the simulation model circuit shows the driver status. There are three ranges of conditions that continuously measure the driver's BAC and report the BAC level.

Condition One: When the BAC of the driver is lower than 0.5 g/L, the LCD display shows the driver "NORMAL DRIVE", as shown in Figure 5.1. Therefore, the pedal control system operates under normal conditions. The stepper motor pedal actuator stops. The buzzer and LED are off.

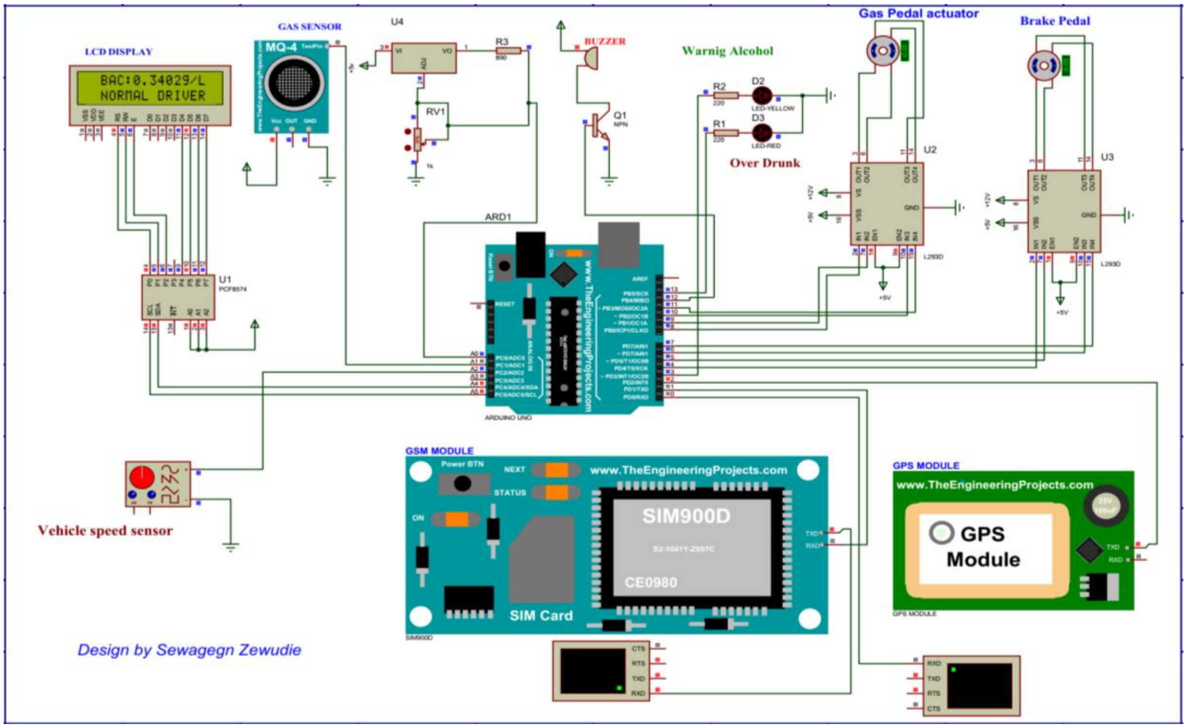

Figure 5.1: System simulations under normal condition

Condition Two: When the driver's BAC is greater than 0.5 mg/L and less than 0.8 g/L. The pedal control system operates under normal conditions. However, the LCD display the message “ALCOHOL WARNING” to the driver and the yellow LED flash continuously to warn the driver to be careful as shown in Figure 5.2.

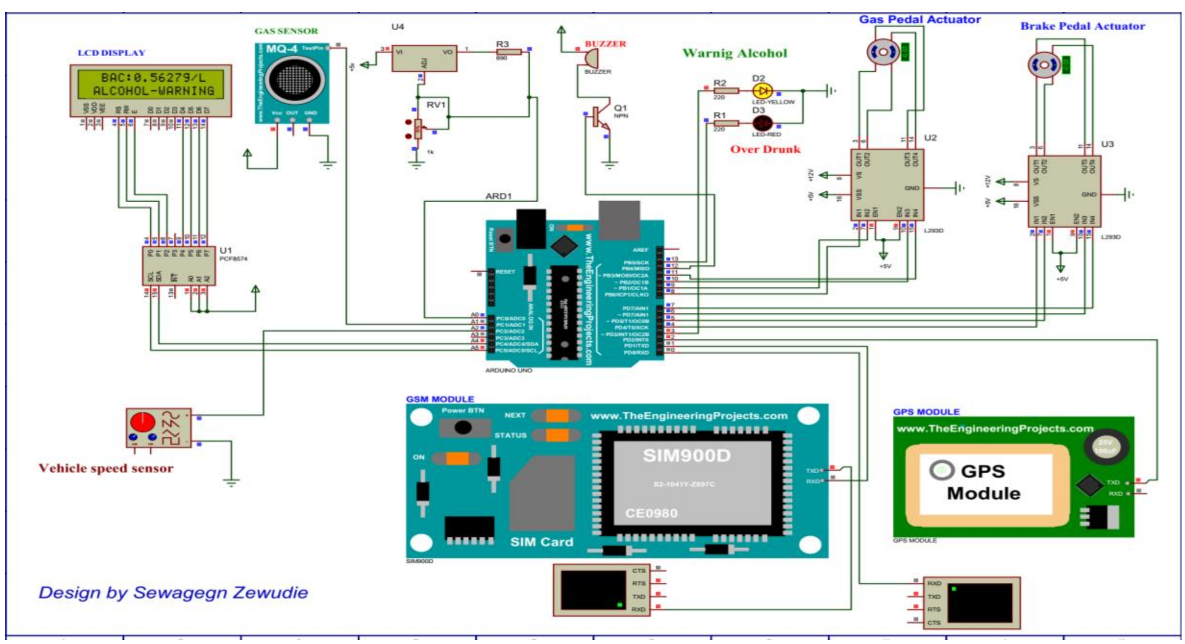

Figure 5.2: System simulations under alcohol warning condition

Condition Three: when the driver's BAC exceeds 0.8 g/L, the LCD displays the message "OVER DRUNK" to the driver, and the stepper motors rotate to control the pedals. The pedal control system remains off until the vehicle speed sensor signal is below 1390 Hz or 36 km/h then control brake pedal. The red LED flashes continuously, the buzzer beeps to surrounding drivers to take caution, as shown in Figure 5.3. The GSM module sends the location of the car to the owner or to the police station and virtually displays the message sent.

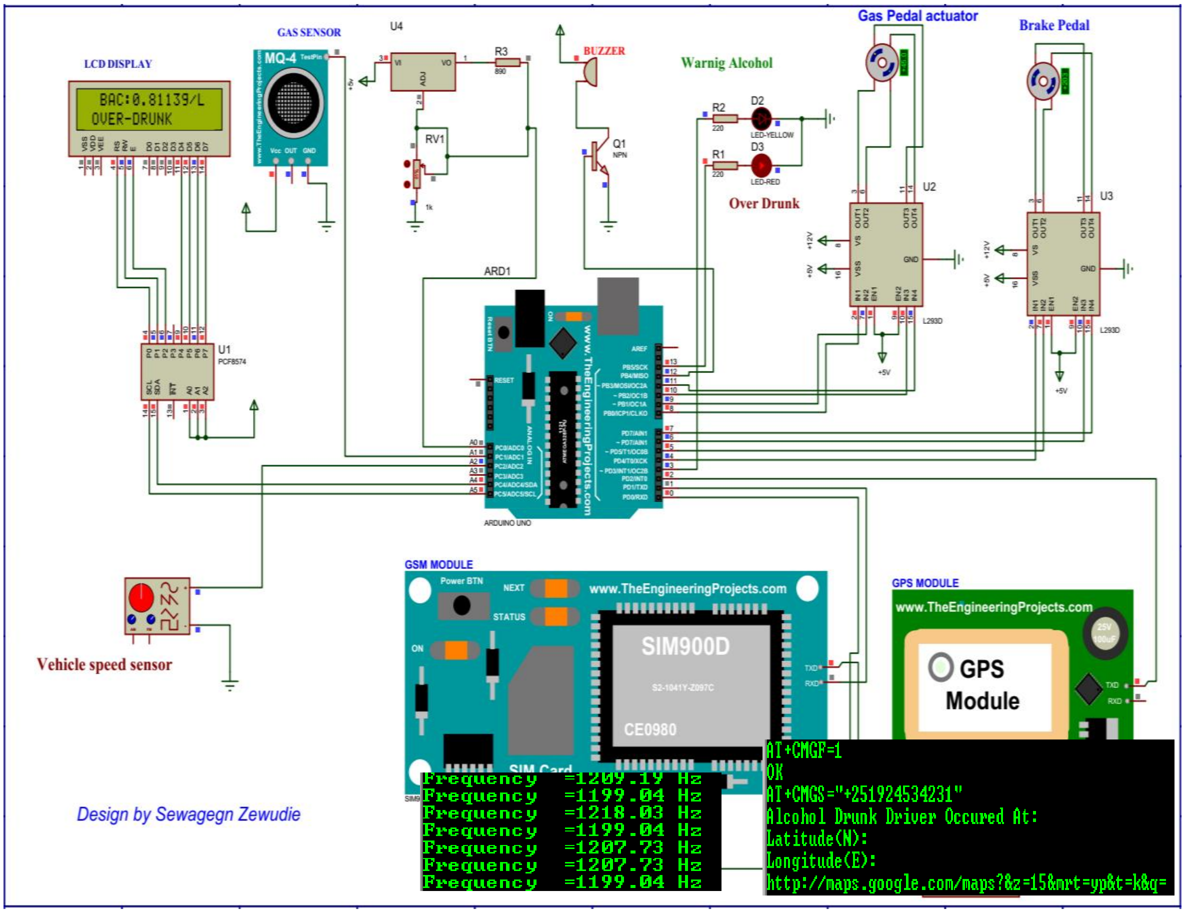

Figure 5.3: System simulations during over drunk condition

5.3 Analysis of the LS-DYNA simulation results

In this LS-DYNA simulation, the assumption was simulated that the vehicle would stop immediately when braking without delay. The analysis, values of the maximum chest deflection, head injury criteria (HIC), femur strength, and upper neck strength of the dummy are evaluated during emergency braking. These values can then be compared to the Federal Motor Safety Standards for occupant injuries.

The deflection values of the dummy's head, chest, and femur are sufficient to compare the requirements of crash regulations. The simulation test results show that the safety of the vehicle is good during emergency braking.

Driver injury criteria result from LS-Dyna post-processing that is results compared to the standard value of the criteria for a head injury, chest deviation, index of chest severity, and maximum force exerted on the femur as stipulated by the Federal Motor Safety Standard (FMSS) and the National Highway Traffic Safety Administration (NHTSA).

5.3.1 Head Injury Criteria (HIC)

Head injuries, which primarily affect skull fractures and brain injuries, are among the most commonly considered injuries. According to FMVSS No. 208, HIC_{15} and HIC_{36} in the center of gravity of the head for 50% dummy were partially developed for the assessment of the risk of injury to the head, the safety standard values are 700 for HIC_{15} and 1000 HIC_{36}, respectively.

According to the graph in Figure 5.4, the maximum value of HIC_{15} at the center of gravity of the head (at 15-millisecond intervals) is 494.5, 588.4, and 714.6/h at 35 km/h, 36 km/h, and 37 km, respectively. These values are below the 700 limit at 35 km/h and 36 km/h, which means that the degree of the head is safe. However, at 37 km/h, the HIC_{15} value is higher than the limit, which means more head injuries.

According to the diagram in Figure 5.5, the maximum value of HIC_{36} (over a time interval of 36 milliseconds) at the head's center of gravity is 934.2, 983.9, and 1224 at 35 km/h, 36 km/h, and 37 km/h, respectively. These values are below the 1000 limit at 35 km/h, 36 km/h, which means less head injury. However, at 37 km/h, the HIC36 exceeds the 1000 limit, which means a higher degree of head injury.

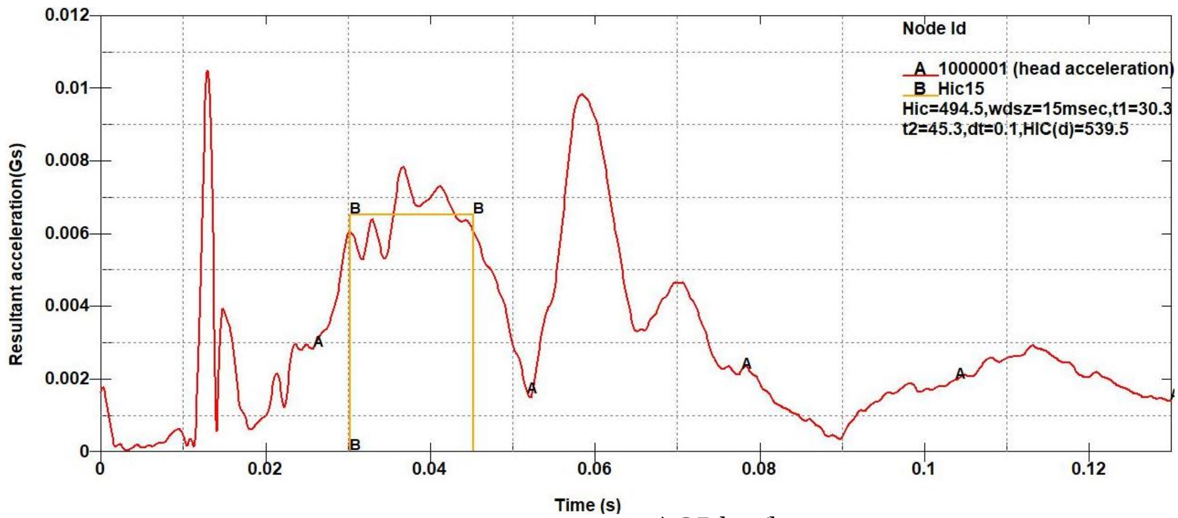

a) 35 km/h

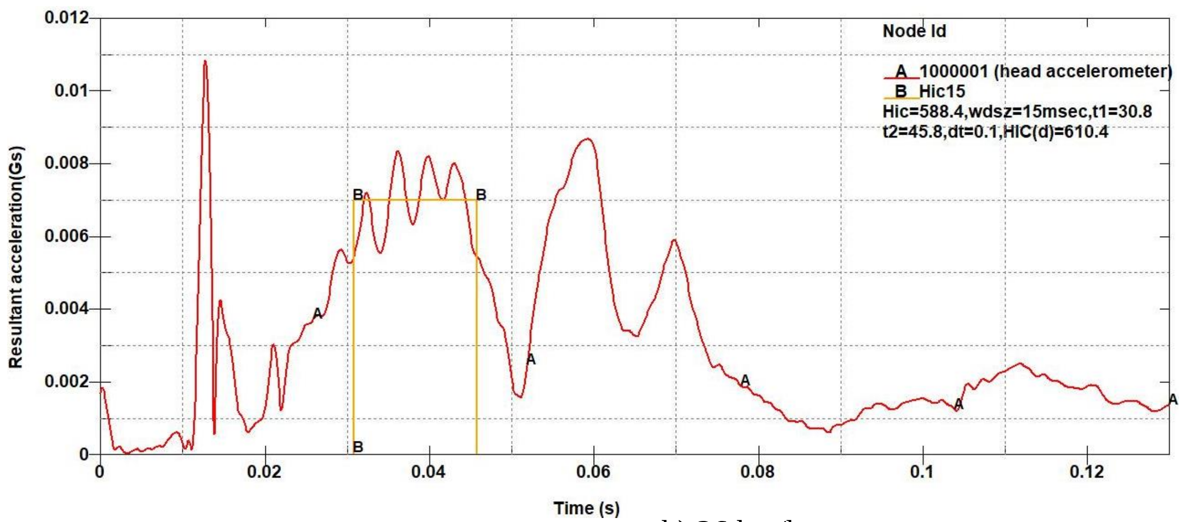

b) 36 km/h

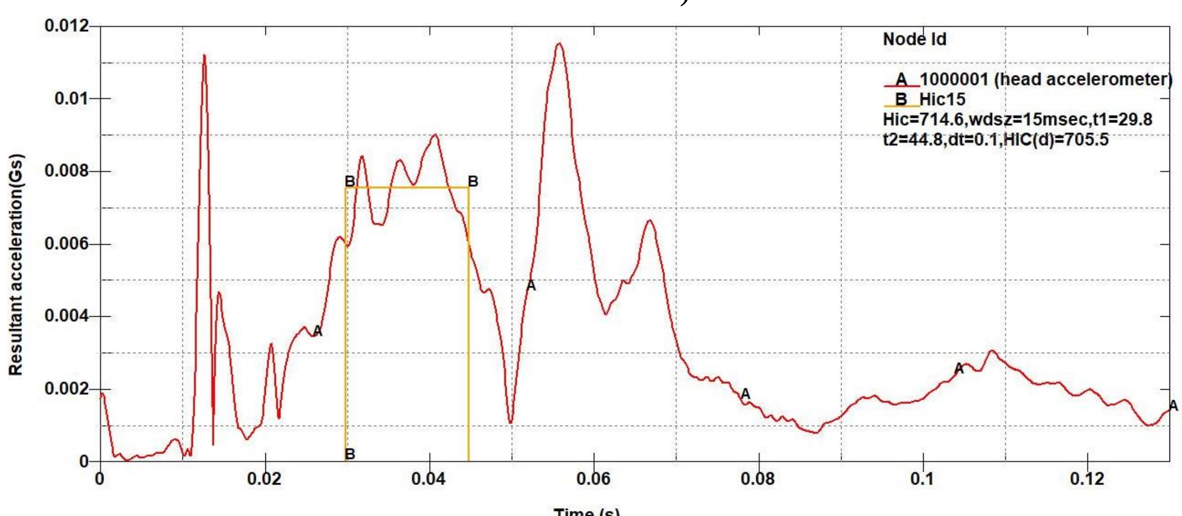

c) 37 km/h

Figure 5.4: Head injury criteria (HIC_{15}) at different vehicle speed

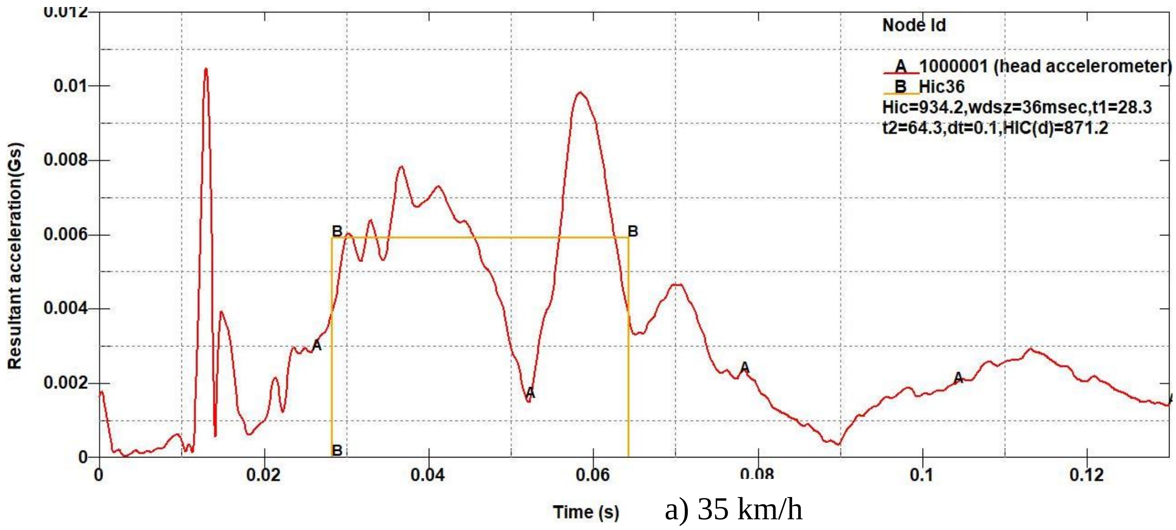

a) 35 km/h

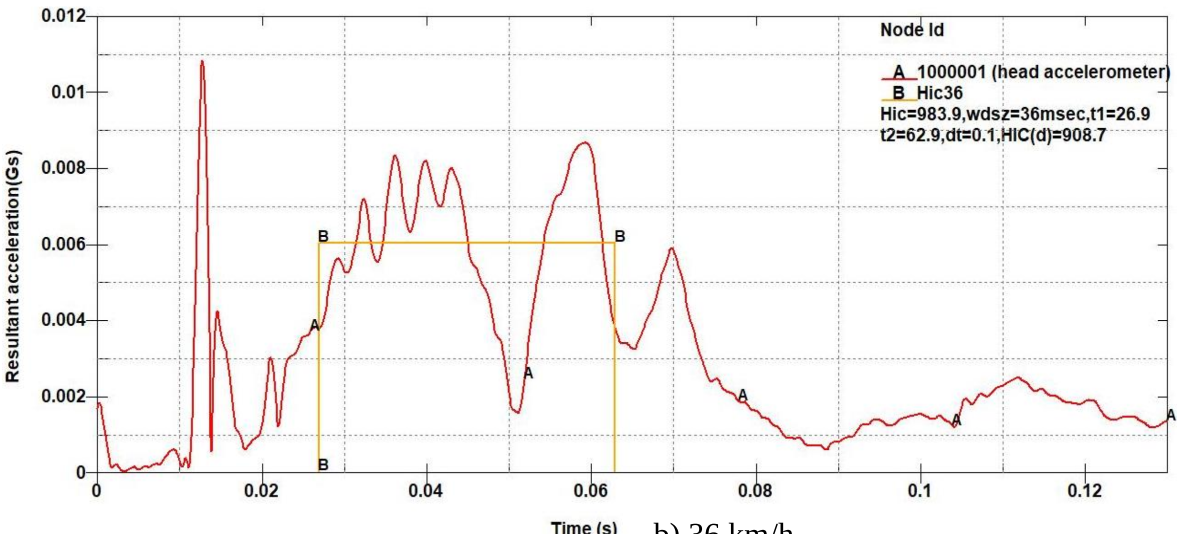

b) 36 km/h

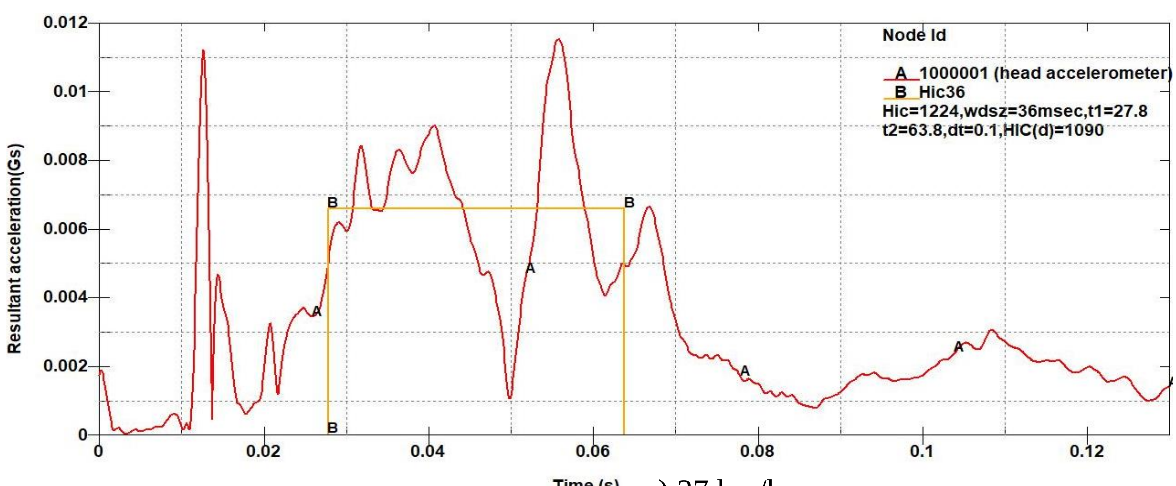

c) 37 km/h

Figure 5.5: Head injury criteria (HIC_{36}) at different vehicle speed

5.3.2 Maximum Force on the Femur

The axial force developed in the femur was measured in the longitudinal direction of the femur bone. A good prediction of the axial femur force is important to assess the safety of femur bone and hip joint.

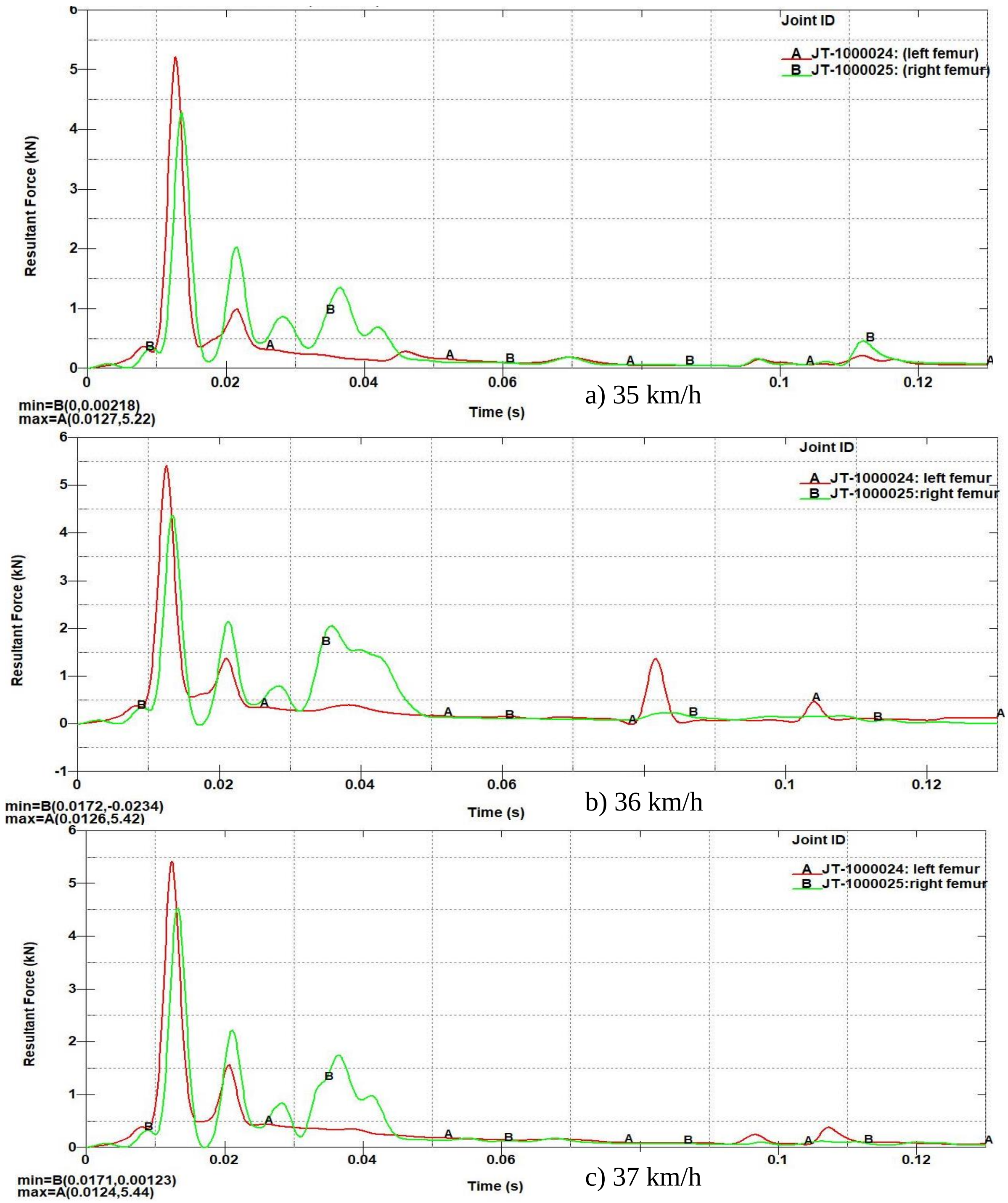

Figure 5.6: Maximum force on femur at different vehicle speed

As shown in Figure 5.6, the maximum femur forces were captured by the simulation for both the left and right femurs. It was measured with a linear chest potentiometer installed in the Hybrid III dummy. According to FMVSS No. 208, the risk of femur injury is assessed in part based on the force exerted on the femur. The maximum femoral strength of 50% dummy is 10 kN. The maximum force exerted on the femur from the LS-DYNA simulation is 5.2 kN, 5.42 kN, and 5.44 kN at 35 km/h, 36 km/h, and 37 km/h, respectively. Therefore, based on maximum femur force exerted on the driver at three different speeds is lower than the standard, which means that the femur is safe.

5.3.3 Maximum deflection of the chest

Chest deflection is another important measurement besides chest acceleration in the assessment of chest injury upon emergency braking. It is measured by a linear chest potentiometer installed in the Hybrid III dummy. According to FMVSS No. 208, part of the basis for assessing the risk of chest injury is chest deflection. The maximum chest deflection of 50^{th} % of the dummy is 63 mm. As shown in Figure 5.7, the maximum chest deflection obtained from LS-DYNA simulation is 45 mm, 47.1 mm, and 48 mm at 35 km/h, 36 km/h, and 37 km/h, respectively. Therefore, based on the maximum chest deflection, the driver's chest deflection is below the standard limit at three different speeds. This means that the degree of chest injury is safe.

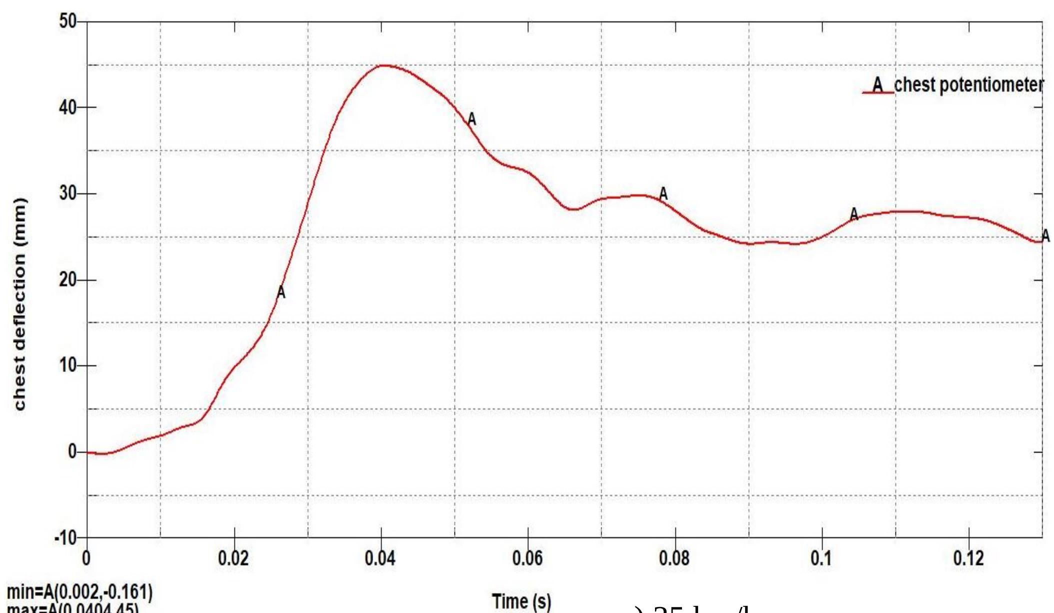

a) 35 km/h

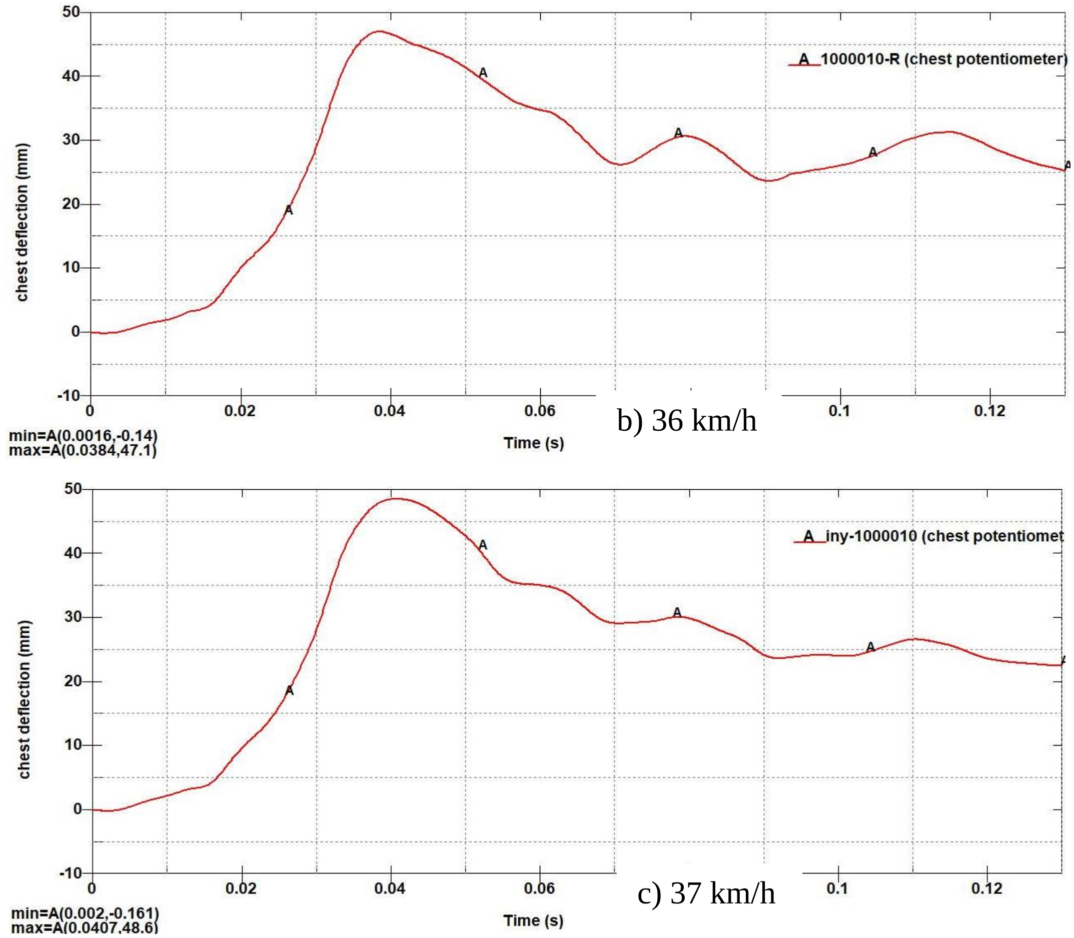

Figure 5.7: Maximum chest deflection at different vehicle speed

5.3.4 Maximum force on the upper neck

Neck injuries are usually related to damage to the spinal cord. Injuries to the neck and spinal cord typically result from a combination of axial and bending loads. Due to the geometric and structural complexity, there are currently no generally accepted criteria for neck injuries. In a simple form, the neck could be modeled as a slender column or beam. The standard permissible neck load on the neck specified by FMVSS No. 208 to avoid neck injuries is axial compression 4000 N, axial tensile force 3300 N, and shear force 3200 N. As shown in Figure 5.8, the maximum resulting forces on the neck obtained from LS-DYNA simulations are 2960 N, 3120 N and 3910 N at 35 km/h, 36 km/h and 37 km/h, respectively. Therefore, based on the maximum force on the driver's neck at 35km/h and 36km/h speed is lower than the standard limit, this means that the neck and spinal cord area are safe. However, at 37km/h, the maximum neck force is greater than the standard limit, resulting in a high degree of injury.

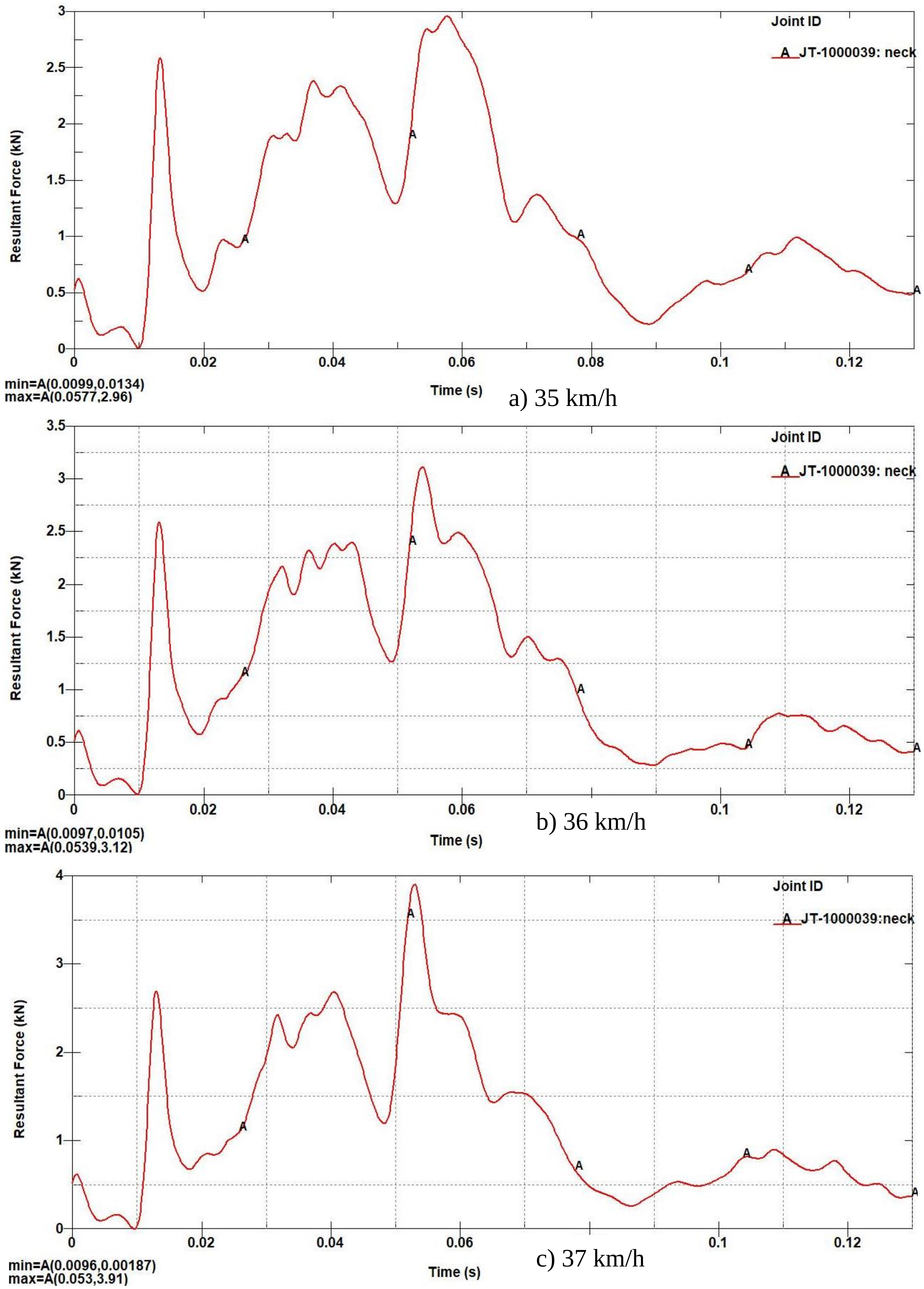

Figure 5.8: Maximum force on the upper neck at different vehicle speed

From the above analysis of driver injury criteria at 35 km/h and 36 km/h, maximum HIC15, HIC36 of the head, maximum chest deflection, femur force, and neck force are below the standard limits of FMSS No. 208. Hence the safe degree of driver injury. However, with a neck force, the HIC15 and HIC36 values exceed the FMSS No. 208 limit at 37 km/h, resulting in higher driver injuries. Therefore the automatic brake pedal control system must activate when the vehicle speed drops to 36 km/h from high speed in order to stop the vehicle without injuring the driver and passenger.

5.3.5 Simulation result verification

In order to verify that the model is stable and able to produce physical results, some controls were performed taking into account the basic energy and mass balances. In particular, it is checked that the global energy and mass involved in the simulation vary within a reasonable range. The verification of energy and mass conservation was performed according to the verification evaluation criteria (Mongiardini, M. 2010). See Table 5.1.

Table 5.4: Analysis solution verification for the numerical model (Mongiardini, M. 2010)

Verification Evaluation Criteria	Change (%)	Pass
Total energy of the analysis solution (i.e., kinetic, potential, contact) must not vary more than 10 percent from the beginning to the end run.	4	✓
Hourglass Energy of the analysis solution at the end of the run is less than five percent of the total initial energy at the beginning of the run.	0.001	✓
The part/material with the highest amount of hourglass energy at a time during the run is less than five percent of the total initial energy at beginning of the run.	0.001	✓
Mass added to the total model is less than five percent of the total model mass at the beginning of the run.	0.08	✓
The part/material with the most mass added had less than 10 percent of its initial mass added.	0.08	✓
The moving parts/materials in the model have less than five percent o Mass added to the initial moving mass of the model.	0.08	✓
Are there any shooting nodes in the solution?	No	✓
Are there any solid elements with negative volumes?	No	✓

All the criteria listed in Table 5.4 passed, the model is considered stable.

5.3.5.1 Verification of dummy response

In order to verify the association between the values of injury indices, the biomechanical response of each part of the occupant model is analyzed in LS-DYNA. These responses are particularly important to check more accurately whether the impact between the body parts of the dummy and the seat structures occurs approximately at the same time instant for simulation. Dummy response during braking at LS-DYNA compared to European Economic Commission for Europe (ECE) sled test video (https://www.youtube.com/watch?v=M7zoaDta5xs).

The response of the dummy during emergency automatic braking of the vehicle is shown in Figures 5.9 to 5.15.

- At a time of 0 millisecond, the dummy is placed in the backrest.
- At 20ms, the dummy's back leaves the backrest, bends its neck slightly, and begins to move forward. The dummy slides forward along the seat as a whole, and the legs move forward and begin to collide under the dashboard.
- At the 40ms time point, the lower part of the dummy slides backward along the seat due to the impact on the dummy legs (due to Newton's Law of Action and Reaction). However, the head tends to tilt, the arms move forward and up. The belt keeps the dummy moving forward and deflects the chest.
- When the time reaches 60ms, the head goes down and the arms keep moving the head forward to reach the extreme position.
- When the time reaches 80ms, after the head reaches an extreme position, the front part of the vehicle begins to wind backward as the neck stretches.
- When the time reaches 100ms, the head and neck gradually bounce due to the traction of the muscles.
- When the time is 120ms, the head bounces back highly.

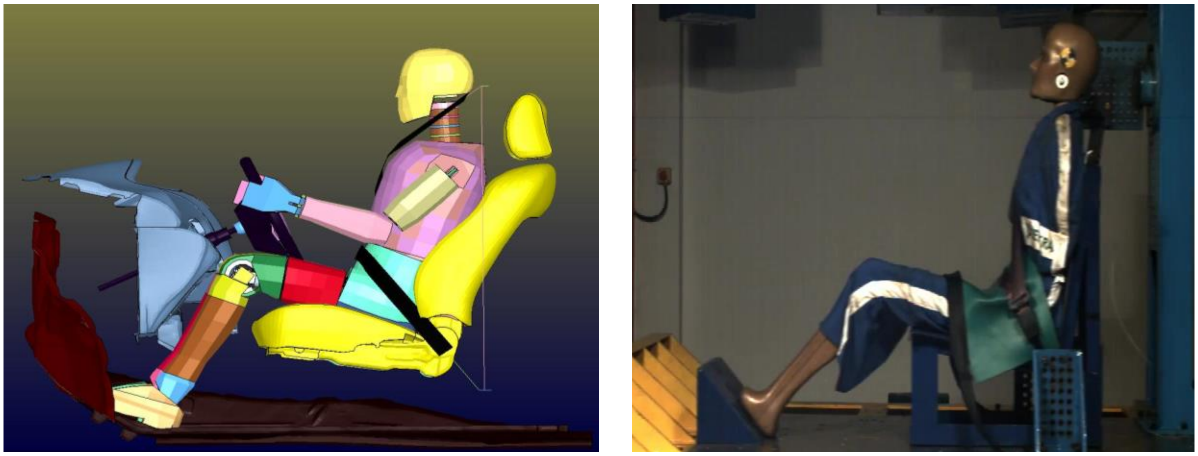

a) LS-DYNA analysis b) ECE laboratory sled test

Figure 5.9: Dummy responses at 0 millisecond

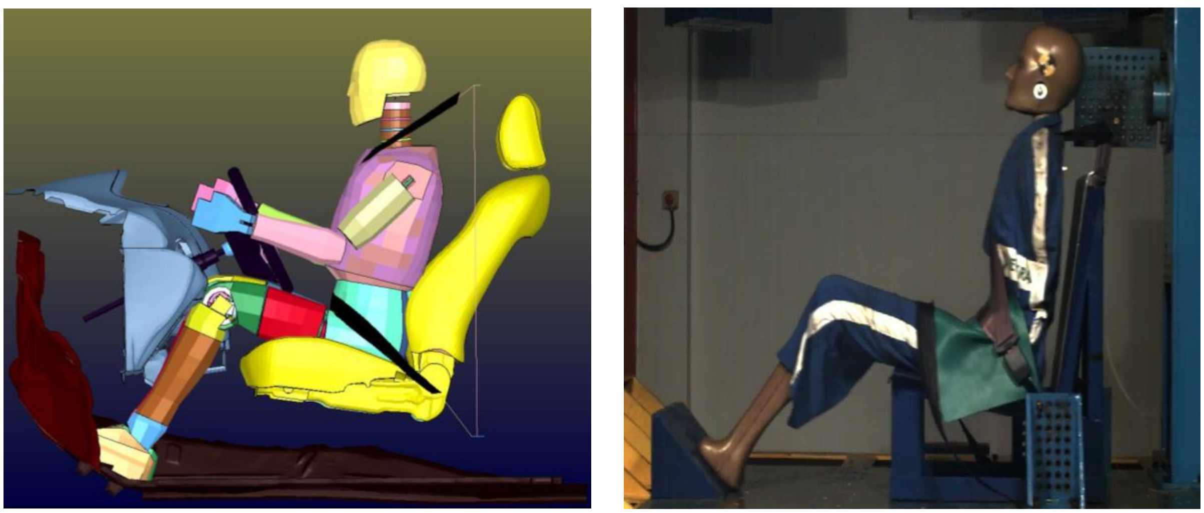

a) LS-DYNA analysis b) ECE laboratory sled test

Figure 5. 10: Dummy responses at 20 millisecond

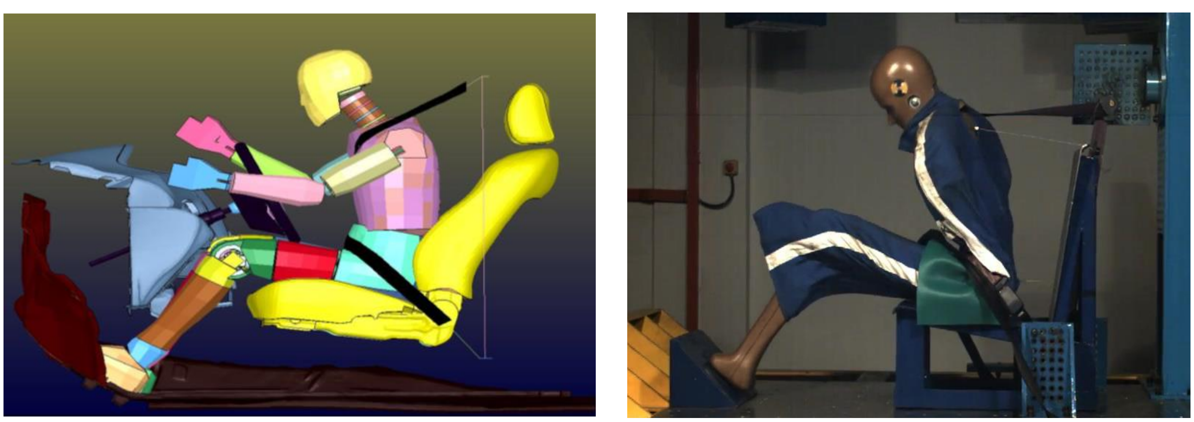

a) LS-DYNA analysis b) ECE laboratory sled test

Figure 5.11: Dummy responses at 40 millisecond

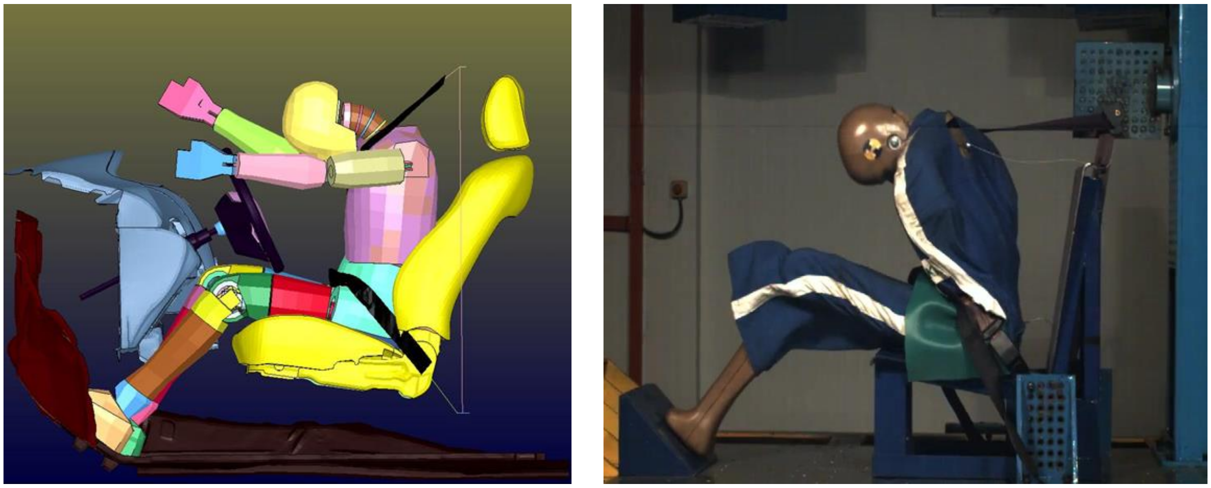

a) LS-DYNA analysis b) ECE laboratory sled test

Figure 5.12: Dummy responses at 60 millisecond

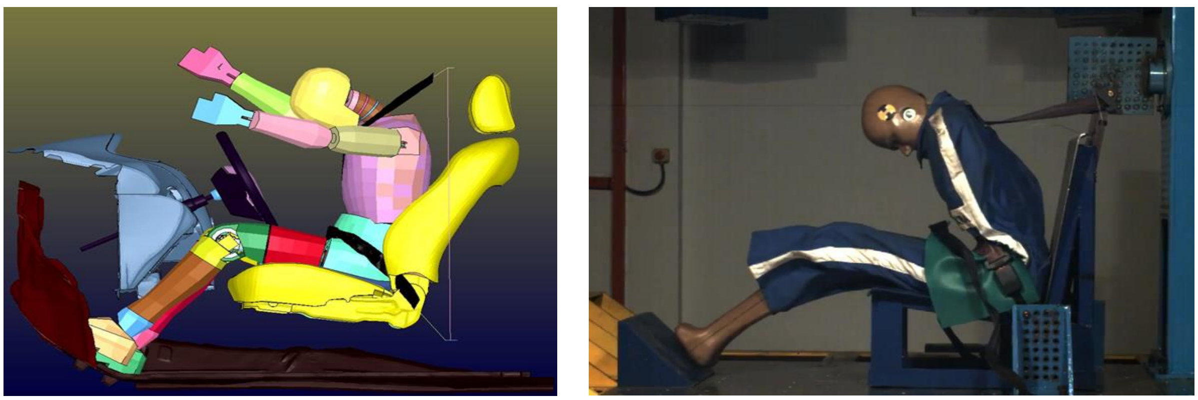

a) LS-DYNA analysis b) ECE laboratory sled test

Figure 5.13: Dummy responses at 80 millisecond

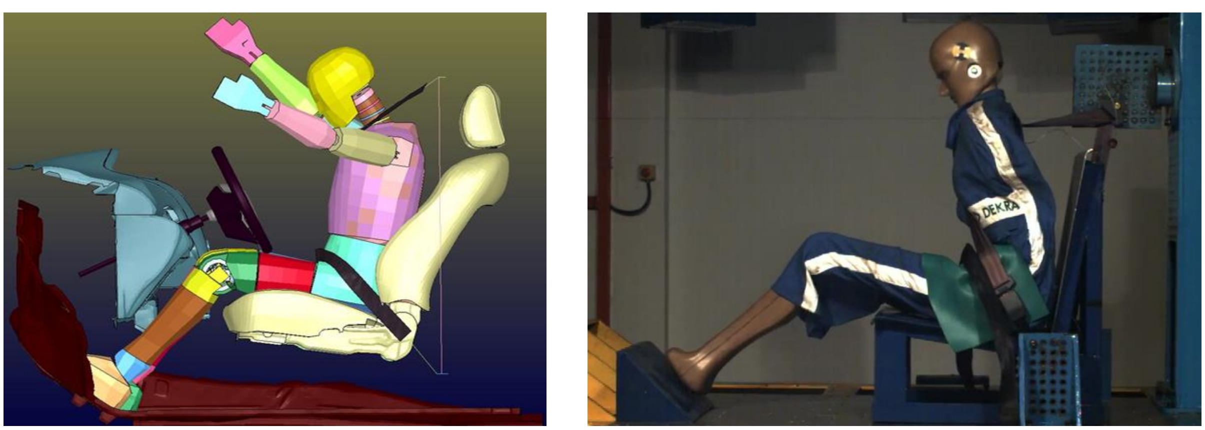

a) LS-DYNA analysis b) ECE laboratory sled test

Figure 5.14: Dummy responses at 100 millisecond

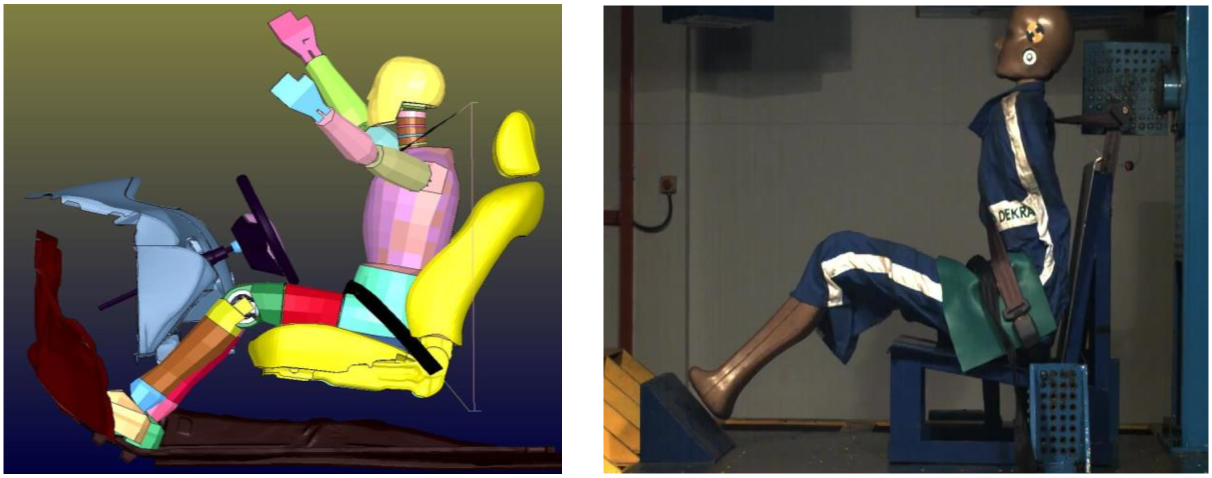

a) LS-DYNA analysis b) ECE laboratory sled test

Figure 5.15: Dummy responses at 120 millisecond

5.4 Stopping distance for alcohol drunk driver vs automatic system

Vehicle stopping distance is the sum of driver reaction distance and vehicle braking distance. Vehicle stopping distance depends on the initial speed of the vehicle and road condition. By using an analytical method the stopping distance of alcohol drunk drivers and automatic pedal control system is stated in Table 5.5 and the graph given in Figure 5.16. Finally, vehicle total stopping distance for automatic braking is best for all road conditions (level, uphill, and downhill) than alcohol drunk drivers. If the driver is drunk above the limit he may not able to take a brake and it is hard to stop the vehicle.

Table 5.5: Stopping distance for the drunk driver and automatic control (Excel)

V (m/s)	Total stopping distance (m)					
	Alcohol drunk driver			Automatic pedal control		
	uphill road	Level road	Downhill	Downhill road	Level road	uphill road
0	0	0	0	0	0	0
5	26.35707	26.5625	27.33951	17.33951	16.5625	16.35707
10	55.42829	56.25	59.35804	39.35804	36.25	35.42829
15	87.21366	89.0625	96.05559	66.05559	59.0625	57.21366
20	121.7132	125	137.4322	97.43215	85	81.71317
25	158.9268	164.063	183.4877	133.4877	114.0625	108.9268
30	198.8546	206.25	234.2223	174.2223	146.25	138.8546
35	241.4966	251.563	289.636	219.636	181.5625	171.4966
40	286.8527	300	349.7286	269.7286	220	206.8527
45	334.9229	351.563	414.5003	324.5003	261.5625	244.9229
50	385.7073	406.25	483.951	383.951	306.25	285.7073
55	439.2058	464.063	558.0807	448.0807	354.0625	329.2058

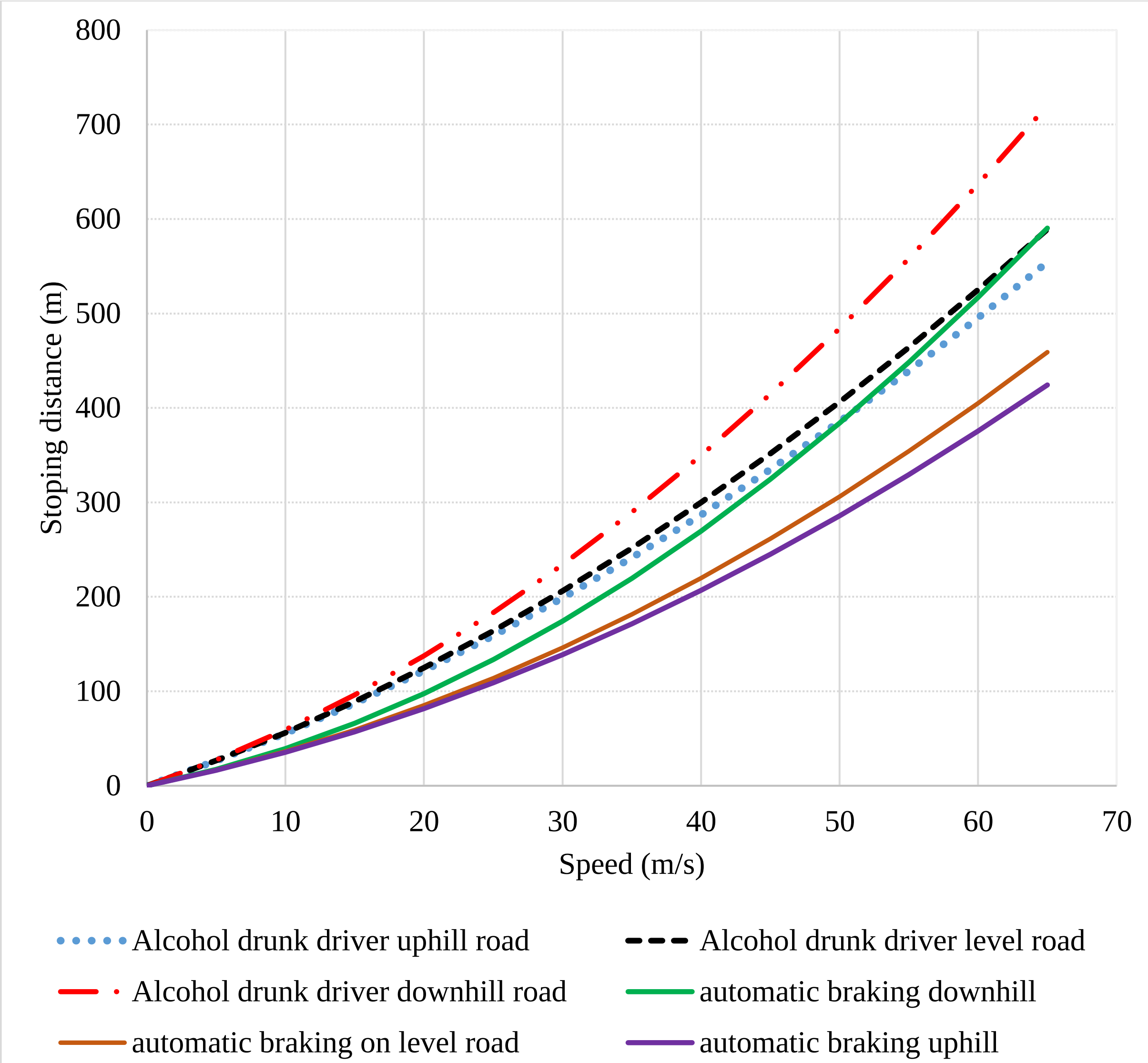

Figure 5.16: Stopping distance for the drunk driver and automatic at the different road (Excel)

5.5 SOLIDWORKS Vehicle Pedal Locking System Simulation

The pedal lock system is a device that plays a very important role in controlling the accelerator and brake pedals. The system has an electric linear actuator that receives commands from the microcontroller. The automatic control operation of the vehicle pedals (Accelerator and brakes) can be performed using two different actuators of the system. If no alcohol is detected, the driver can control all pedals as needed, as shown in Figure 5.17a. When alcohol detects that the brake pedal is depressed and the accelerator pedal is not depressed, as shown in Figure 5.17b.

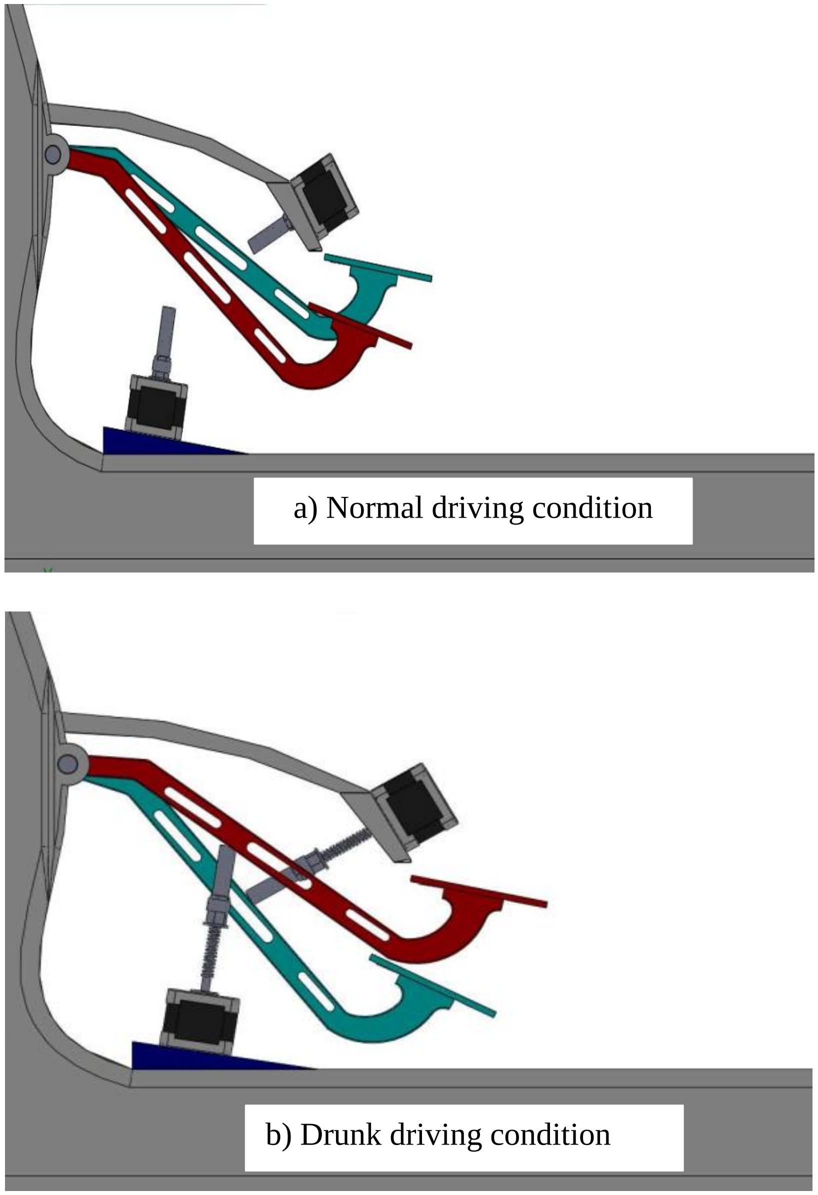

Figure 5.17: SOLIDWORKS Pedal Locking model

5.5 Model development for demonstration purpose

The developed demonstration model includes a microcontroller, liquid crystal display, electric actuator, alcohol sensor, buzzer, GPS, and GSM modules, as shown in Figure 5.18.

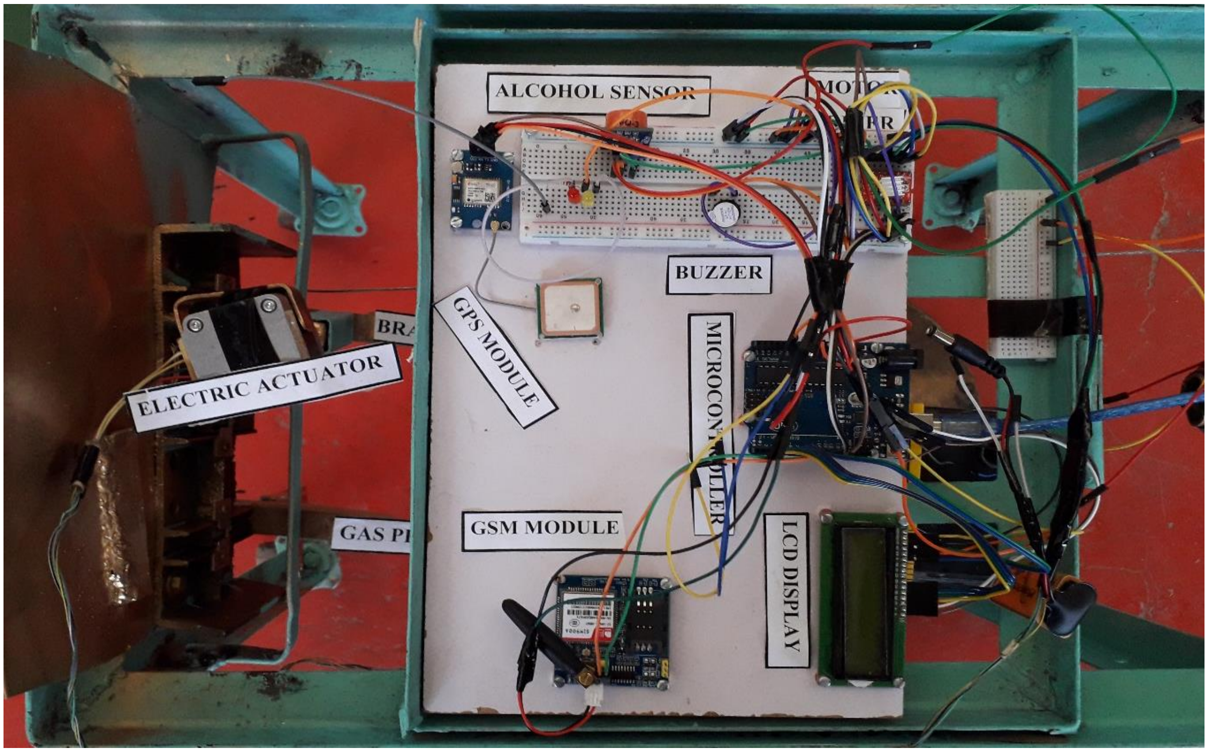

Figure 5. 18: Developed model

The developed model shows the three conditions of the ranges of the concentration of alcohol in the driver's blood, just like simulated by the Proteus program.

Condition One: When the BAC of the driver is lower than 0.5 g/L, the LCD display shows the driver "NORMAL DRIVE", as shown in Figure 5.19. Therefore, the pedal control system operates under normal conditions. The stepper motor pedal actuator stops. The buzzer and LED are off.

Condition Two: When the driver's BAC is greater than 0.5 mg/L and less than 0.8 g/L. The pedal control system operates under normal conditions. However, the LCD display the message “ALCOHOL WARNING” to the driver and the yellow LED flash continuously to warn the driver to be careful as shown in Figure 5.20.

Condition Three: when the driver's BAC exceeds 0.8 g/L, the LCD displays the message “OVER DRUNK” to the driver, and the stepper motors rotate to control the pedals. The pedal control system is controlled by a stepper motor. The red LED flashes continuously, the buzzer beeps to surrounding drivers to take caution, as shown in Figure 5.21. The GSM module sends the location of the car to the owner or the police station and virtually displays the message sent.

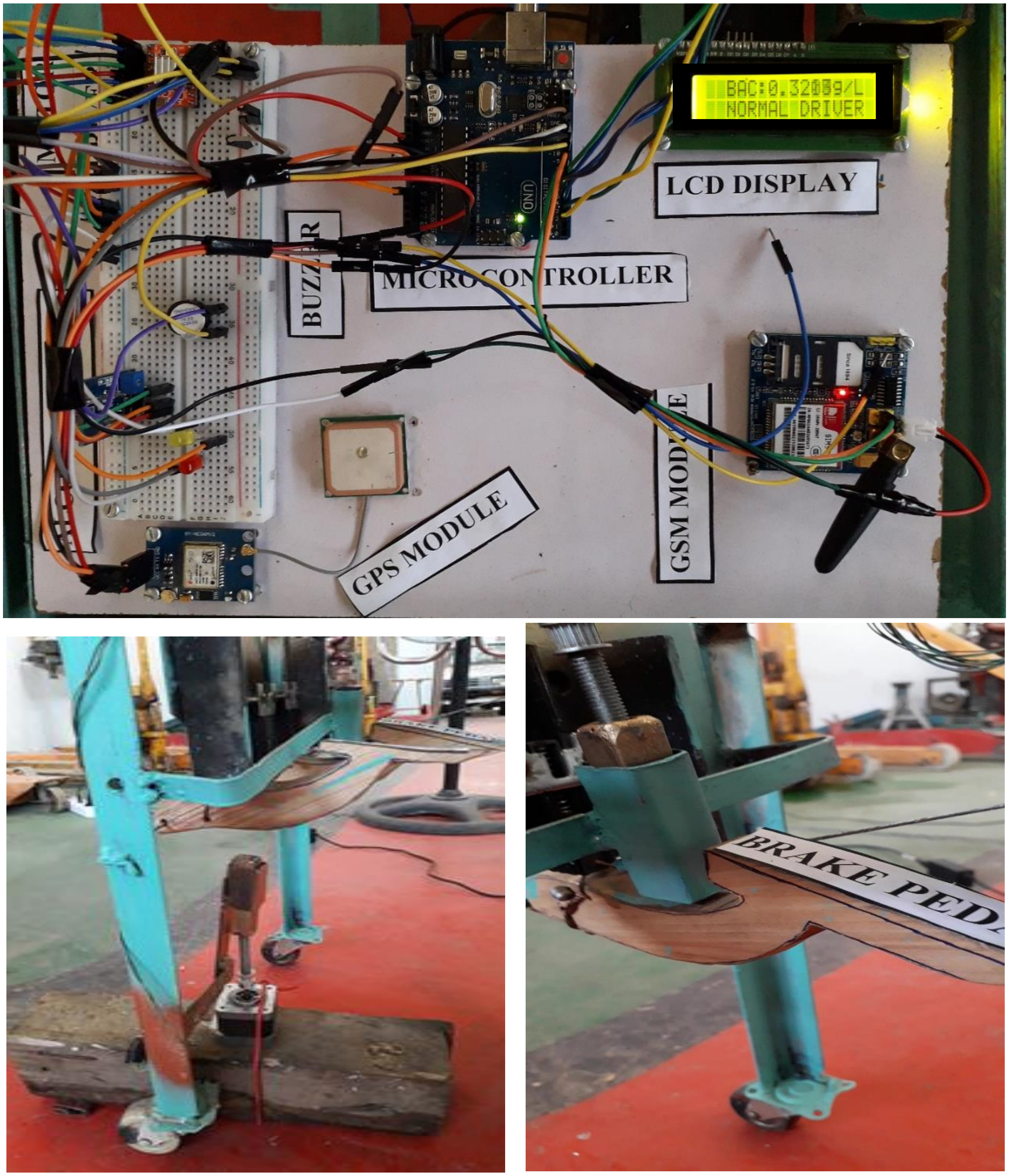

Figure 5. 19: Model demonstration when BAC below 0.5g/L

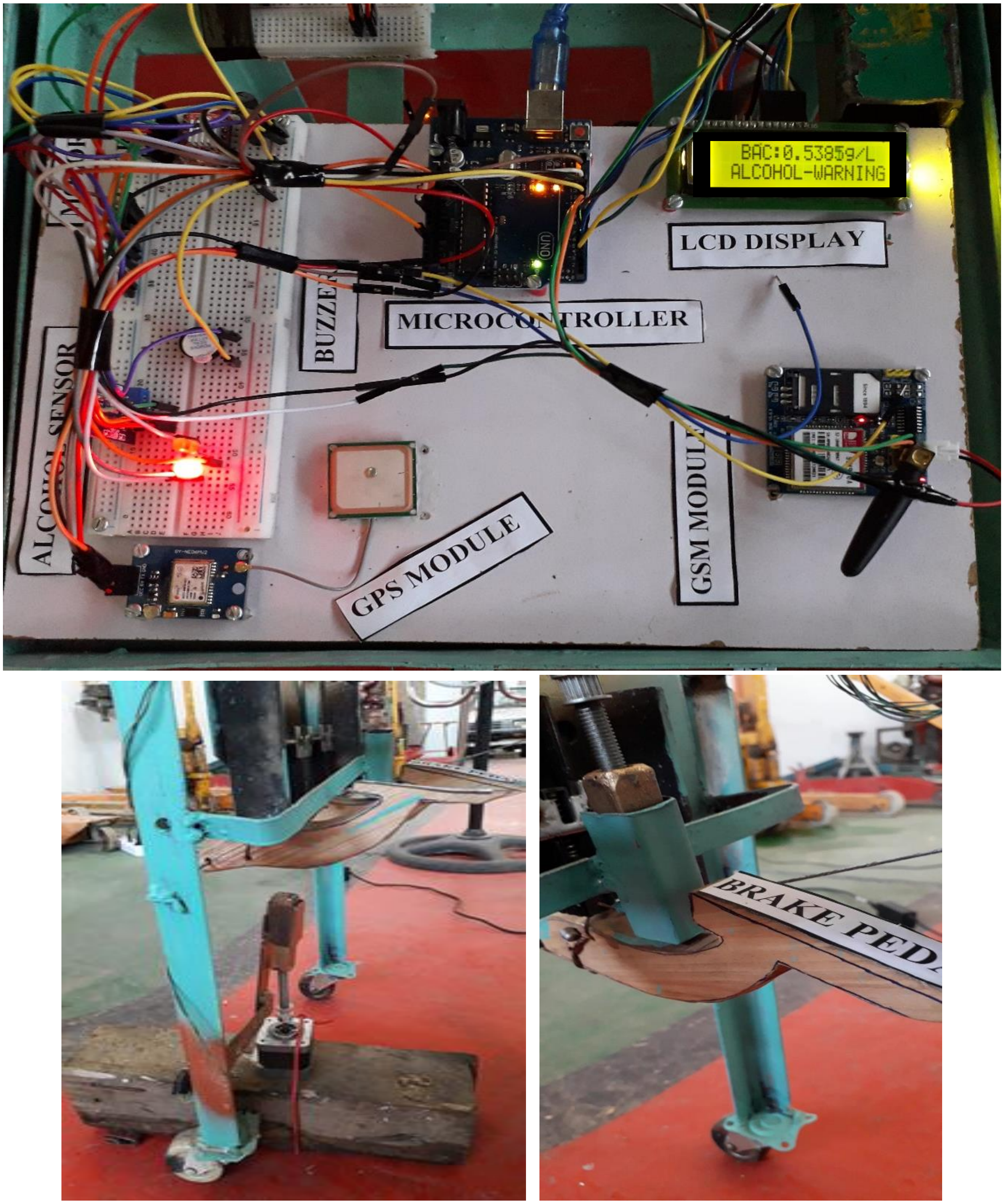

Figure 5. 20: Model demonstration when BAC between 0.5 and 0.8 g/L

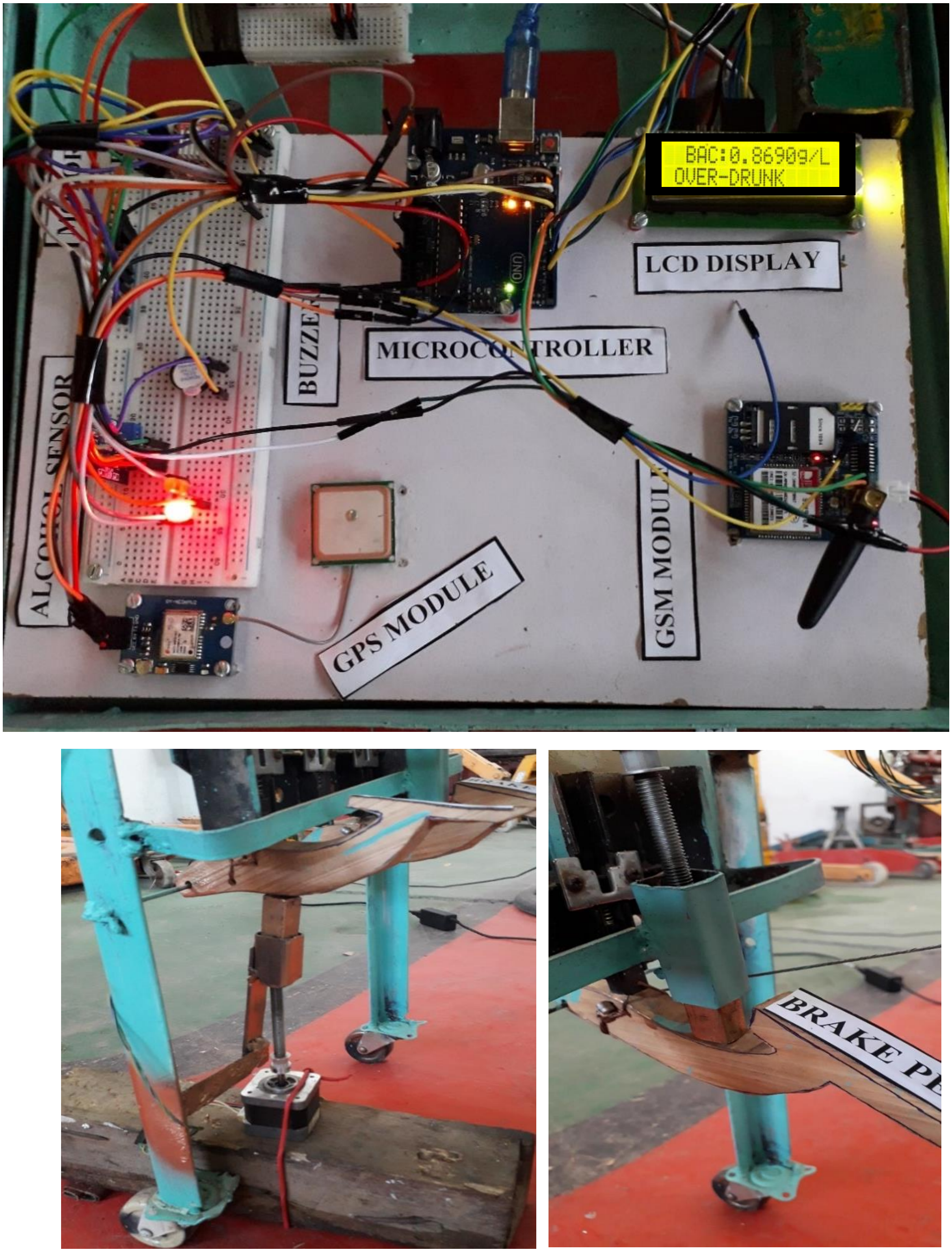

Figure 5. 21: Model demonstration when BAC greater than 0.8g/L

GPS devices transmit position information in accordance with the National Marine Electronics Association (NMEA) standard. The Arduino serial programming monitor can be used to parse GPS data from NMEA sentences. The serial port monitor displays parsed GPS data from NMEA sentences as shown in Figure 5.22. The NMEA standard has many sentences for all types of equipment that can be used in the marine environment. Some of those related to GPS receivers are listed below. All messages start with $ GP.

- GGA - Fix information
- GLL - Lat/Lon data
- GSA - Overall Satellite data
- GST - GPS Pseudo range Noise Statistics
- GSV - Detailed Satellite data
- RMB - recommended navigation data for GPS
- RMC - recommended minimum data for GPS

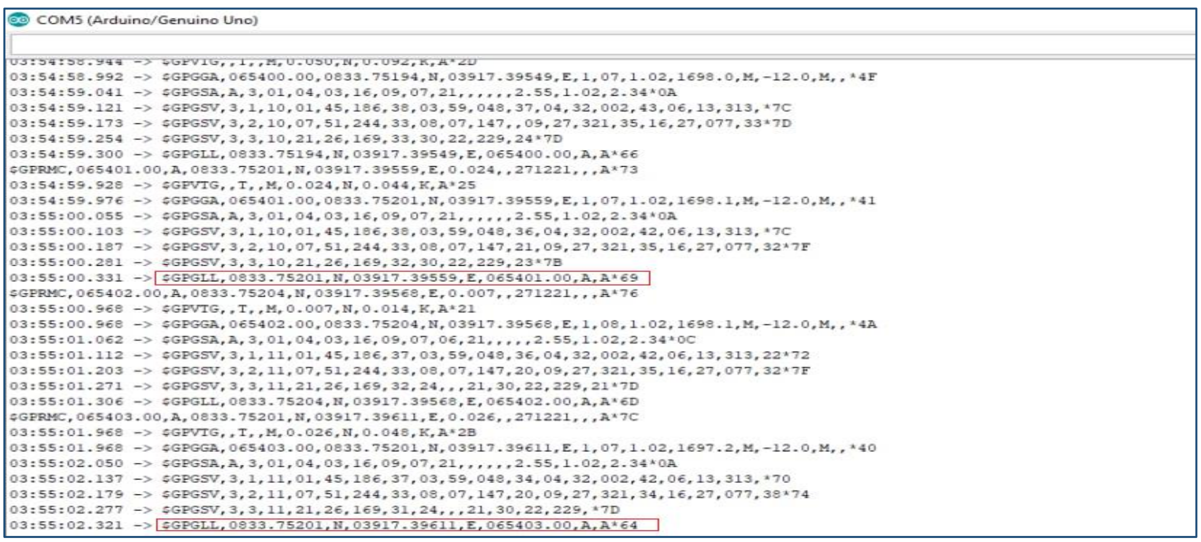

Figure 5.22: Arduino serial port monitor displays of GPS data

It is necessary to verify the latitude and longitude data collected to give the correct vehicle location using the free online NMEA Decoder tool at (http://freenmea.net/decoder). The GPS unit is tested at Adama University of Science and Technology between the auto shop and manufacturing.

The $GPGLL NMEA message $GPGLL,0833.75238,N,03917.39872,E,065451.00,A,A*64 is obtained. Now copy $GPGLL the NMEA message structure from the Arduino serial display and paste it into the free NMEA Decoder tool as shown in Figure 5.23.

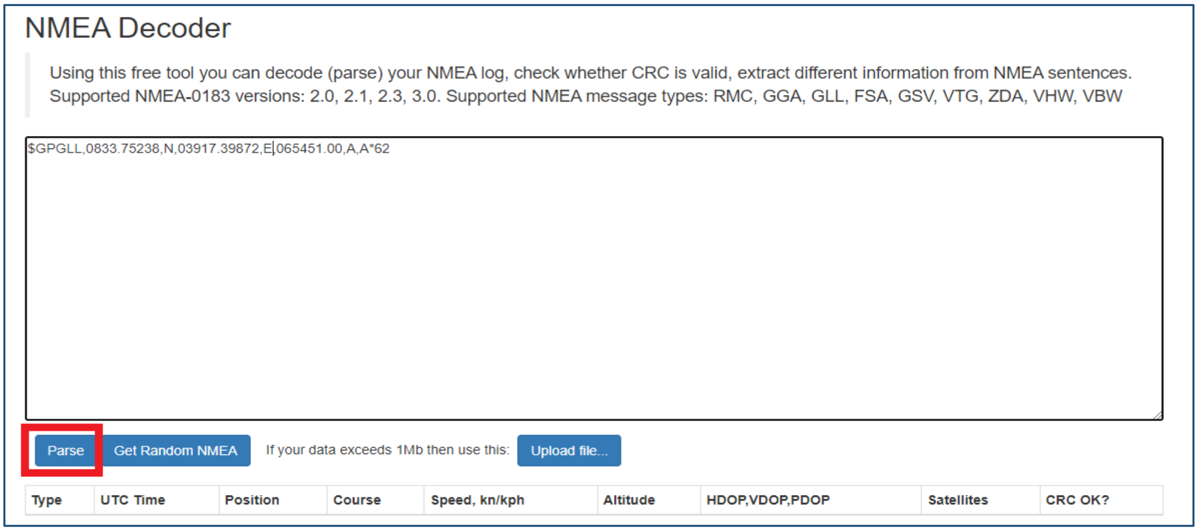

Figure 5.23: NMEA Decoder tool

Then parse the NMEA message structure of $GPGLL in the NMEA Decoder free tool. The position displayed by the NMEA Decoder free tool is shown in Figure 5.24.

Figure 5. 24: Coordinates of the position from the NMEA decoder

When you click on the coordinates of the position from the NMEA decoder, it goes to Google Maps. The location of the car is obtained from a Google map. The specific location is the red point circled by the blue rectangle as shown in Figure 5.25.

Figure 5.25: Location of the vehicle on Google map

5. 6 Summary

Alcohol is a substance that reduces the function of the brain, impairing thinking, reasoning, and muscle coordination. All these abilities are essential to operating a vehicle safely. Driving a vehicle while impaired with alcohol is deadly. This thesis work aims to control alcohol drunk drivers by automatic vehicle pedals lock system to prevent traffic accidents. When the alcohol content exceeds the threshold, the system automatically controls the vehicle's pedals to ensure the driver's safety and sends an SMS to the registered mobile phone number including the vehicle's location. A buzzer starts alarm and LED blink to indicate that nearby drivers are drinking high levels of alcohol. The system is designed for three conditions. The first one when the BAC of the driver is lower than 0.5 g/L, the LCD display shows the driver "NORMAL DRIVE". The pedal control system operates under normal conditions. The stepper motor pedal actuator stops. The buzzer and LED are off. The second one is when the driver's BAC is greater than 0.5 mg/L and less than 0.8 g/L. The pedal control system operates under normal conditions. The LCD displays the message "ALCOHOL WARNING" to the driver and the yellow LED flashes continuously to warn the driver to be careful. The third one is when the driver's BAC exceeds 0.8 g/L, the LCD displays the message "OVER DRUNK" to the driver, and the stepper motors rotate to control the pedals. The pedal control system is controlled by a stepper motor. The red LED flashes continuously, the buzzer beeps to surrounding drivers to take caution. The LS-DYNA simulation shows that when this pedal control system was fully activated, the vehicle stopped with the brakes applied at 36 km/h and the vehicle stopped immediately without seriously injuring the driver. The injury criteria's at vehicle speeds of 35, 36, and 37 km/h are summarized as follows:

- The maximum HIC36 of the head's center of gravity (within a 36 millisecond time interval) is 934.2, 983.9, and 1224 at 35 km/h, 36 km/h, and 37 km/h, respectively. These values are below the limit of (1000) at 35 km/h and 36 km/h, which means that the degree of head injury is low. However, at 37 km/h, the HIC_{36} value is higher than the limit of 1000, which means head safe.
- The maximum resulting forces on the neck determined from the LS-DYNA simulation are 2960 N, 3120 N, and 3910 N at speeds of 35 km/h, 36 km/h, and 37 km/h, respectively. The maximum force of the neck on the driver is lower than the standard limit at speeds of 35 km/h and 36 km/h, which means the neck and spinal cord are safe. However, at 37 km/h,

the maximum neck force is greater than the standard limit, which leads to a high degree of injury.

- The maximum chest deflections obtained from the LS-DYNA simulation are 45 mm, 47.1 mm, and 48 mm at 35 km/h, 36 km/h, and 37 km/h, respectively. Therefore, based on the maximum chest deflection lower than the standard limit (63mm) at three different speeds, which means the chest is safe.
- The maximum force exerted on the femur from the LS-DYNA simulation is 5.2 kN, 5.42 kN, and 5.44 kN at 35 km/h, 36 km/h, and 37 km/h, respectively. Therefore, based on the maximum femoral force on the driver, lower than standard at three different speeds, which means the femur is safe.

The accelerator pedal is controlled immediately when the alcohol content in the breath is greater than the standard limit. The brake pedal is controlled after the accelerator pedal is released and the vehicle speed is less than or equal to 36 km/h to avoid injury to the driver and passengers.

CHAPTER SIX

CONCLUSIONS AND RECOMMENDATIONS

6.1 Conclusions

Based on the design analysis and the results obtained the following conclusions are drawn.

- The automatic vehicle pedal controlling system for alcohol drunk drivers is better in-vehicle stopping distance at maximum speed than alcohol drunk drivers.
- The automatic vehicle pedal controlling brake system operates when the alcohol sensor detects alcohol level. Before controlling brakes automatically. First, the system notifies the driver for taking pre-safety measures.
- The system is feasible and less expensive and it can be implemented on vehicles by making simple modifications for controlling vehicle pedals.
- The GSM and GPS tracking system help to find the location of the vehicle with a drunk driver. The drunk driver cannot control himself and maybe lost the whole night on the road. So this system helps in locating the vehicle with a drunk driver.
- The total stopping distance of the vehicle with an automatic braking system is better on all road conditions (level, inclined) when compared to a vehicle without an automatic braking.

6.2 Recommendations

- Before implementing this system, it is recommended to know the wheel speed sensor output pulse signal corresponding to 36 km/h speedometer reading (vehicle speed).
- It is recommended to implement this system on other types of vehicles like buses, trucks, etc. in addition to automobiles.
- It is recommended that before implementing this system it is necessary to test in the laboratory.
- It is recommended that automotive industries should try to implement the system on the vehicles for reducing vehicle collisions.

6.3 Future Work

The following can be considered as the future scope of this work.

- The alcohol sensor used in this work gets affected by the exhale of other passengers as well in addition to the driver. A touch alcohol sensor mounted on the steering wheel can be used. So that replacing it with touch alcohol sensor by on steering wheel, Usage of other sensors like facial recognition sensor, heartbeat sensor, eye blink detection sensors, etc. can improve the performance of the system.
- Implement on manual transmission vehicles by study designing clutch pedal control system in addition to gas and brake pedal control system.
- Further study is required to place the modified pedal system appropriately.
- Study the effect of this system on driver ergonomics.
- Integrating the alcohol sensing system with other vehicle systems to prevent drivers from deactivating the system by cutting or plugging out wires.

Research Fund Acknowledgment

This research project is funded by Adama Science and Technology University under the grant Number ASTU/SM-R/289/21, Adama, Ethiopia.

REFERENCES

Ahmed M. T. Ibraheem Al-Naib (2019). Stepper Motor, Mosul, Northern Technical University.

Altaf, S. V., Abhinay, S., Ebran Ansari, M., & Kaunain, R. A. (2017). Alcohol Detection and Motor Locking System.

Alonso, F., Pastor, J. C., Montoro, L., & Esteban, C. (2015). Driving under the influence of alcohol: frequency, reasons, perceived risk and punishment.

Ashish C. (2019). Controlling NEMA 17 Stepper Motor with Arduino and A4988 Stepper Driver Module

Asmare, T. (2018). Design of Vacuum Bath Components and Optimization of Cooling Parameter's in Pipe Factory: A Case of Amhara Pipe Factory, Bahir Dar, Ethiopia (Doctoral dissertation, ASTU).

Bhandari, V. B. (2010). Design of machine elements. Tata McGraw-Hill Education.

Budynas, R. G., & Nisbett, J. K. (2011). Shigley's mechanical engineering design (Vol. 9). New York: McGraw-Hill.

Christian C. (2021). Stepper Motors vs. DC Motors retrieved from

https://www.thomasnet.com/articles/machinery-tools-supplies/stepper-motors-vs-dc-motors/

Crolla, D. (2019). Automotive engineering: powertrain, chassis system and vehicle body.

Dietrich, A. (2016). Electric rod actuators vs. hydraulic cylinders: A comparison of the pros and cons of each technology. Machine Design.

Droździel, P., Tarkowski, S., Rybicka, I. & Wrona, R. (2020). Drivers 'reaction time research in the conditions in the real traffic.

El Nagar, A. Y. (2017). Alcohol sensing alert with engine lock.

Elsherif, D. M., Abd El-Wahab, A. A., & Abdellatif, M. H. (2019, September). Factors affecting stress distribution in a wind turbine blade.

Evans, B. (2011). Beginning Arduino Programming (Vol. 6). New York, NY, USA: Apress.

Fan, C., Liu, X., Ling, R., & Si, B. (2018). Application of Proteus in experimental teaching and research of medical electronic circuits.

Firgelli Automations Team. (2018). Inner Workings of a Linear Actuator, Retrieved from https://www.firgelliauto.com/blogs/news/inside-a-linear-actuator-how-a-linear-actuator works.

García-Echalar, A., & Rau, T. (2020). The Effects of Increasing Penalties in Drunk Driving Laws.

Gbenga, D. E., Hamed, H. I., Lateef, A. A., & Opeyemi, A. E. (2017). Alcohol detection of drunk drivers with automatic car engine locking system.

Gebremichael, M., Guta, M., Gedefaw, M., Bekele, A., Shiferaw, F., Gelibo, T. ... & Bekele, A. (2017). Prevalence and determinants of road traffic injuries in Ethiopia

Genta, G., & Morello, L. (2019). The automotive chassis: volume 2 system design. Springer

Gill, H. (2016). Stepper motor or servo motor which should it be, White Paper, Kollmorgen-2016.

Gopinath, R. (2014). Design of a power screw.

Guha, S., Bhalsod, D., & Krebs, J. (2011). LSTC hybrid III 50th fast dummy, positioning & post-processing. LSTC, Michigan.

Gujar, S. N., & Panchal, J. R. (2014). Smart car system using Sensor, GPS and GSM.

Hassen, M. A. (2015). Strategies in the teaching of Geography in higher education preparatory secondary schools of Ethiopia

Indraneel Bhattacherjee, Namrata Singh, Tiwari (2017). Vehicle Tracking and Locking System Using GPS and GSM.

Jadon, V. K., & Verma, S. (2010). Analysis and design of machine elements.

Jakkar, R. K., Pahuja, R., Saini, R. K., & Sahu, B. (2017). Drunk-Driver Detection and Alert System (DDDAS) for Smart Vehicles.

Jain, A., Goyal, V., & Varma, C. (2021). Reflection of epidemiological impact on burden of injury in tertiary care centre, pre-COVID and COVID era:

Jazar, R. N. (2017). Vehicle dynamics: theory and application. Springer.

James, D. H., & Mitchell, C. D. (2019). Automotive Technology: Principles, diagnosis, and service. New York: Prentice Hall.

John Searle. (2015). Alcohol calculations and their uncertainty.

Juvinall, R. C., & Marshek, K. M. (2020). Fundamentals of Machine Component Design.

Khurmi, R. S., & Gupta, J. K. (2014). A textbook of machine design.

Kim, I. H., Bong, J. H., Park, J., & Park, S. (2017). Prediction of driver’s intention of lane change by augmenting sensor information using machine learning techniques. Sensors,

Li, N. (2014). Finite element modelling and simulation of occupant responses in highway crashes (Doctoral dissertation, The University of North Carolina at Charlotte).

Liu, Y. P. (2013). Simulation of Vehicles Frontal Crash with Dummy Inside. In Advanced Materials Research.

Ljungblad, J. (2017). High performance breathe alcohol analysis (Doctoral dissertation, Malardalen University Press).

Ljungblad, J., Hök, B., Allalou, A., & Pettersson, H. (2017). Passive in-vehicle driver breathe alcohol detection using advanced sensor signal acquisition and fusion. Traffic injury prevention.

Maria Vegega (2010). Driver Alcohol Detection System for Safety (DADSS). A Technological Solution to Eliminate Drunk Driving

Macuzic, I., Lukić, J., Glisovic, J., & Miloradović, D. (2017). Pedal force determination respect to ride comfort. Materials Science and Engineering.

Maurya, K., Singh, M., & Jain, N. (2012). Real time vehicle tracking system using GSM and GPS technology-an anti-theft tracking system.

McGehee, D. V., Mazzae, E. N., & Baldwin, G. S. (2000). Driver reaction time in crash avoidance research: Validation of a driving simulator study on a test track. In Proceedings of the human factors and ergonomics society.

Mihradi, S., Golfianto, H., Mahyudin, A. I., & Dirgantara, T. (2017). Head Injury Analysis of Vehicle Occupant in Frontal Crash Simulation: Case Study of ITB's Formula SAE Race Car.

Miller, J. K. (2018). Turbo: Real world high-performance turbocharger systems. Car-Tech Inc.

Mohammed, M. (2016). Developing Drunk Driving Detection and Automatic Engine Locking System.

Mongiardini, M. (2010). Development of a computer program for the verification and validation of numerical simulations in roadside safety. Department of Civil Engineering, Worcester Polytechnic Institute, Worcester, MA.

Monisha V, Priyanga M, Yamini c, Sobiyaa P. (2018). Automatic engine locking system through alcohol detection in Arduino using IOT.

N. Shankar, B.Indurani (2018). Smart Vehicle Monitoring with Accident Detection and Prevention System.

N. Subhalakshmi, R. Aswathi, D. Gobigadharani, S. Hemalatha, Joezeet F. (2017). Arduino Based Automatic Engine Locking System for Drunken Drivers.

Negi, N. S., Schmidt, K., Morozova, I., Addis, T., Kidane, S., Nigus, A., & Murukutla, N. (2020). Effectiveness of a Drinking and Driving Campaign on Knowledge, Attitudes, and Behavior Among Drivers in Addis Ababa.

Nerijus Kudarauskas (2017). Analysis of emergency braking of a vehicle.

Nikhil Agnihotri. (2011). Stepper Motor Basics, Types and Working. Retrieved from https://www.engineersgarage.com/stepper-motor-basics-types-and-working/

Nowak, A., & Nowak, I. (2017). Consumption and sale of alcoholic beverages: selected legal and health-related issues. Ius Novum, 11(4), 154-177.

Owen, C. E., & Erjavec, J. (2018). Automotive brake systems. Thomson Delmar Learning.

Ramani, R., Valarmathy, S., SuthanthiraVanitha, N., Selvaraju, S., Thiruppathi, M., & Thangam, R. (2013). Vehicle tracking and locking system based on GSM and GPS

Ranjana, P., Mukesh, R., Kumar, A., Sujith, N. N. S. S., & Sathyasai, C. H. (2019). Vehicle, engine lock system for theft and alcohol detection.

Rasekh, M., Karami, H., Wilson, A. D., & Gancarz, M. (2021). Classification and Identification of Essential Oils from Herbs and Fruits Based on a MOS Electronic-Nose Technology. Chemosensors, 9(6), 142.

Jazar, R. N. (2017). Vehicle dynamics: theory and application. Springer.

Ricci, P. (2018). Head form impact test under ECE R043 regulation: analysis and processing of data on dedicated program developed to calculate the HIC index and several correlate results.

SAE (2011). Automotive Engineering International University of California.

Safety Net (2009) Alcohol 16/10/2009.

Sahu, P., Dixit, S., Mishra, S., & Srivastava, S. (2017). Alcohol detection based engine locking system using MQ-3 sensor. International Research Journal of Engineering and Technology.

San Hlaing, N. N., Naing, M., & San Naing, S. (2019). GPS and GSM based vehicle tracking system. International Journal of Trend in Scientific Research and Development (IJTSRD).

Satria, D., Yana, S., Munadi, R., & Syahreza, S. (2017). Prototype of Google maps-based flood monitoring system using Arduino and GSM module.

Shafi, S., Tanmay, N. T. S., Tarunya, D., Vinay, G., & Reena, K. (2016). Automatic Vehicle Engine Locked Control System to Prevent Drunken Driving Using Virtual Instrumentation.

Shinde, N., Giri, A., Rima, S., & Singh, P. (2018). Alcohol detection and vehicle engine locking system. International Journal of Industrial Electronics and Electrical Engineering.

Shivam Chauhan (2016). GSM based alcohol detection for vehicles.

Siliquini, R., Bert, F., Alonso, F. et al. Correlation between driving-related skill and alcohol use in young-adults from six European countries: the TEN-D by Night Project. BMC Public Health 11, 526 (2011). https://doi.org/10.1186/1471-2458-11-526

Singh, H., Ganesan, V., James, D., Paramasuwom, M., & Gradischnig, L. (2018). Vehicle interior and restraints modelling development of full vehicle finite element model including vehicle interior and occupant restraints systems for occupant safety analysis using THOR dummies (No. DOT HS 812 545)

Tadesse, S., Chandravanshi, B. S., Ele, E., & Zewge, F. (2017). Ethanol, methanol, acid content and other quality parameters of Ethiopian traditional fermented, distilled and factory-produced alcoholic beverages. SINET: Ethiopian Journal of Science, 40(1), 16-35.

Theraja, B. L., Theraja, A. K., & Tarnekar, S. G. (2010). A Textbook of Electrical technology.

Thomson Industries, Inc. (2020). Linear Actuators for Industrial, Mobile and Structural Applications.

Tolomatic excellence (2019). Selecting the Optimal Screw Technology, Retrieved from https://www.tolomatic.com/info-center/resource-details/acme-ball-roller screw-selection.

Tummanapally, S. S., & Sunkari, S. (2021). Smart Vehicle Tracking System using GPS and GSM Technologies. Available at SSRN 3884903.

Toyota Brake Inspection Quick Training Guide QT512A, USA, December 10, 2013

United Nations economic commission for Africa, (2020). Road Safety Performance Review Ethiopia.

Viral M. Vyas, Viraj Choksi, M.B. Potdar (2018). Alcohol Sensing and Accident Alert System for Car Based on Internet of Things (IoT).

Vukovic J, Modun D, Markovic D, Sutlovic D (2015) Comparison of Breath and Blood Alcohol Concentrations in a Controlled Drinking Study. J Subst Abuse Alcohol 3(2): 1029

Wegman, F. (2017). The future of road safety: A worldwide perspective. IATSS research.

World Health Organization. (2008). Speed management: a road safety manual for decision-makers and practitioners.

World Health Organization. (2015). Global status report on road safety 2015. World Health Organization.

Yonas W. (2021). Design and Development of Intellegent Braking with brake Failure Indicator System for Bus

Yubin, Xi. (2015). Understanding the Automotive Pedal Usage and Foot Movement Characteristics of Older Drivers.

Zhang, D., Wang, J., Qian, L., & Yi, J. (2019). Stepper motor open-loop control system modelling and control strategy optimization. Archives of Electrical Engineering.

Zulhilmi, I. M., Peeie, M. H., Eiman, R. I. M., Izhar, I. M., & Asyraf, S. M. (2019). Investigation on vehicle dynamic behaviour during emergency braking at different speed.

https://community.parker.com/technologies/electromechanicalgroup/w/electromechanical-knowledge-base/433/general grades-of-steel-used-in-servo-motor-shafts

https://www.alcoholproblems and solutions.org/geography-of-alcohol-and-drinking/.

https://www.freepik.com/premium-photo/man-drinking-alcohol-while-driving car_5444975.htm/

https://www.makerspaces.com/arduino-uno-tutorial-beginners/,Thur, 12/03/2020

https://www.pngitem.com/middle/imhRmRx_clipart-don-t-drink-and-drive-images-png/

https://www.moonsindustries.com/series/nema-17-standard-hybrid-stepper-motors-b020105

https://www.backpackways.com/guide-to-ethiopian-beers/

https://americanaddictioncenters.org/alcoholism-treatment/how-long-in-system

APPENDICES

Appendix A: Part and assembly drawings

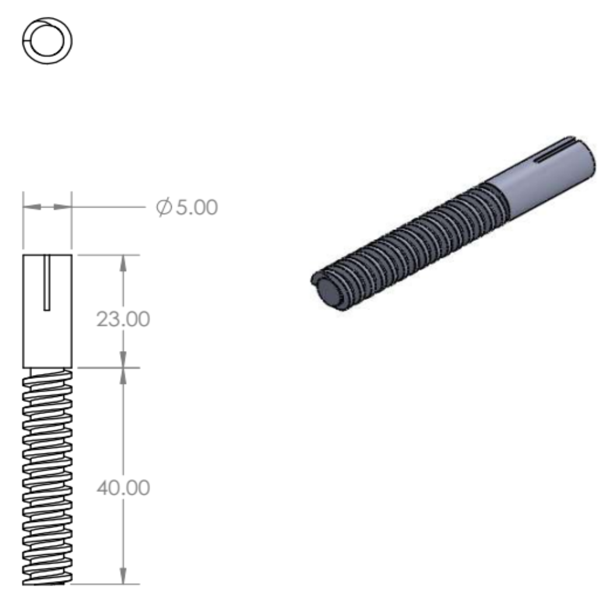

SEWAGEGZEWUDIE	TITLE: Lead Screw	ASTU
SCALE: 1:1	Dimenshion (mm)	DRAWING No 1

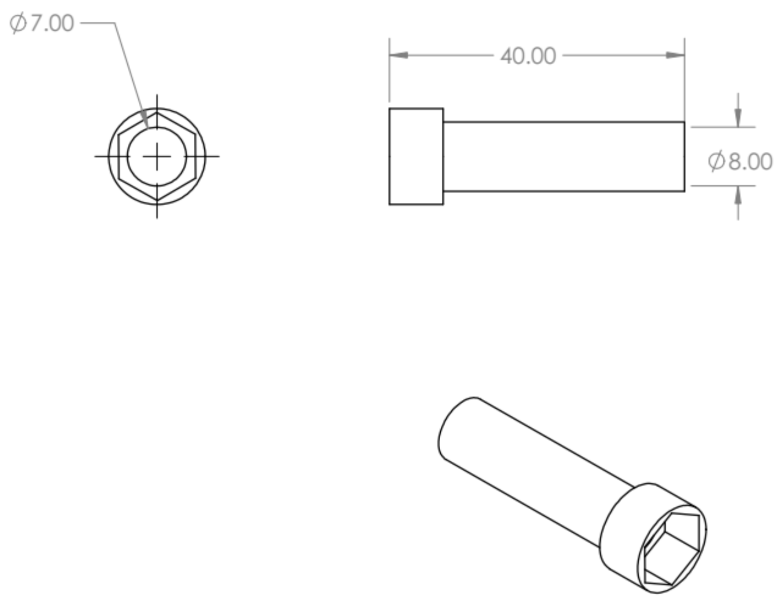

SEWAGEGZEWUDIE	TITLE: inner tube	ASTU
SCALE: 1:1	dimension (mm)	DRAWING No 2

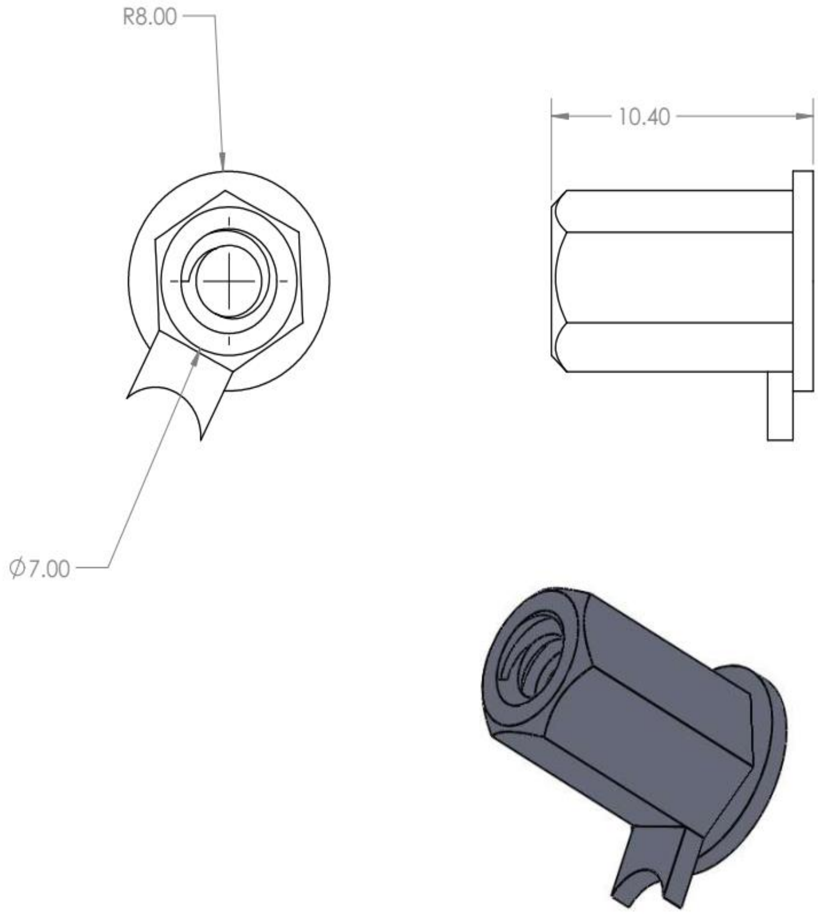

SEWAGEGZEWUDIE	TITLE: driving nut	ASTU
SCALE: 1:1	dimension (mm)	DRAWING No 3

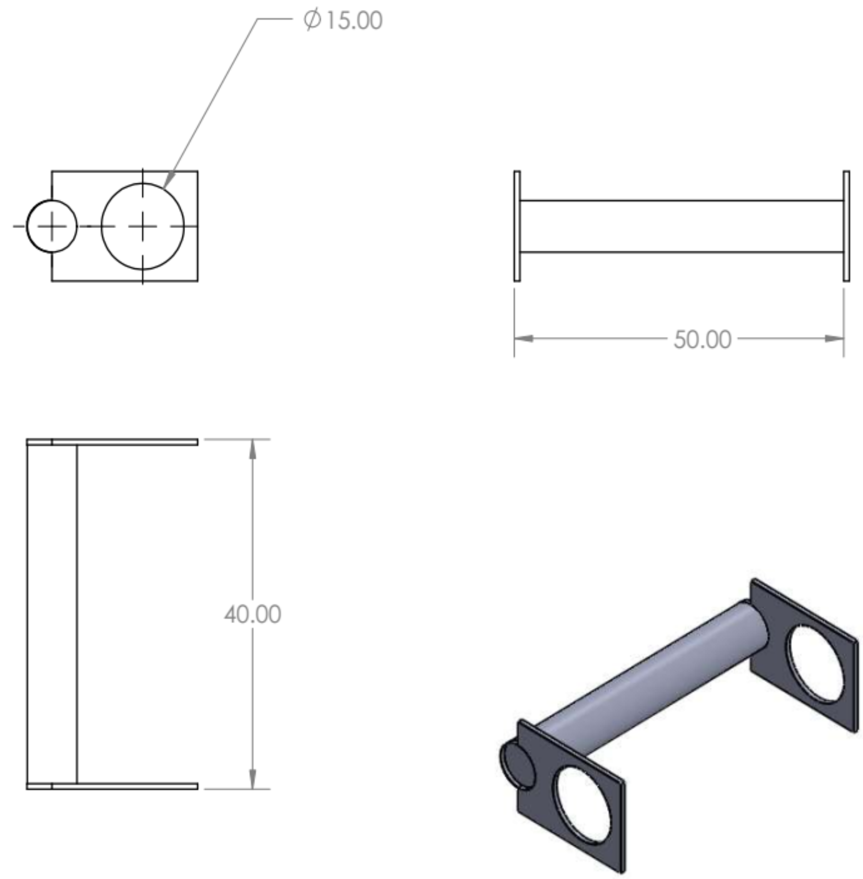

SEWAGEGZEWUDIE	TITLE: nut and leadscrew guide	ASTU
SCALE: 1:1		DRAWING No 5

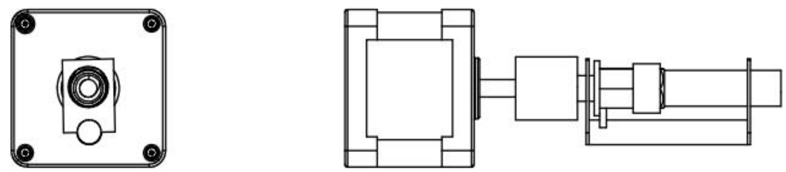

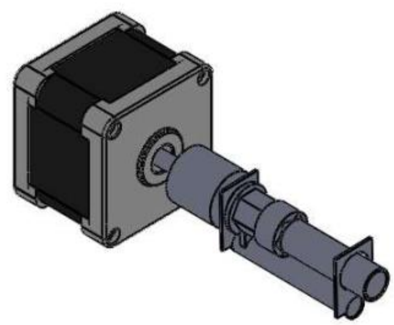

SEWAGEGZEWUDIE	TITLE: Pedal control assembley	ASTU
SCALE: 1:1	dimension (mm)	DRAWING No 4

Appendix B: Arduino programming code

```
#include <LiquidCrystal_I2C.h>
#define MQPin A0
#include <Stepper.h>
const int stepsPerRevolution=200;
// create an instance of the stepper class, specifying
// the number of steps of the motor and the pins it's
// attached to
Stepper stepperA(stepsPerRevolution, 8, 9, 10, 11);
Stepper stepperB(stepsPerRevolution, 4, 5, 6, 7);
int stepperCounter = 0;
LiquidCrystal_I2C lcd(0x27,16,2);
const int pulsePin = A2;
int pulseHigh; // Integer variable to capture High time of the incoming pulse
int pulseLow; // Integer variable to capture Low time of the incoming pulse
float pulseTotal; // Float variable to capture Total time of the incoming pulse
float frequency; // Calculated Frequency
int led1=13;
int led2=3;
const int buzzer = 12; //buzzer to arduino pin 12
char str[70];
char *test="$GPGGA";
char logitude[10];
char latitude[10];
int i,j,k;
int temp;
//int Ctrl+z=26;    //for sending msg
int pos = 0;
void setup() {
  pinMode (3, OUTPUT);
  pinMode (4, OUTPUT);
```

```
  pinMode (5, OUTPUT);
  pinMode (6, OUTPUT);
  pinMode (7, OUTPUT);
  pinMode (8, OUTPUT);
  pinMode (9, OUTPUT);
  pinMode (10, OUTPUT);
  pinMode (11, OUTPUT);
  pinMode (13, OUTPUT);
  stepperA.setSpeed (60);
  stepperB.setSpeed (60);
   lcd.begin(16, 2);
   pinMode(MQPin, INPUT_PULLUP);
   pinMode(buzzer, OUTPUT);
    pinMode(A2,INPUT);
    lcd.setCursor(2, 0);
    lcd.print("ALCOHOL DRUNK");
    lcd.setCursor(0, 1);
    lcd.print("  DRIVER TESTING");
    delay(100);
    lcd.clear();
}
void loop()
{
  pulseHigh = pulseIn(pulsePin,HIGH);
  pulseLow = pulseIn(pulsePin,LOW);
  pulseTotal = pulseHigh + pulseLow; // Time period of the pulse in microseconds
  frequency=1000000/pulseTotal;      // Frequency in Hertz (Hz)
  Serial.print("Frequency  =");
  Serial.print(frequency);
  Serial.println(" Hz");
  delay(300);
```

```
 int gas_value = digitalRead(MQPin);
 float adcValue=0;
 for(int z=0;z<10;z++)
 {
   adcValue+= analogRead(MQPin);
   delay(10);
 }
float v= (adcValue/10) * (5.0/1024.0);
   float gpL= 0.67 * v;
   Serial.print("BAC:");
   Serial.print(gpL);
   Serial.print("g/L");
   lcd.setCursor(2,0);
   lcd.print("BAC:");
   lcd.print(gpL,4);
   lcd.print("g/L");
   lcd.setCursor(0,1);
if (gpL >= 0.8 && frequency <=1390)
 {
   lcd.print(" OVER-DRUNK");
  digitalWrite(buzzer, HIGH);
 digitalWrite(led1, HIGH);

         for(i=18;i<27;i++)          //extract latitude from string
   {
     latitude[j]=str[i];
     j++;
   }

   for(i=30;i<40;i++)          //extract longitude from string
```

```
  {
   logitude[k]=str[i];
   k++;
  }
  Serial.begin(9600);
   Serial.println("AT+CMGF=1");    //select text mode
  delay(10);
  Serial.println("AT+CMGS=\"+251924534231\"");  // enter receipent number
  Serial.println("Alcohol Drunk Driver Occured At:");
  Serial.print("Latitude(N): ");             //enter latitude in msg
  Serial.println(latitude);                  //enter latitude value in msg
  Serial.print("Longitude(E): ");            //enter Longitude in Msg
  Serial.println(logitude);                  //enter longitude value in msg
  Serial.print("http://maps.google.com/maps?&z=15&mrt=yp&t=k&q=");
  Serial.println(latitude);
  Serial.println("+");
  Serial.println(logitude);
  Serial.write(26);                    //send msg  Ctrl+z=26
  temp=0;
  i=0;
  j=0;
  k=0;
  delay(20);                        // next reading within 20 seconds
{
 stepperA.step(stepsPerRevolution*2); //Gas Pedal
 delay (500);
 stepperA.step(-stepsPerRevolution*0); //Gas Pedal
}
 if (gpL >= 0.8 && frequency <= 1390)

  {
```

```
    stepperB.step(stepsPerRevolution*2);//Brake Pedal
    delay (200);
   stepperA.step(-stepsPerRevolution*2); //Gas Pedal
  delay (200);
   stepperB.step(-stepsPerRevolution*2); //Brake Pedal
  delay (200);
   }
}
else if(gpL >=0.5 && gpL < 0.8)
  {
  digitalWrite(buzzer, LOW);
  digitalWrite(led2, HIGH);
  delay(50);
  digitalWrite(led2, LOW);
  delay(50);
  lcd.print(" ALCOHOL-WARNING");
stepperA.step(stepsPerRevolution*0);
stepperB.step(stepsPerRevolution*0);
}
else
{
 lcd.print("  NORMAL DRIVER");
 digitalWrite(buzzer, LOW);
stepperA.step(stepsPerRevolution*0);
stepperB.step(stepsPerRevolution*0);
}
}
void serialEvent()
{
  while (Serial.available())            //Serial incomming data from GPS
  {
```

```
    char inChar = (char)Serial.read();
     str[i]= inChar;                    //store incomming data from GPS to temparary string str[]
     i++;
     if (i < 7)
     {
      if(str[i-1] != test[i-1])         //check for right string
      {
        i=0;
      }
     }
    if(i >=60)
    {
     break;
    }
  }
}
```

Appendix C: Breath Alcohol Tested vehicle in Addis Ababa city

2011E.C Breath Alcohol Testers in Addis Ababa city			
Sub-city	Number of vehicles towed	drink above limit	drink below limit
Bole	10101	119	311
Kirkos	13651	83	240
Yeka	3219	10	80
Gullele	4024	43	165
Arada	7161	101	173
Addis Ketema	5266	0	18
Lideta	6850	15	275
Kolfe Keranio	4336	20	77
Nifas Silk Lafto	5407	64	207
Akaki	4660	173	613
Total	71347	750	2506
2012E.C Breath Alcohol Testers in Addis Ababa city			
sub-city	Number of vehicles towed	drink above limit	drink below limit
Bole	10828	120	534
Kirkos	27829	132	416
Yeka	0	0	0
Gullele	741	35	53
Arada	2366	25	36
Addis Ketema	1198	17	33
Lideta	145	0	1
Kolfe Keranio	0	0	0
Nifas Silk Lafto	2350	40	86
Akaki	975	78	13
Total	47543	556	1260

Appendix D: Vehicle statics in Ethiopia

Type of Vehicles and Number in the Regions (up to tahsas 30.2013) Registration												
Description	AA	AM	AF	BN	DD	SO	TG	GM	HA	SN	OR	Total
Ambulance	322	0	88	55	6	45	187	0	4	61	525	1293
Automobile	255793	1786	85	54	2413	648	1994	0	1303	102	5670	269848
Bajaji	0	9308	4306	0	3302	0	0	1439	4909	11595	60847	957060
Tri cycle	0	0	0	0	0	0	0	0	0	0	0	0
Bus (<12seats)	31330	9197	492	390	1666	979	5656	2125	80	13431	28513	93859
Bus (>11seats)	19206	13953	698	511	860	871	4473	859	3000	10869	37549	92849
Combiner	106	54	0	0	2	1	5	0	0	0	82	250
Dozer	16	0	0	3	0	1	4	0	0	0	0	24
Dry cargo (<10 Quintal)	52338	3597	347	106	1083	1104	1298	0	0	1659	2069	63601
Dry cargo (>10 Quintal)	139376	3653	262	115	4670	2604	5148	0	0	3731	8119	167678
Dual Purpose	56063	4068	476	342	1704	989	2266	0	56	1453	2968	70385
Field Vehicle	53233	1835	384	161	524	1148	1282	0	300	154	3206	62227
Grader	6	2	0	0	2	1	4	0	0	0	0	17
Forklift	351	0	4	1	10	1	18	0	0	0	2	387
Not Specified	21185	1532	72	58	291	511	397	0	0	126	1251	25423
Gotach	7235	0	0	0	67	5	624	0	0	0	0	7931
Liquid Cargo	8307	313	38	2	244	186	658	0	0	67	183	9998
Liquid Trailer	0	14	0	0	0	0	0	0	0	0	171	185
Motor Bicycle	28235	45137	1389	6920	8111	1651	14405	2643	1076	78463	62129	250159
Other	12526	718	35	39	137	33	485	0	0	44	4277	18294
Three-Wheeler dry load	17	42	0	56	10	250	1874	0	0	0	4	2253
Three-Wheeler public	350	10311	0	2959	0	8523	16647	0	0	0	0	38790
Tractor	1505	401	54	143	21	0	317	0	0	17	526	2984
Trailer	32676	360	8	1	450	1	2913	0	0	1	377	36787
Vehicle with machine	1004	153	20	1	134	27	145	0	0	0	0	1484
Total	721180	106434	8758	11917	25707	19579	60800	7066	10728	121773	218470	1312412

Type of Vehicles and Number in the Regions (up to sene 30.2012) Registration												
Description	AA	AM	AF	BN	DD	SO	TG	GM	HA	SN	OR	Total
Ambulance	303	0	82	55	6	45	187	0	4	58	438	1178
Automobile	222683	1786	83	53	2360	648	1994	322	1303	98	5258	236588
Bajaji	0	9308	3925	0	3086	0	0	0	4909	11325	55462	88015
Tri cycle	0	0	0	0	0	0	0	0	0	0	0	0
Bus (<12seats)	28432	9197	493	375	1656	979	5656	2125	80	13300	27315	89608
Bus (>11seats)	17707	13953	678	467	786	871	4473	859	3000	9617	32289	84700
Combiner	27	54	0	0	1	1	5	0	0	0	79	167
Dozer	16	0	3	3	0	1	4	0	0	0	0	27
Dry-cargo(<10Quint)	44898	3597	338	105	1041	1104	1298	0	0	1577	1839	55797
Dry cargo (>10 Quintal)	119032	3653	259	108	4522	2604	5148	0	0	3612	7325	146263
Dual Purpose	49234	4068	461	330	1569	989	2266	0	56	1701	2889	63563
Field Vehicle	48837	1835	371	160	507	1148	1282	330	300	149	3037	57956
Grader	5	2	0	0	2	1	4	0	0	0	2	16
Forklift	281	0	4	1	9	1	18	0	0	0	2	316
Not Specified	19955	1532	71	56	283	511	397	231	0	295	1650	24981
Gotach	5854	0	0	0	66	5	624	0	0	0	0	6549
Liquid Cargo	6866	313	37	2	241	186	658	0	0	67	181	8551
Liquid Trailer	0	14	0	0	0	0	0	0	0	0	171	185
Motor Bicycle	25726	45137	1355	6108	7656	1651	14405	2370	1076	76563	61386	243435
Other	10786	718	35	30	124	33	485	0	0	43	3796	16050
Three-Wheeler-dry	16	42	0	50	9	250	1874	0	0	0	4	2245
Three-Wheeler public	356	10311	0	2612	0	8523	16647	0	0	0	0	38449
Tractor	1325	401	54	138	21	0	317	0	0	16	526	2798
Trailer	27266	360	8	1	431	1	2913	0	0	1	377	31358
Vehicle with machine	835	153	20	1	134	27	145	0	0	0	0	1315
Total	630440	106434	8277	10655	24510	19579	60800	6237	10728	118424	204026	1200110

Type of Vehicles and Number in the Regions (up to Sene 30.2011) Registration											
Description	AA	AM	AF	BN	DD	SO	TG	GM	HA	SN	OR	Total
Ambulance	253	0	38	44	7	14	164	0	4	28	365	917
Automobile	205773	1701	66	49	2246	609	1660	228	1273	80	6012	219699
Bajaji	0	4722	2889	0	2318	0	0	0	536	9307	48822	68594
Tri cycle	0	37	0	0	0	0	0	0	0	27	0	64
Bus (<12seats)	27357	8805	465	347	1607	837	5201	0	0	12503	3024	60146
Bus (>11seats)	16698	12840	532	378	681	677	3886	1375	357	10029	38439	85892
Combiner	23	53	0	0	1	2	5	0	357	0	78	519
Dozer	17	0	3	3	0	1	5	0	20	0	0	49
Dry cargo (<10 Quintal)	41333	2396	301	102	993	1036	1163	0	176	102	1868	49470
Dry cargo (>10 Quintal)	115023	4591	240	103	4313	2348	5030	0	2	153	7188	138991
Dual Purpose	47278	3907	380	310	1370	684	2188	0	36	1438	97	57688
Field Vehicle	47059	1767	318	153	487	1037	1228	0	445	123	3299	55916
Grader	6	2	0	0	2	1	4	0	3	0	2	20
Forklift	237	0	4	1	8	0	18	0	317	0	2	587
Not Specified	18943	1462	34	48	248	0	396	436	1179	3118	7929	33793
Gotach	5756	0	0	0	67	2	613	0	1699	0	0	8137
Liquid Cargo	6703	318	35	2	226	148	650	0	7	65	437	8591
Liquid Trailer	0	14	0	0	0	0	0	0	336	0	187	537
Motor Bicycle	24700	40229	1181	4865	6689	1366	12358	2166	1178	54084	49903	198719
Other	10279	643	36	1	105	33	485	1353	72	78	2903	15950
Three-Wheeler dry load	15	9625	0	39	7	233	1417	0	1	0	4	11341
Three-Wheeler public	368	0	0	2259	0	6106	12953	0	0	0	0	2186
Tractor	1199	392	51	136	21	0	304	0	0	10	530	2643
Trailer	26326	329	8	1	427	1	2891	0	0	0	217	30210
Vehicle with machine	738	148	17	1	125	25	132	0	0	0	0	1186
Total	596084	94001	6598	8842	21938	15160	52751	5558	8000	91105	171308	1071345

Type of Vehicles and Number in the Regions (up to sene 30.2010) Registration											
Description	AA	AM	AF	BN	DD	SO	TG	GM	HA	SN	OR	Total
Ambulance	198	0	37	35	9	2	91	0	4	25	238	639
Automobile	184227	1485	59	49	2057	558	1421	228	1275	16162	4796	212317
Bajaji	0	2132	2644	0	289	0	0	0	536	8721	34339	48661
Tri cycle	0	40	0	0	0	0	0	0	0	27	0	67
Bus (<12seats)	26408	7146	448	324	1468	755	4768	0	0	709	14174	56200
Bus (>11seats)	15242	9747	449	325	514	537	3335	1375	357	1144	22772	55797
Combiner	20	17	0	0	1	2	5	0	357	0	75	477
Dozer	16	0	3	3	0	1	5	0	20	0	0	48
Dry cargo (<10 Quintal)	37384	1602	289	101	890	953	1069	0	176	3070	7063	52597
Dry cargo (>10 Quintal)	109952	4099	229	98	4089	2152	4886	0	2	1195	1810	128512
Dual Purpose	44954	3443	348	301	1157	515	2063	0	36	1435	372	54624
Field Vehicle	45081	1590	303	148	447	912	1185	0	445	117	5421	55649
Grader	7	2	0	0	1	1	4	0	3	0	1	19
Forklift	188	0	4	1	6	0	13	0	317	0	2	531
Not Specified	18154	8121	32	25	222	263	602	0	0	1534	6020	34973
Gotach	5598	0	0	0	59	0	572	0	1699	0	0	7928
Liquid Cargo	6341	272	35	2	206	114	645	0	7	65	189	7876
Liquid Trailer	0	11	0	0	0	0	0	0	336	0	117	464
Motor Bicycle	22931	26442	1152	4129	5891	1157	10744	2166	0	49409	29328	153399
Other	9912	442	36	1	88	33	494	1353	72	36	1763	14230
Three-Wheeler dry load	12	0	0	24	2	166	888	0	1	0	4	1097
Three-Wheeler public	375	0	0	1909	0	5145	9962	0	0	0	0	17391
Tractor	1059	281	46	134	21	0	265	0	0	7	503	2316
Trailer	25336	292	8	1	394	1	2793	0	0	0	302	29127
Vehicle with machine	543	135	15	1	113	27	115	0	0	0	0	949
Total	553938	67299	6137	7611	17924	13294	45925	5122	5643	83656	129339	935888

Type of Vehicles and Number in the Regions (up to tahsas 30.2009) Registration

Description	AA	AM	AF	BN	DD	SO	TG	GM	HA	SN	OR	Total
Ambulance	180	0	34	27	9	2	69	0	4	7	165	497
Automobile	171523	1485	55	34	1967	558	927	228	1275	51	6376	184479
Bajaji	0	2132	2302	0	0	0		0	536	4671	5152	184479
Tri cycle	0	40	0	0	0	0	0	0	0	27	16861	16928
Bus (<12seats)	25929	7146	442	260	1376	755	2799	0	0	50	126	38883
Bus (>11seats)	14524	9747	372	229	457	537	1521	1375	357	178	2126	31423
Combiner	10	17	0	0	1	2	8	0	357	0	6322	6717
Dozer	0	0	3	0	0	1	5	0	20	0	252	281
Dry cargo (<10 Quintal)	34446	1602	273	94	847	953	733	0	176	95	1067	40286
Dry cargo (>10 Quintal)	105150	4099	224	92	3916	2152	4372	0	2	15	527	120549
Dual Purpose	43253	3443	339	255	1104	515	1665	0	36	21	131	50762
Field Vehicle	43681	1590	298	138	426	912	1034	0	445	16	7168	55708
Grader	5	2	0	0	1	1		0	3	0	17517	17529
Forklift	145	0	3	0	6	0	2	0	317	0	19880	20353
Not Specified	18370	8121	25	16	214	2630	187		0	50762	13480	91438
Gotach	5178	0	0	0	57	0	308	0	1699	0	1305	8547
Liquid Cargo	5057	272	34	2	203	114	621	0	7	65	358	6733
Liquid Trailer	0	11	0	0	0	0		0	336	0	2189	2536
Motor Bicycle	21509	26442	1048	3237	5761	1157	5705	2166	0	4	642	67671
Other	9766	442	35	1	89	33	524	1353	72	22	3	12340
Three-Wheeler dry load	8	0	0	6	2	166	65	0	1	0	263	511
Three-Wheeler public	506	0	0	1508	299	5145	5046	0	0	0	7	12511
Tractor	1027	281	46	124	20	0	184	0	0	1	239	1922
Trailer	23810	292	8	1	379	1	2485	0	0	0	13	26989
Vehicle with machine	367	135	14	1	109	27	62	0	0	0	164	879
Total	524444	67299	5555	6025	17243	13294	28322	5122	5643	55985	102333	831265

Type of Vehicles and Number in the Regions (up to sene 30.2008) Registration

Description	AA	AM	AF	BN	DD	SO	TG	GM	HA	SN	OR	Total
Ambulance	15229	0	26	27	7		69	8	4	5	160	15535
Automobile	122637	1341	46	27	1693	478	927	21	1275	10281	6372	145098
Bajaji	98	1108	1776	1146				185	536	4105	5146	14100
Tri cycle	0	3605	0	0	0	0	0	0	0	0	16526	20131
Bus (<12seats)	20847	5956	417	215	952	633	2799	0	0	0		31819
Bus (>11seats)	12636	6781	276	171	375	434	1521	143	357	1257	2067	26018
Combiner	16	19			1	2	8	59	357	98	6322	6882
Dozer	14	0	3			1	5	0	20	1	252	296
Dry cargo (<10 Quintal)	25898	1167	225	90	630	762	733	48	176	35	1063	30827
Dry cargo (>10 Quintal)	81641	3584	210	87	3290	1947	4372	2	2	0	509	95644
Dual Purpose	36084	2804	314	231	870	335	1665	1	36	65	131	42536
Field Vehicle	41684	1433	277	128	348	718	1034	45	445	67	7162	53341
Grader	4	2			1	1		23	3	218	17517	17769
Forklift	16	0	2		3		2	214	317	30276	19880	50710
Not Specified	38416	991	20	6	2624	1134	187	0	0	0	1	43389
Gotach	665	0	0	0	48	0	308	0	1699	3133	1305	7158
Liquid Cargo	4745	201	33	2	186	98	621	13	7	1315	358	7579
Liquid Trailer	559	10						24	336	25	2188	3142
Motor Bicycle	16353	17154	864	2351	5331	931	5705	2	0	1	401	49093
Other	12117	320	39	1	93	33	524	0	72	3207	2	16408
Three-Wheeler dry load	0		0	0	0	0	65	0	1	0	263	329
Three-Wheeler public	13			2	74	2	5046	0	0	0	7	5144
Tractor	715	213	44	114	16	3141	184	0	0	1	238	4666
Trailer	17133	248	8	1	296	1	2485	0	0	0	13	20185
Vehicle with machine	149	99	12	1	103	27	62	0	0	0	164	617
Total	447669	47036	4592	4600	16951	10678	28322	788	5643	54090	88047	708416

Appendix E: Road traffic accident report in Ethiopia

year	bicycle	motor cycle	automobile	small wagen	pickup	truck 11-41 kuntal	truck 41-100 kuntal	truck with trailer	tanker cars
2006E.C	150	562	5652	2082	3100	1852	1863	904	328
2007E.C	284	747	5,236	2,487	3,220	2,055	1,859	949	199
2008E.C	128	1,349	4,239	2,309	3,714	1,516	2,398	712	325
2009E.C	127	881	4,963	2,369	4,950	3,215	2,759	1,214	304
2010E.C	113	1,671	6,701	2,375	5,785	3,287	2,490	1,173	252
2011E.C	122	1,311	7,299	2,601	4,928	2,745	2,507	912	303
2012E.C	194	1,146	8,952	2,549	3,799	2,715	2,213	669	380

year	taxi	bus up to 120	bus 13-45	bus above 46	special Mobile device	special mobile with trailer	cart	others	unknown
2006E.C	4864	3142	1269	804	272	251	288	305	458
2007E.C	7,588	3,508	1,285	699	145	151	468	348	633
2008E.C	9,443	3,441	1,740	917	163	162	379	319	75
2009E.C	7,927	4,830	2,232	1,048	124	92	175	706	534
2010E.C	6,476	4,702	3,249	667	171	91	171	962	660
2011E.C	8,284	5,082	2,267	966	129	85	132	533	664
2012E.C	6,672	5,449	1,745	1,345	211	162	180	491	752